Embryonic stem cells express a transforming oncogene.

Kazutoshi Takahashi

Laboratory of Animal Molecular Technology,
Research and Education Center for Genetic Information,
Nara Institute of Science and Technology

Ph.D. advisor; Professor Shinya Yamanaka

31/ 01/ 2005

Contents

1. Introduction

Embryonic stem (ES) cells were first established from inner cell mass of mouse blastocysts in 1981 [1, 2]. These cells can proliferate infinitely while maintaining the undifferentiated state. Pluripotent cells were subsequently generated from human blastocysts in 1998, which are considered to be promising sources for cell therapy to treat patients with degenerative diseases such as diabetes and Parkinson disease [3]. However, ES cells have a propensity to produce tumors called teratoma when transplanted, which may preclude their therapeutic usage [4].

Transcription factors expressed predominantly in ES cells, such as Oct3/4 [5, 6] and Nanog [7, 8], are essential for the maintenance of pluripotency. Several cytokines including leukemia inhibitory factor (LIF), bone morphogenetic protein 4 (BMP4) and Wnt could sustain self-renewal of ES cells [9, 10, 11, 12]. However, it remains elusive why ES cells possess tumor-like properties without chromosomal abnormalities.

We have identified ~20 genes that are specifically expressed in mouse ES cells and preimplantation embryos. We designated these genes ECAT for ES cell associated transcript. One of them, ECAT5, encodes a polypeptide with ~40% identify with HRas, KRas and NRas. In this study, I studied its expression, transcriptional control, intracellular localization, protein-protein interaction and functions in cells and *in vivo*.

2. Materials and Methods

2.1 ES cell lines and culture conditions.

In this study, RF8 and MG1.19 ES cells were used [14, 15]. RF8 ES cells which used for gene targeting, production of knockout mice or some assays were maintained in Dulbecco's modified eagle medium (DMEM, Nacalai tesque) containing 15% fetal bovine serum (FBS, selected batches for ES cells, Hyclone), 1 x 10^{-4} M non-essential amino acids (Invitrogen), 2 mM L-glutamine (Invitrogen), 1 x 10^{-4} M 2-mercaptoethanol (Invitrogen) and 50U penicillin/streptomycin (Invitrogen). Most of cases, RF8 ES cells were cultured on mitomycin C-treated STO feeder layer. To maintain the pluripotency of ES cells in feeder-free condition, ES cells were plated on gelatin-coated tissue culture plates, and LIF was supplemented into the medium. To prepare LIF, 293T cells were transfected with pPyCAG-IP encoding human *LIF* by using Fugene 6 transfection reagent as described below. Twenty-four hours after transfection, medium was replaced with fresh one and incubated for 3 days. After incubation, supernatant was collected and filtrate through a 0.22 μm pore size filter (Millipore). LIF was stored in small quantity in sterile tubes at -20^{o}C until use. MG1.19 ES cells were grown on gelatin-coated tissue culture plates in the medium containing LIF. MG1.19 ES cells are derived from CCE ES cells and stably express

the large T antigen of murine polyoma virus. When plasmids containing the replication origin of polyoma virus (pPyCAG-IP etc.) are introduced into these cells, they can be replicated without being integrated into chromosomes. The episomal expression system developed by Dr. Austin Smith's laboratory is suitable. This method provides rapid and efficient establishment of both poly-clonal and mono-clonal ES cells expressing genes of interest (Fig. 15A).

2.2 Feeder cells.

I used SNL cells (expressing LIF and neomycin resistance gene based on STO cells) as feeder cells. To establish STO-PH cells which resisted against puromycin and hygromycin B, SNL cells were infected pMX-IP and pMX-IH. All of SNL sublines were maintained STO medium (7% FBS, 2 mM L-glutamine and 50U penicillin/streptomycin in DMEM).

2.3 Other cells.

PLAT-E packaging cells were used for production of retroviruses[16]. PLAT-E cells were maintained in DMEM containing 10% FBS and 50U penicillin/streptomycin supplemented with 1 μg/ml of puromycin (Sigma) and 100 μg/ml of blastcidine S

(Funakoshi). NIH3T3 mouse fibroblasts were cultured in DMEM containing 10% calf serum (Sigma) and 50U penicillin/streptomycin.

Primary mouse embryonic fibroblasts (PMEFs) were isolated by standard protocol. The uterus were isolated from 13.5 day pregnant mice and washed with PBS, briefly. Embryos were isolated and removed the head and liver, and then bodies were washed in fresh PBS. These bodies were pooled, minced with a pair of scissors, and then put into 0.1 mM Trypsin/1 mM EDTA solution (3 ml per embryo) and incubated at 37^{o}C for 20 minutes. After incubation, another 0.1 mM Trypsin/1 mM EDTA solution (3 ml per embryo) was added and incubated at 37^{o}C for 20 minutes. When trypsinization was finished, the equal amount of the medium (6 ml per embryo) was added and pippeted up and down a few times to help break up the tissue. The tissue/medium mixture was left for 5 minutes at room temperature, and then the supernatant was transferred into a new tube. The cells were collected by centrifugation and resuspended in new medium. Ten million cells were plated on 100 mm dishes and incubated at 37^{o}C with 5% CO_2. This period was designated passage 1. In this study, PMEFs were used for assays within passage 3 to avoid replicative senescence.

2.4 Plasmid constructions.

Most of expression vectors were modified for using Gateway Technology. And most of coding regions of the genes used in this study were amplified by RT-PCR, subcloned into pDONR201 (Invitrogen), pENTR-1A (Invitrogen) or pENTR-D-TOPO (Invitrogen) and verified by sequencing. Information of plasmid constructions and primer sequences used in this study were described in Appendix 1 and 2, respectively.

2.5 Transfection and retroviral infection.

For transiently expression, the lipofection method was used. ES cells were plated on gelatin-coated 24-well plates at 1 x 10^5 cells per well in the medium supplemented with LIF and cultured overnight. Next day, DNA was introduced into ES cells with Lipofectamine 2000 (Invitrogen); one microgram of plasmid DNA and 2 μl of Lipofectamine 2000 were diluted each in 150 μl of DMEM. The diluted DNA/Lipofectamine 2000 was mixed by vortex briefly and incubated for 20 minutes at room temperature. During incubation, the medium was removed and cells were washed once with DMEM. After incubation, the DNA/Lipofectamine 2000 mixture was applied to ES cells and incubated for 4 hours at 37^{o}C with 5% CO_2. The parent plasmid (Mock) and/or enhanced green fluorescence protein (EGFP) control plasmid

were transfected at the same time as controls. After 4-hour incubation, the cells were washed once with PBS and treated with 100 μl of 0.25% tripsin/1 mM EDTA for 5 minutes at room temperature. Then four hundreds microliters of the ES medium was added, suspended the cells by pipetting and replated the cells on gelatin-coated 60 mm dishes. Twenty-four hours after transfection, selection of transfected cells were started with 2 μg/ml of puromycin. The medium was changed every day until non-transfected control cells were completely eliminated.

For stable gene expression, the expression vectors were integrated into the genome of ES cell by electoroporation. All of plasmids were linearized by restriction enzyme. After digestion, DNA was purified by phenol-chloroform isoamylalcohol and ethanol precipitation. Purified DNA was dissolved in PBS (1 mg/ml) and stored at 4^{o}C until use. RF8 ES cells were harvested by trypsinization, and neutrized by addition of the medium. These cells were centrifuged at 800 rounds per minute (rpm) for 5 minutes at 4^{o}C. The pellet was resuspended with PBS, cell number was counted by using Coulter counter (Beckman) and then adjusted to 1 x 10^{7} cells per 780 μl with PBS. Twenty micrograms of linearized DNA and 1 x 10^{7} of ES cells were mixed (total 800 μl) and transferred into the cuvette. Electroporation was performed under the condition (250 V, 500 μF, infinitely resistance) and cell suspension was incubated in the hood at room

temperature for 10 minutes. After incubation, the cells were plated on mitomycin C-treated STO cells. Next day, the medium was replaced with new one. Two days after electroporation, the cells were selected with an appropriate drug (250 μg/ml of G418, 1.5 μg/ml of puromycin or 100 μg/ml of hygromycin B) for 10 days. The drug resistant colonies were picked up and harvested by trypsinization and transferred individually to 24-well plates. Expression level of the gene was confirmed by northern blotting or immunoblotting.

The day before transfection, PLAT-E cells from a semiconfluent 100 mm dish were harvested with 4 ml of 0.05% trypsin/0.53 mM EDTA (Sigma), resuspend in 10 ml of the medium devoid of puromycin and blastcidine S by pipetting. Then this cell suspension was centrifuged at 1200 rpm for 5 minutes, resuspended with the medium and seeded at 2 x 10^6 cells per 60 mm dish and incubated overnight. Next day, pMX based retroviral vectors were introduced into PLAT-E with Fugene 6 transfection reagent according to the manufacturer's recommendation: nine microliters of Fugene 6 transfection reagent (Roche) was diluted in 100 μl of DMEM and incubate for 5 minutes at room temperature. Three micrograms of plasmid DNA (pMX-IP retroviral vectors with gene of interest) were added into the mixture and incubated for 15 minutes at room temperature. After incubation, the DNA/Fugene 6 complex was added drop

by drop into PLAT-E plate and incubated overnight at 37^{o}C with 5% CO_2. Twenty-four hours after transfection, the medium was replaced with new one. PMEFs or NIH3T3 cells were prepared by seeding at 2 x 10^5 cells (at subconfluent density) per 60 mm dishes. Twenty-four hours later, virus-containing supernatant of PLAT-E dishes were filtered through a 0.45 μm cellulose acetate filter (Schleicher & Schuell) and added 4 μg/ml of polybrene (Nacalai tesque). The medium of PMEFs or NIH3T3 cells was replaced with virus- and polybrene-containing supernatant. The cells were incubated for 4 hours to overnight. After infection, the virus-supernatant was removed from the PMEFs plate and add 10 ml fresh medium. Forty-eight hours after infection, cells were selected with 2 μg/ml of puromycin for 4 or 5 days.

2.6 Immunoblotting and Immunoprecipitation.

In all of experiments, cell lysates were collected at subconfluent density (log-phase). Normally, cells were washed once with PBS, lysed with M-PER (PIERCE) and then incubated for 15 minutes at 4^{o}C. Cells were scraped, transferred to microcentrifuge tubes and centrifuged at 15000 rpm for 15 minutes. The supernatants were transferred to new microcentrifuge tubes. The concentrations of total protein were measured by Bradford method. The cleared lysates were added with one-fifth volume of 5 x SDS

sample buffer (250mM Tris-HCl, pH6.8, 10% SDS, 0.5% Bromophenol Blue, 50% Glycerol and 100 mM of 2-mercaptoethanol) and boiled at 100^{o}C for 5 minutes. Fifty-micrograms of proteins were separated by SDS-polyaclylamide gel electrophoresis (SDS-PAGE) and transferred to PVDF membranes (Millipore). Then membranes were incubated in blocking solution for 1 hour at room temperature with gently agitation. Primary antibodies were diluted at appropriate concentrations in fresh blocking buffer and membranes were placed in the primary antibody solution overnight at 4^{o}C. Next day, membranes were washed three times for 10 minutes each with TBS-T (20 mM Tris-HCl, pH7.6, 136 mM NaCl and 0.1% Tween20) at room temperature with agitation. Then membranes were incubated in secondary antibody solution for 1 hour at room temperature with agitation. All of secondary antibodies used for immunoblotting in this study were conjugated with horse radish peroxydase. After incubation, membranes were washed three times for 10 minutes each with TBS-T at room temperature with agitation. Detection was performed using enhanced chemiluminescence (ECL, Amersham) reagents. Information of antibodies used in this study is described in Appendix 3. Immunoprecipitation were performed as described by Rosario *et al*.[17]

2.7 Analysis of GTP/GDP association.

MG1.19 ES cells seeded on 100 mm dishes were transfected pPyCAG-IP encoding EGFP or Myc-tagged Ras proteins with Lipofectamine 2000. Twenty four hours after transfection, GTP/GDP association was evaluated as described by Quilliam *et al*.[18], except that the lysis buffer consisted of 20 mM Tris-HCl (pH 7.5), 150 mM NaCl, 1 mM Na_3VO_4, 20 mM $MgCl_2$, 0.5% Triton X100 and protease inhibitor cocktail (Nacalai tesque). Signals were analyzed with an imaging plate scanner (BAS 5000, FUJIFILM). The ratio of GTP-bound form was calculated as GTP/(GTP + 1.5 x GDP).

2.8 Subcellular fractionation.

Cytosol and membrane fractions were prepared as described previously by Cox, A. D. *et al* [19]. Cells were washed once with PBS, collected in 1 ml of PBS and transferred to microcentrifuge tubes. These cell suspensions were centrifuged at 10000 rpm for 30 seconds. Pellets were resuspended in 1225 μl of buffer A (10 mM Tris-HCl, pH7.5, 1 mM $MgCl_2$, and protease inhibitors) and incubated on ice for 10 minutes. These cells were disrupted with a Dounce tissue homogenizer (20 strokes in pestle B; Wheaton) and then added 225 μl of 1 M NaCl. Four-hundreds and fifty microliters of samples were transferred to new microcentrifuge tubes as total lysate (T).

To separate the crude membrane fraction (P100) from the cytosolic fraction (S100), the remaining 1000 µl of homogenized sample was transferred into polycarbonate tube (TLS-55, Beckman) and centrifuged at 38000 rpm (100000 x *g*) for 30 minutes at 4°C in a swinging bucket rotor (TLS-55) in a tabletop ultracentrifuge. All of the supernatant was collected into a new tube (S100) and the pellet was resuspended with 850 µl of buffer A and 150 µl of 1 M NaCl (P100). Fifty microliters of 10 x Hi-SDS RIPA buffer (50% SDS, 10% Nonidet-P 40 and 10% deoxycholate) was added to total lysate and added 110 µl to S100 and P100 samples, for a final concentration of 1 x. And then samples were incubated on ice for 10 minutes. After incubation, these samples were centrifuged at 15000 rpm for 30 minutes, and supernatants were transferred into new microcentrifuge tubes. SDS-PAGE and immunoblotting were performed as described above.

2.9 Immunocytochemistry.

The cells were seeded on coverslips at normal density and incubate overnight. Next day, the coverslips were washed three times for 5 minutes each with PBS. The cells were fixed with PBS containing 4% formaldehyde for 5 minutes at room temperature. After fixation, the coverslips were washed three times for 10 minutes

each with PBS. Then the cells were permeabilized with PBS containing 0.5% TritonX-100 for 10 minutes at room temperature. The coverslips were washed three times for 10 minutes each with PBS. The coverslips were placed in blocking solution (PBS containing 1-5% skim milk or 1% bovine serum albumin) for 30 minutes at room temperature or overnight at 4^{o}C. The coverslips were washed three times with PBS for 15 minutes. The primary antibody diluted as appropriate with blocking buffer to the cells on coverslips and incubated for one hour at room temperature or overnight at 4^{o}C. Anti-ERas antiserum was diluted 1:500 in PBS containing 5% skim milk. Pre-immune rabbit serum was used as negative control at the same time. Anti-GM130 antibody was diluted 1:100 in PBS containing 1% bovine serum albumin. After primary antibody reaction, the coverslips were washed three times for 15 minutes each with PBS. The coverslips were incubated with fluorescently labeled secondary antibody diluted as appropriate with blocking buffer for one hour at room temperature in the dark. Cyanine 3-labbeled anti-rabbit IgG (Chemicon) and cyanine 3-labbeled anti-mouse IgG (Chemicon) were diluted 1:100 in blocking solution. After incubation, the coverslips were washed three times for 15 minutes each with PBS in the dark. Then the coverslips were mounted on slides with PBS containing 50% glycerol, sealed with nail vanish and then observed with a confocal microscope (LSM510, Carl Zeiss).

2.10 Colony formation in soft agar.

MilliQ water containing 1% agar was autoclaved and then incubated in 42^{o}C water bath. When the 1% agar solution cooled down, equal amount of 20% calf serum-containing medium pre-warmed to 42^{o}C was mixed. The agar-containing medium was applied to 60 mm tissue culture dishes (3 ml per dish). The mixture (DMEM containing 0.5% agar and 10% calf serum) in the dishes was solidified on bench for 15 minutes. The remaining mixture was kept in 42^{o}C water bath to avoid solidification. NIH3T3 cells were harvested by trypsinization, suspended with the medium and the cell number was counted by using a Coulter counter. The cell suspension was suspended with the medium at 7500 cells per milliliter. The cell suspension were mixed with DMEM containing 0.5% agar and 10% calf serum at 1 : 2 ratio and seed on the prepared 0.5% agar dishes (3 ml per dish). The dishes were incubated for 2 or 3 weeks in 37^{o}C CO_2 incubator and colony number was counted under microscope.

2.11 X-gal staining.

The cells were washed once with PBS, fixed with PBS containing 1 % glutaraaldehyde (Nacalai tesque) for 5 minutes at room temperature. After fixation, the cells were washed once with PBS, permeabilized with PBS containing 1 % Triton

X-100 and PBS, and replaced with PBS for 5 minutes each at room temperature. Then the cells were incubated in PBS containing 1 mM $MgCl_2$ (Nacalai tesque), 3 mM $K_3Fe(CN)_6$ (Nacalai tesque), 3 mM $K_4Fe(CN)_6$ (Nacalai tesque) and 1 mg/ml X-gal (Nacalai tesque) at 37^{o}C.

2.12 Luciferase assay.

One microgram of each reporter constructs were transfected into ES cells or NIH3T3 cells seeded on 24-well culture plates along with 0.025 μg of pRL-TK (Promega) by using Lipofectamine 2000. Twenty-four hours after transfection, cells were lysed and measured the luciferase activities by using Dual-reporter assay system (Promega) as a manufacturer's protocol.

2.13 PCR genotyping.

Genotypes of ERas were determined by PCR with the primers ERas-U527, ERas-L826 and bgeo-screening1. PCR with these primers produces a 340-base pairs (bps) fragment from the wild-type locus and a 600-bps fragment from the targeted locus. Embryos were incubated in 5 μl of the lysis buffer (10 mM Tris-HCl, pH7.5, 50 mM KCl, 2.5 mM $MgCl_2$, 0.45% NP-40, 0.45% Tween-20 and 200 μg/ml of protease K) at

55°C overnight and then boiled at 100°C for 5 minutes. The genomic DNA derived from ES cells was purified using PUREGENE (Gentra systems). The PCR program consisted of an initial denaturation at 94°C for 10 seconds, 36 cycles of 94°C for 5 seconds, 55°C for 5 seconds, and 72°C for 1 minute and a final extension at 72°C for 5 minutes. PCR products were resolved by TAE based gel containing 2% agarose electrophoresis.

2.14 Reverse transcription.

Total RNA derived from cultured cells was collected with Trizol reagent (Invitrogen). Samples were purified by phenol-chloroform isoamylalcohol purification and ethanol precipitation. Purified RNA was dissolved in DEPC-treated water, and then treated with DNase I (Ambion). One microgram of RNA was used for reverse transcript (RT) reaction. RT reaction was performed by using Reva Tra Ace (Toyobo) and oligo-dT primer.

2.15 Mice

All of mice used in this study were maintained in specific pathogen free area. To generate mice carrying *ERas* heterozygous or null mutation, *ERas* $^{\beta\text{-geo/Y}}$ RF8 ES cells

were injected into blastocysts (derived from C57BL6) and then embryos were transferred to the uterus of pseudo pregnant female mice (ICR) at 3.5 dpc. High percentage chimeric mice (judged by coat color) were mated with C57BL6 female mice. The genotypes of littermate were confirmed by southern blotting or PCR.

2. 16 Chromatin immunoprecipitation assay

Formaldehyde was added directly to the culture medium to a final concentration of 1 % (v/v) and the dishes were gently shaken on a shaker at room temperature for 8 minutes. Glycine was added to 125 mM, and the dishes were returned to the shaker for an additional 5 minutes. Dishes were washed three times with ice-cold PBS and harvested by scraping into 3 ml of cold PBS. Cells from dishes were collected by centrifugation at 2000 rpm for 5 minutes at 4^{o}C, and the supernatants were discarded. Cell pellets were resuspended in 10 ml of cold PBS plus 200μM phenylmethyl-sulfonylfluoride (PMSF). Cells were collected by centrifugation as above and resuspended in 5 ml of an ice cold solution containing 5 mM HEPES, pH 8.0, 85 mM KCl, 0.5% (v/v) Nonidet P-40 plus protease inhibitors (200 μM PMSF, 1.4 μg/ml pepstatin and 1 μg/ml leupeptin). Samples were allowed to swell on ice for 10 minutes before homogenization with three strokes of a glass Dounce homogenizer to release

nuclei. Nuclei were collected by centrifugation as above, and the supernatants were discarded. Nuclei were resuspended in 50 mM Tris-HCl, pH 7.6, 10 mM EDTA, 1% SDS plus protease inhibitors as above (50 µl/100 mm dish of cells). Samples were incubated on ice for 10 minutes, and immunoprecipitation dilution buffer A (0.01% SDS, 1.1% (v/v) Triton X-100, 1.2 mM EDTA, 16.7 mM Tris-HCl, pH 7.6, 167 mM NaCl) was added to bring the volume to 750 µl. Samples were sonicated 30 seconds ON and 1 minute OFF using a Bioruptor (Cosmo bio). Routinely, ten repetitions of the sonication were performed. Chromatin samples (500 µl) were first precleared with normal mouse IgG (5 µl) in the presence of protein G-Sepharose (Amersham) beads slurry (60 µl of a 50/50 slurry of beads in TBS, 1 mg/ml bovine serum albumin and 200 µg/ml salmon sperm DNA). Samples were incubated for 2 hours at 4°C on a rotator, and beads were collected by centrifugation in a microcentrifuge at 2000 rpm. The unbound material (chromatin) was transferred to a new tube and 5 µg of each antibody were added. Samples were incubated overnight at 4°C on a rotator, 60 µl of blocked protein G slurry were added, and incubation was continued on the rotator for an additional 2 hours at 4°C. Beads were collected by centrifugation in a microcentrifuge at 12000 rpm for 1 minute. Beads were first washed twice with 500 µl of ice-cold buffer B (0.05% (w/v) SDS, 1% (v/v), Triton X-100, 20 mM Tris-HCl, pH 7.6, 2 mM

EDTA, 150 mM NaCl), washed once sequentially with buffer D (0.05% (w/v) SDS, 1% (v/v) Triton X-100, 20mM Tris-HCl, pH 7.6, 2 mM EDTA, 500 mM NaCl), buffer 3 (0.25 M LiCl, 1.0% (v/v) Nonidet P-40, 1.0% deoxycholate, 10 mM Tris-HCl, pH 7.6, 1 mM EDTA), and buffer C (0.1% (v/v) Triton X-100, 150 mM NaCl, 20 mM Tris-HCl, pH 7.6, 2 mM EDTA). Beads were transferred to a microcentrifuge tube, and bound material was eluted by incubating the beads with 75 µl of elution buffer (0.1 mM sodium bicarbonate, 1.0% (w/v) SDS) while vortexing for 10 minutes. This was repeated a total of four times. The four eluates were pooled, and NaCl and RNase were added to 300 mM and 10 µg, respectively, and samples were heated at 65^{o}C for 6 hours to reverse the Schiff's base linkage. DNA was collected by ethanol precipitation and diluted a total of 20 µl.

3. Results

3.1 Identification of ERas.

To understand mechanisms underlying the pluripotency of ES cells and their propensity to form tumors *in vivo*, we searched for genes that were expressed specifically in murine ES cells by digital differential display. We found a number of genes that overrepresented in ES-cell derived libraries [8, 13, 20]. We designated these genes ECAT for ES cell associated transcript. We obtained full-length cDNAs of ECATs by the rapid amplification of cDNA ends. Basic local alignment search tool analysis against mouse genomic databases revealed that ECAT5 (Unigene cluster Mm.249524) encodes a protein of 227 amino acids with 43, 46, and 47% identity to HRas, KRas, and NRas, respectively. This protein highly conserves five domains essential for small G-proteins [9] and a CAAX motif [21, 22] (Fig. 1A). These findings indicated that the protein, which I designated ERas, is a novel member of the Ras protein family. By searching mouse genomic databases, I found that the mouse ERas gene consist of two exons and is located on X chromosome. By searching human genomic databases, I found that *ERas* was most similar to human *HRasp (Ha-Ras2)*, which was also located on the X-chromosome and had long been recognized as a processed pseudogene with multiple nonsense and deletion mutations [23]. I

re-determined the nucleotide sequence of *HRasp* and found that the previously reported mutations did not exist. *HRasp* has a single open reading frame encoding a polypeptide 76% identical to mouse ERas (Fig. 1A). Because of the sequence similarity and the common chromosomal localization, I concluded that *HRasp* is the human ortholog of *ERas*.

Northern blot analyses detected a single 1.2-kb *ERas* transcript in undifferentiated RF8 mouse ES cells (Fig. 1B). ERas was also expressed in three other undifferentiated mouse ES cell lines: J1 [24], CGR8 [25], and MG1.19 (Fig. 1C). In contrast, *ERas* was not detected in differentiated ES cells or in 12 somatic tissues from adult mouse (Fig. 1B). Therefore the specific expression of ERas is a common property of ES cells.

3.2 Transforming activity of ERas.

To study whether ERas has the ability to transform cells, I utilized efficient retroviral gene transfer system to generate polyclonal NIH 3T3 cell population expressing ERas or HRasV12 (Fig. 2). Both mouse and human ERas induced morphological changes indicative of transformation, namely high refractivity and spindle-like shape (Fig. 3A), and loss of contact inhibition (Fig. 3B). When I cultured 5000 NIH 3T3 cells expressing mouse ERas, human ERas or HRasV12 in soft agar, I

obtained similar numbers (992 ± 160, 934 ± 49, and 989 ± 86) of colonies showing anchorage-independent growth (Fig. 3C). In contrast, from control cells transfected with the parent vector or ERas inactivated by deletion of the carboxy-terminal region (ERas−ΔC), I obtained a few (7 ± 2 and 15 ± 3) colonies that were much smaller than those from wild-type ERas and HRasV12. When transplanted into nude mice, cells expressing ERas effectively produced tumors (Fig. 3D). ERas was more potent than HRasV12 in promoting cell growth in culture (Fig. 3B, 3C), but produced smaller tumors (Fig. 3D). Their difference was more evident in primary mouse embryonic fibroblast (PMEF): HRasV12 caused premature senescence [26] (Fig. 3E). In contrast, ERas significant increased growth rate. These results demonstrated that ERas induced transformation as effectively as HRasV12, but with different mode of action.

3.3 Posttranslational modification of ERas.

3.3.1 GTP association of ERas.

All small G-proteins have consensus sequences responsible for specific interaction with GDP and GTP and for GTPase activity [27]. Point mutations of several amino acids of HRas, including Gly12, Ala59, or Glu63, render the protein constitutively active [28]. I found that mouse ERas had Ser, Ser, and Ile (and human ERas had Ser, Ala, and Asp)

at the positions corresponding to Gly12, Ala59, and Glu63 of HRas (Fig. 1A), suggesting that both were constitutively active. To explore this possibility, I analyzed the GTP/GDP-association (Fig. 4A) by immunoprecipitation and thin-layer chromatography. As expected, ~95% of mouse and human ERas was in a GTP-bound form. In contrast, ~90% of wild-type HRas existed in a GDP-bound form, whereas ~80% of HRasV12 (a constitutively active mutant in which Gly12 is mutated to Val) was in a GTP-bound form. These data demonstrate that ERas is indeed constitutively active.

3.3.2 Intracellular localization of ERas.

All of Ras proteins have carboxy-terminal consensus motif known as the CAAX motif (C is cysteine, A is aliphatic amino acid and X is any amino acid) [27]. Post-translational modification of this motif is required to associate with cytoplasmic membranes and activation of these proteins. Recent studies have shown that the carboxy-terminal regions, which are unique for each Ras protein and are therefore called hypervaliable region (HVR), contribute to different functions among Ras proteins [29]. I found that endogenous ERas was located at plasma membrane by immunostaining with anti-ERas antiserum (Fig. 4B). However, the carboxyl terminus

of ERas contains an atypical CAAX motif, CSVA (cysteine, serine, valine and alanine) [13]. Thus, I decided to study the post-translational modification of ERas.

The carboxy-terminal sequence is required for activation of ERas.

To study whether the CAAX motif was necessary for the activation of ERas, I constructed ERas-ΔC, in which the CAAX motif and HVR region were deleted, and introduced it into NIH3T3 cells using retroviral infection. The cells expressing ERas-ΔC were normal in morphology (Fig. 5A), did not form colonies in soft agar (Fig. 5C) and did not produce tumors when transplated into nude mice (Fig.5D). In addition, ERas-ΔC could not promote cell growth (Fig. 5B). These data indicate that ERas-ΔC has no transforming activity and the carboxy-terminal region is essential for biological activities of ERas.

ERas is isoprenylated by farnesyl transferase.

The first step of the post-translational modification is isoprenylation of the cysteine residue of the CAAX motif by either farnesyl transferase [30] or geranylgeranyl transferase [31, 32, 33].

To study whether ERas is farnesylated or geranylgeranylated, I generated MEFs

stably expressing EGFP, EGFP-tagged ERas (EGFP-ERas), EGFP-ERas-ΔC, EGFP-HRasV12, EGFP-KRas4BV12 or EGFP-Rap1A. I treated these cells with the 2 μM of farnesyl transferase inhibitor (FTI-277) or 5 μM of geranylgeranyl transferase inhibitor (GGTI-298) for 24 hours. These cells were fixed and observed with a confocal microscope. When treated with DMSO (vehicle), EGFP-ERas, EGFP-HRasV12 and EGFP-KRas4BV12 were located at plasma membrane (Fig. 6). EGFP-ERas-ΔC was diffused in cytoplasm (Fig. 6). When treated with FTI-277, the majority of EGFP-ERas and EGFP-HRasV12 were diffused in cytoplasm, whereas most of EGFP-KRas4BV12 remained at the cytoplasmic membrane (Fig. 6). When treated with GGTI-298, EGFP-ERas, EGFP-HRasV12 and EGFP-KRas4BV12 remained at plasma membranes (Fig. 6).

In these experiments, I used EGFP-Rap1A as a positive control for geranyl-geranylation. EGFP-Rap1A was translocated to cytoplasm by treating with GGTI-298, but not with FTI-277 (Fig. 6). These data demonstrated that farnesylation is required for membrane targeting of ERas.

To confirm that the CAAX motif is required for membrane targeting of ERas, I constructed ERas-SSVA, in which cysteine in the CAAX motif was mutated to serine, and HRasV12-SVLS. In MEFs, both EGFP-ERas SSVA and EGFP-HRasV12-SVLS

were not located at plasma membrane or endomembrane and showed diffused localization in cytoplasm (Fig. 7).

I also made mutants of ERas, HRasV12 and KRas4BV12, in which the CAAX motif was deleted but the HVR was maintained. These CAAX deletion mutants were located at cytoplasm (Fig. 7). These data demonstrated that the CAAX motif is required for membrane targeting of ERas and HRas.

Rce1 is required for localization ERas at plasma membranes.

After isoprenylation of Ras proteins, the AAX tripeptide of CAAX sequence is removed by an endoprotease RCE1 (Ras-converting enzyme 1) [34, 35, 36]. To examine whether ERas was modified by RCE1, *Rce1* KO MEFs were used [37]. Plasma membrane localization of EGFP-ERas, EGFP-HRasV12 and EGFP-KRas4BV12 was partially blocked (Fig. 8). Previous study showed that another Ras-related protein, Ras-homolog enriched in brain (Rheb) was farnesylated and located at plasma membrane [38]. However, I found that EGFP-fused Rheb was located at endomembrane in wild-type MEFs (Fig. 8). In *Rce1*-deficient cells, most of EGFP-Rheb proteins were located in cytoplasm (Fig. 8). These data suggest that RCE1 is required for trafficking to plasma membrane of ERas and to endomembrane of Rheb.

Icmt is also required for localization ERas at plasma membrane.

The third modification required for plasma membrane targeting of HRas is the methylation of isoprenylated-cysteine by ICMT (Isoprenylcysteine carboxy methyltransferase) [39, 40]. To study whether ERas is modified by Icmt, similar experiments using *Icmt* KO MEFs were performed [41] (Fig. 8). In *Icmt*-deficient cells, plasma membrane localization of EGFP-HRasV12 and EGFP-ERas was partially inhibited (Fig. 8). These data suggest that ICMT is required for the localization of ERas at plasma membrane.

To quantify the inhibition of membrane localization by *Rce1*- or *Icmt*- knockout, I performed subcellular fractionations and immunoblotting (Fig. 9). In wild-type cells, most of EGFP-ERas, EGFP-HRasV12 and EGFP-KRas4BV12 were detected in the pellet (P100 insoulble fraction). EGFP and EGFP-ERas-ΔC proteins were detected in soluble (S100) fraction. In *Rce1*- or in *Icmt*-deficient cells, in contrast, approximately 50 % of EGFP-ERas, EGFP-HRasV12 and EGFP-KRas4BV12 were detected in both P100 and S100 fractions.

ERas is located at golgi apparatus in Rce1- or Icmt-deficient cells.

I found that a significant portion of EGFP-ERas was condensed around the nucleus in *Rce1*- or *Icmt*-deficient cells. This pattern was indicative of golgi localization. To test this possibility, I stained these cells with anti-Golgi matrix protein of 130 kDa (GM130) antibody [42]. The observation with a confocal microscope showed that the condensed EGFP-ERas protein around the nucleus was co-localized with GM130 in cells deficient in RCE1 or ICMT (Fig. 10). A smaller portion of EGFP-HRasV12 was merged with GM130 in *Rce1*- or *Icmt*-deficient cells (Fig. 10).

Two cysteine residues in HVR of ERas are palmitoylated.

Both ERas and HRas have two cysteine residues in HVR. Previous studies have shown that HRas was palmitoylated at these cysteine residues by Ras palmitoyltransferase (RPT) [43, 44]. I hypothesized that ERas could be palmitoylated and this modification was required for plasma membrane targeting of ERas. To confirm this hypothesis, I constructed ERas-C220S/C222S, in which the two cysteine residues were mutated to serine residues. I also constructed HRasV12-C181S/C184S, in which the two palmitoylation sites were altered. These mutants were introduced into wild-type, *Rce1*- or *Icmt*-deficient MEFs. EGFP-HRasV12-C181S/C184S was located at endomembrane in wild-type MEFs whereas in cytoplasm in *Rce-1* or *Icmt*-deficient

cells (Fig. 11). In contrast, EGFP-ERas-C220S/C222S protein did not localize at endomembrane even in wild-type MEFs (Fig. 11). These data suggested that the palmitoylation of cysteine residues of ERas were required for plasma- and endomembrane.

To clarify whether difference between EGFP-ERas-C220S/C222S and EGFP-HRasV12-C181S/C184S is attributable to the differential CAAX sequences, I exchange the CSVA sequence of ERas with the CVLS sequence of HRasV12. EGFP-ERas-CVLS and EGFP-HRasV12-CSVA proteins located at plasma membrane and golgi apparatus in wild-type MEFs (Fig. 11). I found that EGFP-ERas-C220S/C222S-CVLS diffused into cytoplasm whereas EGFP-HRasV12 -C181S/C184S-CSVA is located at endomembrane (Fig. 11). This result indicated that the different localization of ERas and HRasV12 is not attributable to the differential CAAX sequences.

I next studied whether the different localization is attributable to HVR. To clarify this end, I exchanged the HVRs between EGFP-ERas-C220S/C222S and EGFP-HRasV12-C181S/C184S. I found that the chimeric protein containing the HVR of HRas was located at emdomembranes whereas the other proteins containing of the HVR of ERas diffused in cytoplasm (Fig. 12).

To further analyze the role of palmitoylation, I treated wild-type MEFs expressing EGFP-ERas or EGFP-HRasV12 with 25 μg/ml of 2-bromopalmitate (BP), which inhibited palmitoylation[44, 45]. I found that both EGFP-ERas and EGFP-HRasV12 were located at endomenbrane in control cells treated with 2-BP (Fig. 13). In *Rce1*- or *Icmt*-deficient cells treated with 2-BP, most of EGFP-ERas and EGFP-HRasV12 were located at cytoplasm. In contrast, most of EGFP-KRas4BV12 proteins remained at plasma membrane even in the presence of 2-BP (Fig. 13). These results confirm the important role of palmitoylation in plasma membrane localization of ERas and HRas.

Intracellular localization of ERas and its biological activity.

To clarify that relationship between intracellular localization and biological activities, I constructed plasma membrane-, endomembrane- or cytoplasma- localized mutants of ERas, Rheb and HRasV12 were constructed. Wild-type ERas, Rheb-HRas (N-terminal region of Rheb fused with HVR of HRas in frame) and wild-type HRasV12 were located at plasma membrane (Fig. 14A). Because of palmitoylation defects, EH-C220S/C222S, wild-type Rheb and HRasV12-C181S/C184S were located at endomembrane. ERas-SSVA, Rheb-SSVM and HRasV12-SVLS were located in cytoplasm because these mutants could not be farnesylated (Fig. 14A). When

introduced into MG1.19 ES cells, wild-type ERas (ERas, P) promoted proliferation of MG1.19 ES cells (Fig. 14B) [13]. EH-C220S/C222S (ERas, E) partially supported ES cell growth, compared with mock- or EGFP- transfected cells, whereas ERas-SSVA (ERas, C) could not promote proliferation.

HRasV12 (HRasV12, P) caused growth retardation of ES cells (Fig. 14B) [13]. HRasV12-C181S/C184S or HRasV12-SVLS were much weaker in this effect than wild-type HRasV12. These data suggest that plasma membrane localization of ERas and HRas is important for their activities.

I next examined the GTP-binding statuses of ERas, Rheb, HRasV12 and their mutants. Immunoprecipitation and separation on thin-layer chromatography (Fig. 15) showed that 86%, 45% and 73% of ERas, Rheb and HRasV12 existed in GTP-bound form, respectively. All of their mutants showed similar ratio to wild-types (Fig. 15). This data suggests that membrane localization have no effect on GTP/GDP association of ERas, Rheb and HRasV12.

I also studied the activation statuses of the downstream targets by immonoblotting with anti-phosphorylated Ser473 AKT or phosphorylated Thr389 p70S6K. ERas and EH-C220S/C222S activated AKT by 10- and 5-folds. ERas and EH-C220/C222S doubled phosphorylation status of p70S6K (Fig. 16A, B). In contrast, ERas-SSVA

could activate neither AKT nor p70S6K (Fig. 16A, B). I obtained similar results with HRasV12 and its mutants. Noteworthy, Rheb-HRas (Rheb, P), wild-type Rheb (Rheb, E) or Rheb-SSVM (Rheb, C) all were able to activate p70S6K (Fig. 16A, B). These data suggest that biological activities of ERas and HRasV12 depend on membrane localization and the CAAX modification. In great contrast, Rheb can activate downstream targets regardless of localization.

3.4 Role of ERas in ES cells.

To study the functions of ERas in ES cells, either the sense or antisense cDNA of ERas were introduced into MG1.19 ES cells (Fig. 17A). After selection with puromycin, these cells were replated at 1 x 10^4 cells per well and counted after 6 days. When the sense cDNA was transfected, the ERas expression increased approximately four fold (Fig 17B) and cell growth was significantly enhanced (Fig. 17C). ERas-ΔC did not show such growth-promoting effect. In contrast, introduction of HRasV12 resulted in differentiation and growth retardation (Fig. 17C) as has been reported [13, 46, 47]. When the antisense cDNA was introduced, the ERas expression decreased to one fifth of the normal level (Fig. 17B) and cell growth was significantly repressed (Fig. 17C). These data suggest that ERas, unlike HRasV12, promotes ES cell growth.

To further clarify the *in vivo* functions, I disrupted the *ERas* gene by homologous recombination in another ES cell line, RF8. I obtained two clones in which the coding region was replaced with a fusion comprising the β-galactosidase and neomycin resistance gene (*β-geo*) (Fig. 18A). As expected from its location on the X-chromosome, southern blotting showed that the wild-type *ERas* allele was absent in both clones (Fig. 18B). Northern blot (Fig. 18C), immunoblot (Fig. 19B) and immunohistochemistry (Fig. 4B) analyses confirmed the absence of *ERas* expression. In addition, I established two clones, one from each knockout clone, in which *ERas* expression was partially recovered by introduction of cDNA (Fig. 19A, B).

ERas-null ES cells were normal in morphology and *Oct3*/4 expression (Fig. 18C). Blastocyst injection of these cells resulted in high percentage chimeric mice and germ line transmission. Mutant mice did not show gross abnormalities or infertility. These results indicate that ERas is not required for pluripotency and normal mouse development.

However, *ERas*-null cells grew significantly slower than wild-type cells (Fig. 19C). The slow growth phenotype was more evident when ES cells were grown without feeder cells. Wild-type ES cells expanded 6×10^5 times under these sub-optimal conditions over 16 days, whereas the *ERas*-null cells expanded only 1×10^3 times.

When transplanted into nude mice, *ERas*-deficient cells produced markedly smaller tumors than wild-type cells (Fig. 19D). Re-expression of *ERas* led to a partial recovery of growth and tumorigenicity (Fig. 19C, D). These results demonstrate the important role of ERas in tumor-like growth property of ES cells.

I hypothesized that the functional differences between ERas and HRasV12 is attributable to different effector preferences. To test this hypothesis, I studied whether ERas could activate Raf [48, 49]. Co-immunoprecipitation experiments showed that HRasV12, but not ERas, associates with Raf1, BRaf and RalGDS (Fig. 20). In reporter assays, AP1 enhancer activity was activated by HRasV12 and repressed by the dominant negative mutant HRasN17 (Fig. 21A). In contrast, ERas did not affect AP1 activity. These data indicate that ERas is not capable of binding to Raf or activating the MAP kinase cascade.

I next examined whether ERas bound to PI3 kinase, since it is another effector of Ras [50] and plays an important role in transformation [51] and ES cell propagation [52, 53]. Co-immunoprecipitation experiments showed that ERas, as well as HRasV12, associated with PI3 kinase p110δ (Fig. 20). Phosphorylation of AKT was decreased in *ERas*-null cells (Fig. 21B). Transgenic re-expression of *ERas* (KO + cDNA) partially recovered this reduction (Fig. 21B). These data demonstrate that ERas constitutively

binds and activates PI3 kinase.

I next examined whether impaired growth and tumorigenicity in *ERas*-null ES cells could be rescued by forced expression of active PI3 kinase [54] (Fig. 22A). In both clones, the phosphorylation level of AKT became higher than the normal level (Fig. 22B). Impaired growth reverted to a normal level (Fig. 22C). Teratoma formation was also rescued and even accelerated than wild-type ES cells (Fig. 22D). These results demonstrated that the PI3 kinase cascade plays an important role in growth-promoting activity of ERas.

3.5 The downstream targets of ERas.

In *ERas*-deficient ES cells, phosphorylation status of AKT was decreased compared to wild-type ES cells. Northern blotting analyses showed that *Akt1*, *Pten* (phosphatase and tensin homolog deleted on chromosome ten, which is a phosphatase of PIP_3) [55], *Tsc1* and *Tsc2* (GTPase activating protein complex of Rheb) [56, 57] were expressed in undifferentiated ES cells (Fig. 23). To study whether PI3 kinase and AKT were important for ES cell proliferation, I constructed a dominant negative form of p110 (p110dnCAAX, which lacked the kinase domain and was fused with HVR of HRas) [58] and of AKT (K179M, in which lysine179 was mutated to methionine).

I introduced EGFP, p110dnCAAX, AKT K179M, PTEN or TSC1 + TSC2 into MG1.19 ES cells and selected with 2 μg/ml of puromycin. I observed massive cell death in the cells expressing p110dnCAAX, PTEN or TSC1 + TSC2 during puromycin selection.

With a lower dose (1 μg/ml) of puromycin selection, the cells expressing p110dnCAAX, PTEN or TSC1 + TSC2 died more rapidly than those expressing EGFP or AKT K179M, but some cells were still alive. These cells were replated at 5 x 10^4 cells per 35 mm dish and cultured for 7 days. Mock-transfected or EGFP-transfected cells formed over 100 undifferentiated colonies (Fig. 24A, B). Cells expressing AKT-K179M formed approximately 40 undifferentiated colonies (Fig. 24A, B). In contrast, cells expressing p110dnCAAX, PTEN or TSC1 + TSC2 produced no stem cell colonies. These cells produced a small number of differentiated colonies (Fig. 24A, B). These data suggest that PI3 kinase activity is important not only for proliferation but also for ES cell self-renewal.

Next, I applied LY294002 (PI3 kinase specific inhibitor) to MG1.19 ES cells at a clonal density (500 cells per 35 mm dish) or at a higher density (subconfluent). With 25 μM (high concentration) of LY294002, most of cells died at the clonal density (Fig. 25). At the higher density, cell showed massive differentiation. With 10 μM (low

concentration) of LY294002, mixed or completely differentiated colonies were produced at the clonal density (Fig. 25). In contrast, MG1.19 ES cells could form stem cell colonies with 20 nM of rapamycin (TOR inhibitor) whereas these colonies were much smaller than cells treated with DMSO (control) or with 25 μM of PD98059 (MEK inhibitor). These data suggest that inhibition of PI3 kinase activity induced ES cell differentiation.

RT-PCR analyses showed that the LY294002 treatment resulted in decrease of the undifferentiated ES cell markers (*Oct3/4* and *Nanog*), increase in endoderm markers (*Gata6* and *Hnf1b*) and parietal endoderm markers (*Lamb* and *Tm*). However, no significant changes were induced in visceral endoderm markers (*Afp* and *Ttr*), other lineage markers (*Cdx2* and *T*) or *Nat1* [8, 59, 60]. Suppression of PI3 kinase may activate the MAP kinase pathway and therefore induce ES cell differentiation. To test this, I performed AP1 reporter assay. However, AP1 activity was not up-regulated by 25 μM of LY294002, whereas it was inhibited by 25 μM of PD98059 (Fig. 26). The second possibility is that inhibition of PI3 kinase suppresses the STAT3 pathway. To test this, I performed CIS1 reporter assay. However, the CIS1 reporter was not inhibited by LY294002 (Fig. 26).

To monitor the short term responses, I treated MG1.19 ES cells with DMSO or 25

μM of LY294002 for 16 hours. Northern blotting showed that *Nanog*, *Oct3/4* or *Esg1* (Embryonal-cell specific gene 1) [61, 62] were decreased by LY294002 (Fig. 27B). These data further support the notion that PI3 kinase inhibition with LY294002 induces ES cell differentiation.

To clarify the reason of ES cell differentiation by inhibition of PI3 kinase, I generated and used Flag-tagged Nanog transgenic (Tg) ES cells. Because this transgene was driven by CAG promoter, these cells could self-renew without LIF. Mock control and FT-Nanog Tg cells were treated with DMSO, 10 μM of LY294002, 20 nM of Rapamycin and 300 nM of retinoic acid for 6 days. MG1.19 ES cells carrying Mock could maintain undifferentiated state and proliferate in the medium supplemented with DMSO or Rapamycin (Fig. 28A). On the other hand, these cells showed morphological changes by LY294002- or retinoic acid-treatment (Fig. 28A). In contrast, Flag-Nanog Tg cells were no morphological changes after treating with LY294002 (Fig. 28A). Retinoic acid-treatment made these cells to fibroblast-like shapes (Fig. 28A).

RT-PCR showed that *Nanog*, *Oct3/4* and *Sox2* transcripts were decreased by LY294002- or retinoic acid-treatment in Mock control cells (Fig. 28B). In Flag-Nanog Tg cells, *Sox2* mRNA was partially reduced by LY294002-treatment whereas expression

level of *Oct3/4* or *ERas* were normally (Fig. 28B). These results suggested that forced-expression of Nanog prevented differentiation of ES cells by treating with LY294002.

For the next, I applied to detect the endogenous Nanog expression by using the primers designed in 3' untranslated region of *Nanog* gene. As results, endogenous *Nanog* expression was significantly decreased by LY294002-treatment (Fig. 28B). These data suggested that LY294002-induced ES cell differentiation included the downregulation of *Nanog* expression.

To clarify the mechanism of Nanog reduction by inhibition of PI3 kinase, I performed luciferase reporter assays with *Nanog* promoter. The 0.1-kbp fragment of upstream region of *Nanog* gene (Nanog-0.1K), the 0.7-kbp fragment (Nanog-0.7K) which included proximal-enhancer (PE), the 3.0-kbp fragment (Nanog-3K) or the 5.0-kbp (Nanog-5K) fragment which contained both PE and distal-enhancer (DE) were amplified by PCR and cloned into promoter-less luciferase vector (Fig. 29, upper panel). These plasmids were transiently introduced into Flag-Nanog Tg cells. Transfectants were cultured in the medium supplemented DMSO, 25 μM of PD98059, 10 μM of LY294002, 20 nM of Rapamycin, 300 nM of retinoic acid or 2 μM of BIO for 24 hours. As results, treatment with LY294002 induced reduction of luciferase activity driven by

Nanog-5K fragment whereas Nanog-0.1K, -0.7K and -3K kept normal levels (Fig. 29). These results suggested that LY294002 inhibited the activity of DE for *Nanog* gene.

Next, the 0.4 kbp fragment which included DE of *Nanog* gene was inserted into the luciferase vector containing SV40 minimal promoter (Fig. 30, upper panel). Reporter assay showed that the enhancer activity of this fragment was also decreased by LY294002-treatment (Fig. 30). These data further suggested that PI3 kinase inhibition with LY294002 induced the reduction of *Nanog* DE activity in ES cells.

M. Maruyama *et al.* showed that SOX2 protein bound to the distal enhancer of *Nanog* gene both *in vivo* and *in vitro*. They also demonstrated that this interaction was crucial for the expression of *Nanog*. I hypothesized that PI3 kinase inhibition prevented the accession of SOX2 to the *Nanog* DE. To confirm this hypothesis, MG1.19 ES cells carrying Mock or Flag-Nanog were treated with DMSO or 10 μM of LY294002 for 6 days. After treatment, these cells were lysed and used for chromatin immunoprecipitation assay with anti-SOX2 antibody. Immunoprecipitants were used for PCR with the PE or DE of *Nanog* gene or *Fgf4* enhancer specific primers. As results, in DMSO-treated cells, anti-SOX2 antibody precipitated fragments located DE or PE of *Nanog* gene or *Fgf4* enhancer (Fig. 31). In contrast, these co-precipitated DNA were significantly decreased by LY294002-treatment (Fig. 31). These results

suggested that PI3 kinase inhibition prevented the interaction of SOX2 protein with DNA.

3.6 Transcriptional control of the mouse ERas gene.

ERas expresses in undifferentiated ES cells but not in blastocysts.

I performed X-gal staining of *ERas* $^{\beta\text{-geo/Y}}$ ES cells, in which the coding region of *ERas* was replaced with the *β-geo* gene. As a control, I used *Nanog* $^{\beta\text{-geo/+}}$ ES cells did (Fig. 32A) [8]. I observed specific staining in both cell lines. In contrast, *ERas* KO blastocysts were not stained with X-gal, whereas *Fbx15* KO blastocysts were strongly stained (Fig. 32B) [20]. These results indicate that ERas is expressed in undifferentiated ES cells, but not in inner cell mass, which is the origin of ES cells.

ERas expression is not regulated by the LIF/STAT3 pathway.

I found that in Nanog-overexpressing ES cells, the STAT3 pathway can be completely blocked by introducing hLIF05 (a LIF antagonist) or SOCS3 without inducing differentiation (Tokuzawa *et al*, unpublished). In these cells, phosphorylation statuses of STAT3 could not be detected (Fig. 33). In contrast, ERas and Oct3/4 were not decreased in these cells (Fig. 33). These data indicated that the expression of ERas

was independent of the LIF/STAT3 pathway.

Transcriptional enhancer of ERas gene was located in the intron.

To identify the transcriptional enhancer of ERas gene, I performed luciferase reporter assays. I subcloned two fragments to the upstream of the luciferase gene in pGV-BM2 [8, 20]. The first fragment started at ~ 4 kb upstream from the transcription initiation site and ended at exon 1 (ERas pro4K). The other 8-kb fragment started at the same position and ended at exon2 (ERas pro8K). The 8-kb fragment activated the reporter in undifferentiated ES cells, but not in differentiated ES cells or NIH3T3 cells (Fig. 34, 35). In contrast, the 4 kb-fragment did not activate the reporter in ES cells or in NIH3T3 cells (Fig. 34, 35). These data suggested that transcription of *ERas* gene required the intron sequence.

I constructed reporter genes with smaller fragments to narrow down the enhancer. I shortened the 5' flanking region to 300 bases or 50 bases. I found that even these shorter fragments promoted the expression of luciferase in undifferentiated ES cells, but not in NIH3T3 cells (Fig. 34, 35). However, when I deleted the 5' end of the exon 1, the enhancer activity was lost. These data indicate that the promoter of *ERas* gene existed within the 50 bases upstream of the exon 1, but the enhancer is likely to exist in

the intron.

To narrow down the ERas enhancer, I constructed a series of reporter genes containing various types of deletion in the introns. These plasmids were transfected into undifferentiated ES cells or NIH3T3 cells. All of these constructs promoted relative luciferase activities in undifferentiated ES cells, but not in NIH3T3 cells (Fig. 34, 35). These data suggest that transcriptional enhancer of *ERas* gene is involved in either the 5' end (130 bases) or 3' end (170 bases) of the intron.

To determine the sequence of enhancer, I performed further deletion of the 5' and 3' portion. I constructed four deletion mutants, A1 (5' ; 5 bp and 3' ; 73 bp), A2 (5' ; 5 bp and 3' ; 94 bp), B1 (5' ; 39 bp and 3' ; 73 bp) and B2 (5' ; 39 bp and 3' ; 73 bp). These plasmids were introduced into undifferentiated ES cells or NIH3T3 cells. The luciferase activities of A1, A2, B1 and B2 remained as high as the full-length intron could induce (Fig. 36, 37).

I then constructed six more deletion mutants: A3 (5' ; 5 bp and 3' ; 60 bp), A4 (5' ; 5 bp and 3' ; 50 bp), A5 (5' ; 5 bp and 3' ; 40 bp), A6 (5' ; 5 bp and 3' ; 30 bp), A7 (5' ; 5 bp and 3' ; 20 bp) and A8 (5' ; 5 bp and 3' ; 10 bp). The luciferase activity of A3 was reduced approximately 30% compared with A1 (Fig. 38). The luciferase activities from A3 to A8 progressively diminished (Fig. 39). These data suggested that the

79-bp sequence at the 3' portion of the intron was required for the ERas enhancer activity.

Finally, I studied CpG mrthylation status of the ERas cis element (79 bp) by bisulfite genomic sequencing in undifferentiated ES cells and retinoic acid-reated ES cells. I found that CpG in ERas cis element was completely demethylated in undifferentiated ES cells (Fig. 40). In contrast, ~70% of CpG in the ERas enhancer were methylated after treatment with retinoic acid (Fig. 40). These data support that CpG methylation status could be involved in ES cell specific expression of ERas.

4. Discussion

Role of ERas and PI3 kinase in proliferation and tumorigenicity of mouse ES cells.

In this study, I identified a novel Ras protein, ERas, expressed specifically in mouse ES cells. The assays with NIH3T3 cells demonstrated that ERas was oncogenic protein because of its constitutive activation. In addition, our study also established a novel pathway that activates PI3 kinase in ES cells. The identification of ERas will facilitate our understanding of signaling pathways that maintain tumor-like propagation of ES cells.

Ras family proteins elicit their functions through binding to downstream effectors. HRas, KRas and NRas use Raf, RalGDS and PI3 kinase as effectors to modify cell proliferation, apoptosis and differentiation. In great contrast, I found that ERas specifically binds to PI3 kinase, but not to Raf1, BRaf or RalGDS. I also found that the phosphorylation status of AKT was significantly decreased in *ERas*-deficient ES cells. These data demonstrated that ERas specifically binds and activates PI3 kinase as an effector.

ERas-deficient ES cells form significantly smaller teratomas and show reduced proliferation rate *in vitro* than wild-type ES cells do, suggesting that PI3 kinase promotes teratoma formation. Important roles of the PI3 kinase pathway have been

reported previously. *Pten*-deficient ES cells form significantly larger tumors than wild-type ES cells do [52]. Pten-null ES cells proliferate much faster *in vitro* [53]. On the other hand, deletion of *Akt1*, also known as protein kinase B alpha, by gene targeting in Pten-null ES cells resulted in suppression of both tumorigenicity and proliferation rate *in vitro* [54]. These data indicated that ERas and its downstream effector PI3 kinase promote ES cell proliferation and tumorigenicity.

Roles of PI3 kinase in cell cycle control of ES cells were recently demonstrated by Jirmanova *et al*., who showed that LY294002 markedly increased G0/G1 phase in ES cells [64]. In contrast, I observed only small changes in cell cycle in *ERas*-null cells compared to wild-type cells (G1, 24.6 ± 0.3%; S, 60.5 ± 1.5%; G2, 14.8 ± 1.3% vs G1, 22.8 ± 0.7%; S, 59.8 ± 1.3%; G2, 17.4 ± 0.8%), suggesting that PI3 kinase might also have a growth-promoting effect independent of cell cycle control. I showed that AKT was one of the downstream effectors of the ERas/PI3 kinase pathway, but other factors should also be involved.

Recently, Murakami *et al*. showed that mammalian target of rapamycin (mTOR), one of downstream target of PI3 kinase, was essential for both ES cell proliferation and mouse development [65]. Taken together, these data suggest that ERas/PI3 kinase/mTOR signaling is crucial for proliferation of undifferentiated ES cells.

However, ERas-null ES cells still produce teratomas, albeit smaller than normal ES cells do, suggesting the existence of other factors activating the PI3 kinase pathway. Factors involved in other signaling pathways might also be involved in tumorigenicity of ES cells. Identification of these factors is essential for understanding of tumor-like properties of ES cells and for their clinical application.

Role of PI3 kinase in the maintenance of undifferentiated state of ES cells

In addition to proliferation and tumorigenicity, my data suggested that PI3 kinase activity is also crucial for self-renewal of ES cells. I found that the PI3 kainse inhibitor LY294002 induced ES cells differentiation and decreased the expression of ES cell marker genes, such as *Oct3/4* and *Nanog*. I could not obtain undifferentiated ES cell clones expressing a dominant negative mutant of the catalytic subunit of PI3 kinase, p110. Recently, Paling *et al*. also reported important roles of PI3 kinase in ES cell self-renewal [66].

I found that constitutive expression of Nanog inhibited LY294002-induced differentiation of ES cells. These cells express flag-tagged Nanog form the constitutive CAG promoter, but the amount of total Nanog is normal, probably due to negative auto regulation of the endogenous expression. In these cells, LY294002 did

not induce differentiation. The expression of *Oct3/4* was also normal. In contrast, LY294002 selectively decreased the expression of the endogenous Nanog. Nanog is essential for maintenance of pluripotency in ES cells and epiblast [7, 8]. These data suggested that the PI3 kinase may positively regulate the Nanog expression and thus contribute to self-renewal.

However, how the PI3 kinase modulates the Nanog expression remains unknown. Lin *et al.* reported that tumor suppressor p53 promoted differentiation of ES cells by suppressing the Nanog expression [67]. They also showed that suppression of Nanog by p53 depended on phosphorylation status of Ser315 of p53. It is known that this residue is a substrate of glycogen synthase kinase 3β (GSK3β) [68, 69]. GSK3 is negatively regulated by PI3 kinase and AKT [70]. Taken together, PI3 kinase may contribute self-renwal of ES cells through GSK3b, p53 and Nanog.

Membrane localization of ERas is essential for its activity

In this study, I also studied the molecular mechanisms underlying membrane targeting of ERas and another Ras-related protein Rheb. The CAAX motifs of ERas and Rheb are atypical in that they have serine at the second position, suggesting that it may undergo unique post-translational modifications. My study demonstrated that

ERas is targeted to plasma membrane, whereas Rheb is targeted to endomembrane through the common mechanism.

I found that three lipid modifications target ERas to plasma membrane through ER and golgi. The modifications include farnesylation of the cysteine in the CAAX motif, methylation of the farnesylated cysteine by ICMT, and palmitoylation of upstream cysteines. In addition, cleavage of the AAX triplet by RCE1 is also required. These data demonstrated that ERas shares the same membrane-targeting mechanisms with HRas.

However, the effect of inhibition of methylation, AAX cleavage, or palmitoylation was not identical between HRas and ERas. In *Rce1*- or *Icmt*- deficient cells, a large portion of HRas remains at plasma membrane. In contrast, ERas has a tendency to localize in golgi apparatus in these cells. When palmitoylation was inhibited by mutating the upstream cysteines, HRas localized in endomembranes, whereas ERas diffused in cytoplasm. These data indicated that ERas depends more on methylation and palmitoylation for membrane localization than HRas.

I found that Rheb localized at endomembrane, but not at plasma membrane. Endomembrane localization was blocked by farnesyl transferase inhibitor, but not by geranyl-geranyl transferase inhibitor. Membrane localization also disappeared in

Rce1- or *Icmt*- deficient cells. These indicate that Rheb utilized the same membrane targeting machinery with HRas and ERas.

However, Rheb lacks upstream cysteines to be palmitoylated. When I introduced upstream cysteines, Rheb was targeted to plasma membrane. Thus, the lack of palmitoylation is likely to be the cause of endomembrane localization.

Forced-expression of farnesylation- or palmitoylation-defected mutant of ERas showed that plasma membrane localization of ERas is important for its biological activity. Endomembrane-targeted ERas showed weaker effect on cell proliferation, whereas cytosol-diffused ERas had no effect. This observation is reasonable since I found that the main effctor of ERas is PI3 kinase, which catalyzes membrane-associated lipids.

In contrast, I found that Rheb can activate p70S6K regardless of its localization. The signaling from Rheb to p70S6K is still unclear. Several studies suggest that mTOR functions downstream of Rheb [71]. Since mTOR abundantly exists in cytoplasm, Rheb does not have to be located at membranes to activate downstream effectors regardless of localization.

Why is the CAAX motif of Rheb conserved in the course of evolution? TSC1 and TSC2 form heterodimer, and then negatively regulate Rheb activity. I found that

EGFP-fused TSC1 was located at endomembrane in MEFs. The CAAX motif of Rheb might be required for efficient interaction with the TSC1-TSC2 complex and for proper regulation. This should be essential for organisms, since enhancement of mTOR activity leads to oncogenesis [72, 73].

Another possibility is that Rheb has other effector(s), which is located at membranes. Previous study has shown that Rheb could interact with the proto-oncogene BRaf and negatively regulate MAP kinase [74, 75]. These data suggest that the CAAX motif of Rheb might be required for downregulation of MAP kinase.

Transcriptional control of the mouse ERas gene

In contrast to other ECATs, such as *Fbx15* and *Nanog*, which are expressed both in ES cells and in blastocysts [8, 20], X-gal staining suggests that *ERas* is expressed in ES cells but not in blastocysts. In addition, no EST containing *ERas* messenger RNA sequence is found in blastocyst-derived libraries. I studied the mechanisms for this specific expression of ERas.

Reporter assays with the deletion of ERas promoter suggest that the 79-bp 3' ternimus of intron is required for the transcriptional activity. Deletion mutants of this region showed reduced enhancer activity. This fragment contains three E-boxes,

which is the basic helix-loop-helix protein binding site. On the other hand, this fragment also includes U2, U5 snRNP binding sequence (5'-TAAC-3'), which is required for splicing. Further studies will be required to determine whether the reduction in enhancer activity is due to deletion of the E-boxes or improper splicing.

Finally, I obtained ES-like tetraploid cells by electric fusion with wild-type ES cells and T cells carrying *β-geo* knocked-into the *ERas* locus. These tetraploid ES-like cells expressed *β-geo* gene at the *ERas* locus derived from T cells. These data suggest that the environment in undifferentiated ES cells, such as specific transcription factors or chromatin remodeling factor, may be required for activation of the *ERas* promoter.

Future plans

All of data in this study propose the further application with ERas. For example, *ERas* promoter may be beneficial in finding the pluripotent cell origin. ES cells are established from inner cell mass of blastocysts. However, inner cell mass maintain their pluripotency only for short term *in vivo*. In contrast, ES cells can grow infinitely and maintain pluripotency. The mechanism of turning inner cell mass into ES cells is still unknown.

Another application is for expansion of stem cells in vitro. Adult stem cells, such as hematopoietic stem cells, proliferate much slower than ES cells. Their expansion is limited *in vitro* and the conditions supporting their *in vitro* self-renewal are still

unclear. On the other hand, human ES cells can self-renew in the presence of FBS, MEF conditioned medium or feeder cells. Recently, Ying *et al*. succeeded in establishing completely chemical-defined culture (serum- and feeder-free) of mouse ES cells [11]. However, human ES cells can not proliferate in this condition. For clinical usage of these cells, unidentified components must be completely precluded from the culture medium. In this study, I demonstrate that ERas can promote proliferation not only of ES cells but of other cells such as NIH3T3 and MEFs. To deliver ERas protein directly to cells, recombinant TAT-ERas protein carrying the protein transduction domain of human immunodeficiency virus transactivating protein (TAT) [76] might be utilized.

5. Acknowledgements

I appreciate to Drs. Kenji Kohno, Hiroshi Itoh, Kinichi Nakashima and Shinya Yamanaka for reading and reviewing for this thesis.

I thank to Drs. Masato Nakagawa, Koji Shimozaki, Keisuke Okita and Yumiko Sasaoka, Kaoru Mitsui and Akihito Adachi, and Eiko Kaiho, Yoshimi Tokuzawa, Masayoshi Maruyama, Mirei Murakami, Yasuaki Oda, Nami Yoshikane, Michimasa Osawa, Hiroaki Ito, Masanori Imamura, Hisayuki Amano, Arufumi Shiota, Noriko Tsubooka, Kyoko Miura and Takaaki Hirano for valuable discussion, to Tomoko Ichisaka, Yukiko Ikeguchi, Tamayo Ozawa, Kanako Sawai, Junko Iida and Masako Shirasaka for helpful supports, to people belonging to KAC for maintenance of animals, Drs. Junya Kato and Kiichiro Tomoda for valuable guidance. I am grateful to Dr. Hitoshi Niwa for MG1.19 ES cells, pBIKS(-)IresBgeopA and pPyCAG-IP, to Drs. Kenji Kohno and Toshio Kitamura for PLAT-E cells and pMX retroviral vectors, to Drs. Kenji Kohno and Akio Tsuru for anti-GM130 antibody, to Drs. Masaru Okabe and Jun-ichi Miyazaki for pCX-EGFP, to Dr. Robert Farese, Jr. for RF8 ES cells, to Drs. Rudolf Jaenisch and Tetsuo Noda for J1 cells, to Drs. William Skarnes and Stephen Young for CGR8 cells, and to Dr. Stephen Young for *Rce1*- or *Icmt*-deficient MEFs.

I especially thank to Keisuke Nimura, Ken Itakura, Reiko Sasaki, Chihiro Takigawa,

Naoya Konishi and Akira Watanabe for both personal and scientific talking, Kosuke Yusa and Drs. Masamichi Yamamoto and Yasuaki Kida for advisement of future plan, Yuki Yoshimoto and my family for unlimited love and support.

Finally, I thank to Dr. Shinya Yamanaka for everything. I have been always got to his support and suggestion. The time in Nara is extremely important for my life as a scientist.

This thesis is dedicated to Akiko Hironaka, my aunt.

6. References

1. Evans, M.J. & Kaufman, M.H. (1981). Establishment in culture of pluripotential cells from mouse embryos. *Nature* 292, 154–6.

2. Martin, G.R. (1981). Isolation of a pluripotent cell line from early mouse embryos cultured in medium conditioned by teratocarcinoma. *Proc. Natl. Acad. Sci. U. S. A.* 78, 7634–8.

3. Thomson, J. A., Itskovitz-Eldor, J., Shapiro, S. S., Waknitz, M. A., Swiergiel, J. J., Marshall, V. S. & Jones, J. M. (1998). Embryonic stem cell lines derived from human blastocysts. *Science* 282, 1145-7.

4. Freed, C. R. (2002). Will embryonic stem cells be a useful source of dopamine neurons for transplant into patients with Parkinson's disease? *Proc. Natl. Acad. Sci. U. S. A.* 99, 1755-7.

5. Nichols, J., Zevnik, B., Anastassiadis, K., Niwa, H., Klewe-Nebenius, D., Chambers, I., Scholer, H. & Smith, A. (1998). Formation of pluripotent stem cells in the mammalian embryo depends on the POU transcription factor Oct4. *Cell* 95, 379–91.

6. Niwa, H., Miyazaki, J. & Smith, A. G. (2000). Quantitative expression of Oct-3/4 defines differentiation, dedifferentiation or self-renewal of ES cells. *Nat. Genet.* 24, 372–6.

7. Chambers, I., Colby, D., Robertson, M., Nichols, J., Lee, S., Tweedie, S. & Smith, A. (2003). Functional expression cloning of Nanog, a pluripotency sustaining factor in embryonic stem cells. *Cell* 113, 643-55.

8. Mitsui, K., Tokuzawa, Y., Itoh, H., Segawa, K., Murakami, M., Takahashi, K., Maruyama, M., Maeda, M. & Yamanaka, S. (2003). The homeoprotein Nanog is required for maintenance of pluripotency in mouse epiblast and ES cells. *Cell* 113, 631-42.

9. Smith, A. G., Heath, J. K., Donaldson, D. D., Wong, G. G., Moreau, J., Stahl, M. & Rogers, D. (1988). Inhibition of pluripotential embryonic stem cell differentiation by purified polypeptides. *Nature* 336, 688–90.

10. Williams, R.L., Hilton, D.J., Pease, S., Willson, T.A., Stewart, C.L., Gearing, D.P., Wagner, E.F., Metcalf, D., Nicola, N.A. & Gough, N.M. (1988). Myeloid leukaemia inhibitory factor maintains the developmental potential of embryonic stem cells. *Nature* 336, 684–7.

11. Ying, Q. L., Nichols, J., Chambers, I. & Smith, A. (2003). BMP induction of Id proteins suppresses differentiation and sustains embryonic stem cell self-renewal in collaboration with STAT3. *Cell* 115, 281-92.

12. Sato, N., Meijer, L., Skaltsounis, L., Greengard, P. & Brivanlou, A. H. (2004). Maintenance of pluripotency in human and mouse embryonic stem cells through activation of Wnt signaling by a pharmacological GSK-3-specific inhibitor. *Nat. Med.* 10, 55-63.

13. Takahashi, K., Mitsui, K. & Yamanaka, S. (2003). Role of ERas in promoting tumour-like properties in mouse embryonic stem cells. *Nature* 423, 541-5.

14. Meiner, V. L., Cases, S., Myers, H. M., Sande, E. R., Bellosta, S., Schambelan, M.,

Pitas, R. E., McGuire, J., Herz, J. & Farese, R. V. Jr. (1996). Disruption of the acyl-CoA:cholesterol acyltransferase gene in mice: evidence suggesting multiple cholesterol esterification enzymes in mammals. *Proc. Natl. Acad. Sci. U. S. A.* 93, 14041-6.

15. Gassmann, M., Donoho, G. & Berg, P. (1995). Maintenance of an extrachromosomal plasmid vector in mouse embryonic stem cells. *Proc. Natl. Acad. Sci. U. S. A.* 92, 1292-6.

16. Morita, S., Kojima, T., and Kitamura, T. (2000). Plat-E : an efficient and stable system for transient packaging of retroviruses. *Gene Therapy* 7, 1063-6.

17. Rosario, M., Paterson, H. F. & Marshall, C. J. (1999). Activation of the Raf/MAP kinase cascade by the Ras-related protein TC21 is required for the TC21-mediated transformation of NIH 3T3 cells. *EMBO J.* 18, 1270-9.

18. Quilliam, L. A., Castro, A. F., Rogers-Graham, K. S., Martin, C. B., Der, C. J. & Bi, C. (1999). M-Ras/R-Ras3, a transforming ras protein regulated by Sos1, GRF1, and p120 Ras GTPase-activating protein, interacts with the putative Ras effector AF6. *J.*

Biol. Chem. 274, 23850-7.

19. Cox A. D., Solski P. A., Jordan J. D. & Der C. J. (1995). Analysis of Ras protein expression in mammalian cells. *Methods Enzymol.* 255, 195-220.

20. Tokuzawa Y., Kaiho E., Maruyama M., Takahashi K., Mitsui K., Maeda M., Niwa H. & Yamanaka S. (2003). Fbx15 is a novel target of Oct3/4 but is dispensable for ES cell self-renewal and mouse development. *Mol. Cell. Biol*. 23, 2699-2708.

21. Chen, Z. Q., Ulsh, L. S., DuBois, G. & Shih, T. Y. (1985). Posttranslational processing of p21 ras proteins involves palmitylation of the C-terminal tetrapeptide containing cysteine-186. *J. Virol*. 56, 607-12.

22. Willumsen, B. M., Christensen, A., Hubbert, N. L., Papageorge, A. G. & Lowy, D. R. (1984). The p21 ras C-terminus is required for transformation and membrane association. *Nature* 310, 583-6.

23. Miyoshi, J., Kagimoto, M., Soeda, E. & Sakaki, Y. (1984). The human c-Ha-ras2 is

a processed pseudogene inactivated by numerous base substitutions. *Nucleic Acids Res.* 12, 1821-8.

24. Li, E., Bestor, T. H. & Jaenisch, R. (1992). Targeted mutation of the DNA methyltransferase gene results in embryonic lethality. *Cell* 69, 915-26.

25. Nichols, J., Evans, E. P. & Smith, A. G. (1990). Establishment of germ-line-competent embryonic stem (ES) cells using differentiation inhibiting activity. *Development* 110, 1341-8.

26. Serrano, M., Lin, A. W., McCurrach, M. E., Beach, D. & Lowe, S. W. (1997). Oncogenic ras provokes premature cell senescence associated with accumulation of p53 and p16INK4a. *Cell* 88, 593-602.

27. Takai, Y., Sasaki, T. & Matozaki, T. (2001). Small GTP-binding proteins. *Physiol. Rev.* 81, 153-208.

28. Fasano, O., Aldrich, T., Tamanoi, F., Taparowsky, E., Furth, M. & Wigler, M. (1984).

Analysis of the transforming potential of the human H-ras gene by random mutagenesis. *Proc. Natl. Acad. Sci. U. S. A.* 81, 4008-12.

29. Hancock, J. F. (2003). RAS PROTEINS: DIFFERENT SIGNALS FROM DIFFERENT LOCATIONS. *Nat. Rev. Mol. Cell Biol*. 4, 373-84.

30. Reiss, Y., Goldstein, J. L., Seabra, M. C., Casey, P. J. & Brown, M. S. (1990). Inhibition of purified p21ras farnesyl:protein transferase by Cys-AAX tetrapeptides. *Cell* 62, 81–88.

31. Seabra, M. C., Reiss, Y., Casey, P. J., Brown, M. S. & Goldstein, J. L. (1991). Protein farnesyltransferase and geranylgeranyltransferase share a common a-subunit. *Cell* 65, 429-34.

32. Moores, S. L., Schaber, M. D., Mooser, S. D., Rands, E., O'hara, M. B., Garsky, V. M., Marshall, M. S., Pompliano, D. L. & Gibbs, J. B. (1991). Sequence dependence of protein isoprenylation. *J. Biol. Chem*. 266, 14603-10.

33. Yokoyama, K., Goldwin, G. W., Ghomashchi, F., Glomset, J. A. & Gelb, M. H. (1991). A protein geranylgeranyltransferase from bovine brain: Implications for protein prenylation specificity. *Proc. Natl. Acad. Sci. U. S. A.* 88, 5302-6.

34. Boyartchuk, V. L., Ashby, M. N. & Rine, J. (1997). Modulation of Ras and a-factor function by carboxyl-terminal proteolysis. *Science* 275, 1796–1800.

35. Kim, E., Ambroziak, P., Otto, J. C., Taylor, B., Ashby, M., Shannon, K., Casey, P. J. & Young, S. G.. (1999). Disruption of the mouse *Rce1* gene results in defective Ras processing and mislocalization of Ras within cells. *J. Biol. Chem*. 274, 8383–8390.

36. Otto, J. C., Kim, E., Young, S. G. & Casey, P. J. (1999). Cloning and characterization of a mammalian prenyl protein-specific protease. *J. Biol. Chem*. 274, 8379–8382.

37. Bergo, M. O., Ambroziak, P., Gregor,y C., George, A., Otto, J. C., Kim, E., Nagase, H., Casey, P. J., Balmain, A. & Young, S. G.. (2002). Absence of the CAAX endoprotease Rce1: effects on cell growth and transformation. *Mol. Cell. Biol*. 22,

171-81.

38. Clark, G. J., Kinch, M. S., Rogers-Graham, K., Sebti, S. M., Hamilton, A. D. & Der, C. J. (1997). The Ras-related protein Rheb is farnesylated and antagonizes Ras signaling and transformation. *J. Biol. Chem.* 272, 10608-15.

39. Hrycyna, C. A., Sapperstein, S. K., Clarke, S. & Michaelis, S. (1991). The *Saccharomyces cerevisiae STE14* gene encodes a methyltransferase that mediates C-terminal methylation of a-factor and RAS proteins. *EMBO J*. 10, 1699–1709.

40. Dai, Q., Choy, E., Chiu, V., Romano, J., Slivka, S. R., Steitz, S. A., Michaelis, S. & Philips, M. R. Mammalian prenylcysteine carboxyl methyltransferase is in the endoplasmic reticulum. *J. Biol. Chem*. 273, 15030–15034 (1998).

41. Bergo, M. O., Leung, G. K., Ambroziak, P., Otto, J. C., Casey, P. J. & Young, S. G. (2000). Targeted inactivation of the isoprenylcysteine carboxyl methyltransferase gene causes mislocalization of K-Ras in mammalian cells. *J. Biol. Chem.* 275, 17605-10.

42. Nakamura, N., Rabouille, C., Watson, R., Nilsson, T., Hui, N., Slusarewicz, P., Kreis, T. E. & Warren, G. (1995). Characterization of a cis-Golgi matrix protein, GM130. *J. Cell Biol.* 131, 1715-26.

43. Choy, E., Chiu, V. K., Silletti, J., Feoktistov, M., Morimoto, T., Michaelson, D., Ivanov, I. E. & Philips, M. R. (1999). Endomembrane trafficking of Ras: the CAAX motif targets proteins to the ER and Golgi. *Cell* 98, 69–80.

44. Apolloni, A., Prior, I. A., Lindsay, M., Parton, R. G. & Hancock, J. F. (2000). H-ras but not K-ras traffics to the plasma membrane through the exocytic pathway. *Mol. Cell. Biol*. 20, 2475–2487.

45. Michaelson, D., Ahearn, I., Bergo, M., Young, S. & Philips, M. (2002). Membrane trafficking of heterotrimeric G proteins via the endoplasmic reticulum and Golgi. *Mol. Biol. Cell* 13, 3294–3302.

46. Cheng, A. M., Saxton, T. M., Sakai, R., Kulkarni, S., Mbamalu, G., Vogel, W.,

Tortorice, C. G., Cardiff, R. D., Cross, J. C., Muller, W. J. & Pawson, T. (1998). Mammalian Grb2 regulates multiple steps in embryonic development and malignant transformation. *Cell* 95, 793-803.

47. Burdon, T., Stracey, C., Chambers, I., Nichols, J. & Smith, A. (1999). Suppression of SHP-2 and ERK signalling promotes self-renewal of mouse embryonic stem cells. *Dev. Biol.* 210, 30-43.

48. Moodie, S. A., Willumsen, B. M., Weber, M. J. & Wolfman, A. (1993). Complexes of Ras.GTP with Raf-1 and mitogen-activated protein kinase kinase. *Science* 260, 1658-61.

49. Zhang, X. F., Settleman, J., Kyriakis, J. M., Takeuchi-Suzuki, E., Elledge, S. J., Marshall, M. S., Bruder, J. T., Rapp, U. R. & Avruch, J. (1993). Normal and oncogenic p21ras proteins bind to the amino-terminal regulatory domain of c-Raf-1. *Nature* 364, 308-13.

50. Rodriguez-Viciana, P., Warne, P. H., Dhand, R., Vanhaesebroeck, B., Gout, I., Fry,

M. J., Waterfield, M. D. & Downward, J. (1994). Phosphatidylinositol-3-OH kinase as a direct target of Ras. *Nature* 370, 527-32.

51. Rodriguez-Viciana, P., Warne, P. H., Khwaja, A., Marte, B. M., Pappin, D., Das, P., Waterfield, M. D., Ridley, A. & Downward, J. (1997). Role of phosphoinositide 3-OH kinase in cell transformation and control of the actin cytoskeleton by Ras. *Cell* 89, 457-67.

52. Di Cristofano, A., Pesce, B., Cordon-Cardo, C. & Pandolfi, P. P. (1998). Pten is essential for embryonic development and tumour suppression. *Nat. Genet.* 19, 348-55.

53. Sun, H., Lesche, R., Li, D. M., Liliental, J., Zhang, H., Gao, J., Gavrilova, N., Mueller, B., Liu, X. & Wu H. (1999). PTEN modulates cell cycle progression and cell survival by regulating phosphatidylinositol 3,4,5,-trisphosphate and Akt/protein kinase B signaling pathway. *Proc. Natl. Acad. Sci. U. S. A.* 96, 6199-204.

54. Klippel, A., Reinhard, C., Kavanaugh, W. M., Apell, G., Escobedo, M. A. &

Williams, L. T. (1996). Membrane localization of phosphatidylinositol 3-kinase is sufficient to activate multiple signal-transducing kinase pathways. *Mol. Cell. Biol.* 16, 4117-27.

55. Maehama, T., Dixon, J. E. (1998). The tumor suppressor, PTEN/MMAC1, dephosphorylates the lipid second messenger, phosphatidylinositol 3,4,5-trisphosphate. *J. Biol. Chem.* 273, 13375-8.

56. Zhang, Y., Gao, X., Saucedo, L. J., Ru, B., Edgar. B. A. & Pan, D. (2003). Rheb is a direct target of the tuberous sclerosis tumour suppressor proteins. *Nat. Cell Biol.* 5, 578-81.

57. Inoki, K., Li, Y., Xu, T. & Guan, K. L. (2003). Rheb GTPase is a direct target of TSC2 GAP activity and regulates mTOR signaling. *Genes. Dev.* 2003 17, 1829-34.

58. Klippel, A., Escobedo, J. A., Hirano, M. & Williams, L. T. (1994). The interaction of small domains between the subunits of phosphatidylinositol 3-kinase determines enzyme activity. *Mol. Cell. Biol.*, 14, 2675–85.

59. Yamanaka, S., Poksay, K. S., Arnold, K. S. & Innerarity, T. L. (1997). A novel translational repressor mRNA is edited extensively in livers containing tumors caused by the transgene expression of the apoB mRNA-editing enzyme. *Genes. Dev.* 11, 321-33.

60. Yamanaka, S., Zhang, X. Y., Maeda, M., Miura, K., Wang, S., Farese, R. V. Jr,, Iwao, H. & Innerarity, T. L. (2000). Essential role of NAT1/p97/DAP5 in embryonic differentiation and the retinoic acid pathway. *EMBO J.* 19, 5533-41.

61. Tanaka, T. S., Kunath, T., Kimber, W. L., Jaradat, S. A., Stagg, C. A., Usuda, M., Yokota, T., Niwa, H., Rossant, J. & Ko, M. S. (2002). Gene expression profiling of embryo-derived stem cells reveals candidate genes associated with pluripotency and lineage specificity. *Genome Res.* 12, 1921-8.

62. Bortvin, A., Eggan, K., Skaletsky, H., Akutsu, H., Berry, D. L., Yanagimachi, R., Page, D. C. & Jaenisch, R. (2003). *Development* 130, 1673-80.

63. Vernallis, A. B., Hudson, K. R. & Heath, J. K. (1997). An antagonist for the

leukemia inhibitory factor receptor inhibits leukemia inhibitory factor, cardiotrophin-1, ciliary neurotrophic factor, and oncostatin M. *J. Biol. Chem.* 272, 26947-52.

64. Jirmanova, L., Afanassieff, M., Gobert-Gosse, S., Markossian, S. & Savatier, P. (2002). Differential contributions of ERK and PI3-kinase to the regulation of cyclin D1 expression and to the control of the G1/S transition in mouse embryonic stem cells. *Oncogene* 21, 5515-28.

65. Murakami, M., Ichisaka, T., Maeda, M., Oshiro, N., Hara, K., Edenhofer, F., Kiyama, H., Yonezawa, K. & Yamanaka, S. (2004). mTOR is essential for growth and proliferation in early mouse embryos and embryonic stem cells. *Mol. Cell. Biol.* 24, 6710-8.

66. Paling, N. R., Wheadon, H., Bone, H. K. & Welham, M. J. (2004). Regulation of embryonic stem cell self-renewal by phosphoinositide 3-kinase-dependent signaling. *J. Biol. Chem.* 279, 48063-70.

67. Lin, T., Chao, C., Saito, S., Mazur, S. J., Murphy, M. E., Appella, E. & Xu, Y. (2005). p53 induces differentiation of mouse embryonic stem cells by suppressing Nanog expression. *Nat. Cell Biol.* Advanced Online Publication.

68. Watcharasit, P., Bijur, G. N., Zmijewski, J. W., Song, L., Zmijewska, A., Chen, X., Johnson, G. V. & Jope, R. S. (2002). Direct, activating interaction between glycogen synthase kinase-3beta and p53 after DNA damage. *Proc. Natl. Acad. Sci. U. S. A.* 99, 7951-5.

69. Qu, L., Huang, S., Baltzis, D., Rivas-Estilla, A. M., Pluquet, O., Hatzoglou, M., Koumenis, C., Taya, Y., Yoshimura, A. & Koromilas, A. E. (2004). Endoplasmic reticulum stress induces p53 cytoplasmic localization and prevents p53-dependent apoptosis by a pathway involving glycogen synthase kinase-3beta. *Genes. Dev.* 18, 261-77.

70. Cross, D. A., Alessi, D. R., Cohen, P., Andjelkovich, M. & Hemmings, B. A. (1995). Inhibition of glycogen synthase kinase-3 by insulin mediated by protein kinase B. *Nature* 378, 785-9.

71. Manning, B. D. & Cantley, L. C. (2003). Rheb fills a GAP between TSC and TOR. *Trends Biochem. Sci.* 28, 573-6.

72. Hay, N. & Sonenberg, N. (2004). Upstream and downstream of mTOR. *Genes. Dev.* 18, 1926-45.

73. Bjornsti, M. A. & Houghton, P. J. (2004). The TOR pathway: a target for cancer therapy. *Nat. Rev. Cancer* 4, 335-48.

74. Im, E., von Lintig, F. C., Chen, J., Zhuang, S., Qui, W., Chowdhury, S., Worley, P. F., Boss, G. R. & Pilz, R. B. (2002). Rheb is in a high activation state and inhibits B-Raf kinase in mammalian cells. *Oncogene* 21, 6356-65.

75. Karbowniczek, M., Cash, T., Cheung, M., Robertson, G. P., Astrinidis, A. & Henske, E. P. (2004). Regulation of B-Raf kinase activity by tuberin and Rheb is mammalian target of rapamycin (mTOR)-independent. *J. Biol. Chem.* 279, 29930-7.

76. Krosl, J., Austin, P., Beslu, N., Kroon, E., Humphries, R. K. & Sauvageau, G. (2003). *In vitro* expansion of hematopoietic stem cells by recombinant TAT-HOXB4 protein. *Nat. Med.* 9, 1428-32.

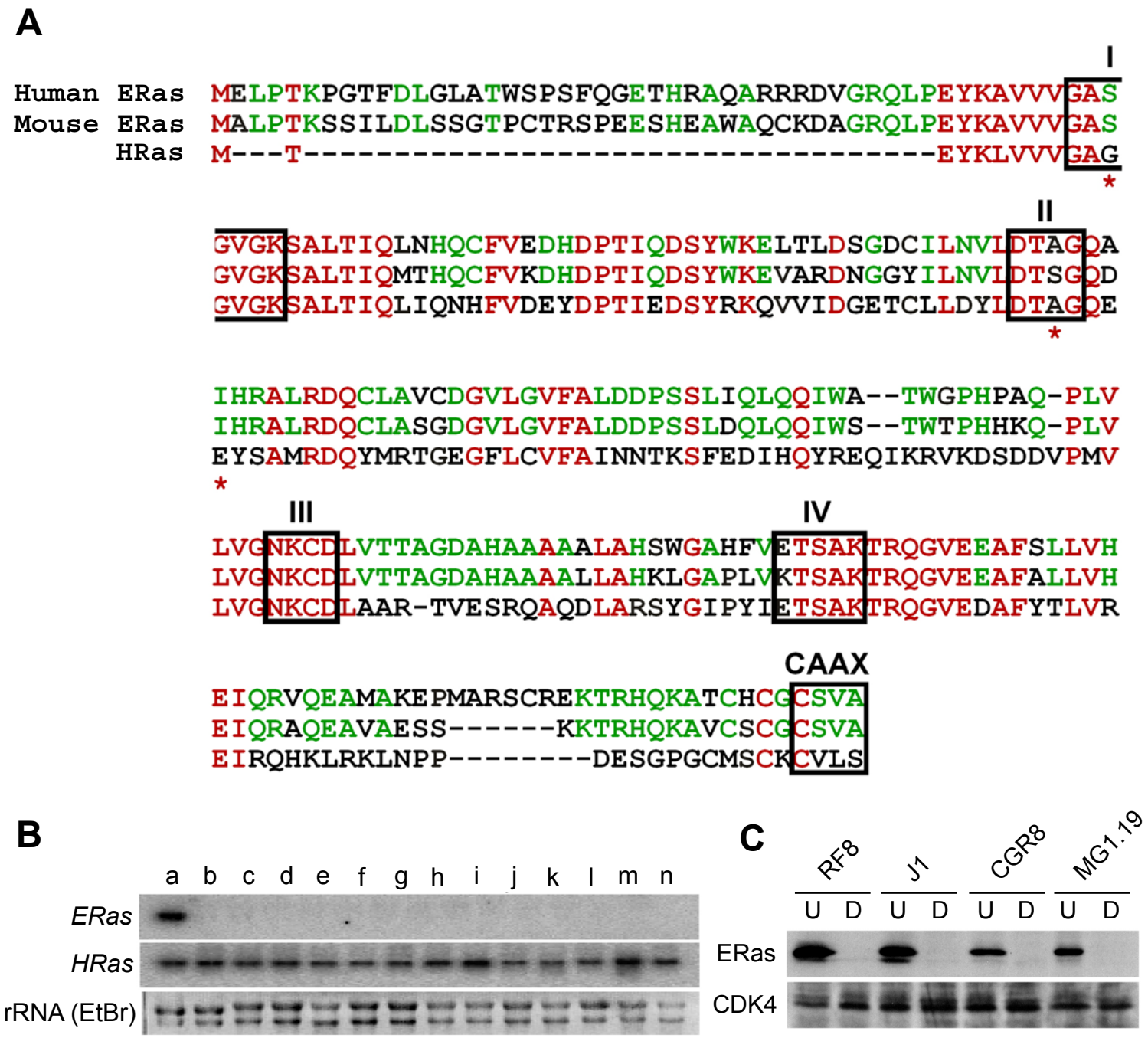

Figure 1. Identification of ERas gene.

A. Amino acid sequence of human ERas, mouse ERas and HRas. Boxes indicate conserved domains (I-IV) and the CAAX motif. Asterisks indicate three amino acid residues that are often mutated in oncogenic HRas mutants. Amino acids conserved among all three proteins are shown in red, and those conserved between human and mouse ERas are shown in green.

B. Northern blot. a, undifferentiated RF8 ES cells; b, retinoic acid treated RF8 ES cells; c, testis; d, lung; e, heart; f, liver; g, stomach; h, kidney; i, brain; j, spleen; k, thymus; l, small intestine; m, skin; n, muscle.

C. Immunoblot. Immunoblotting of ERas expression in four independent ES cell lines. U, undifferentiated; D, differentiated.

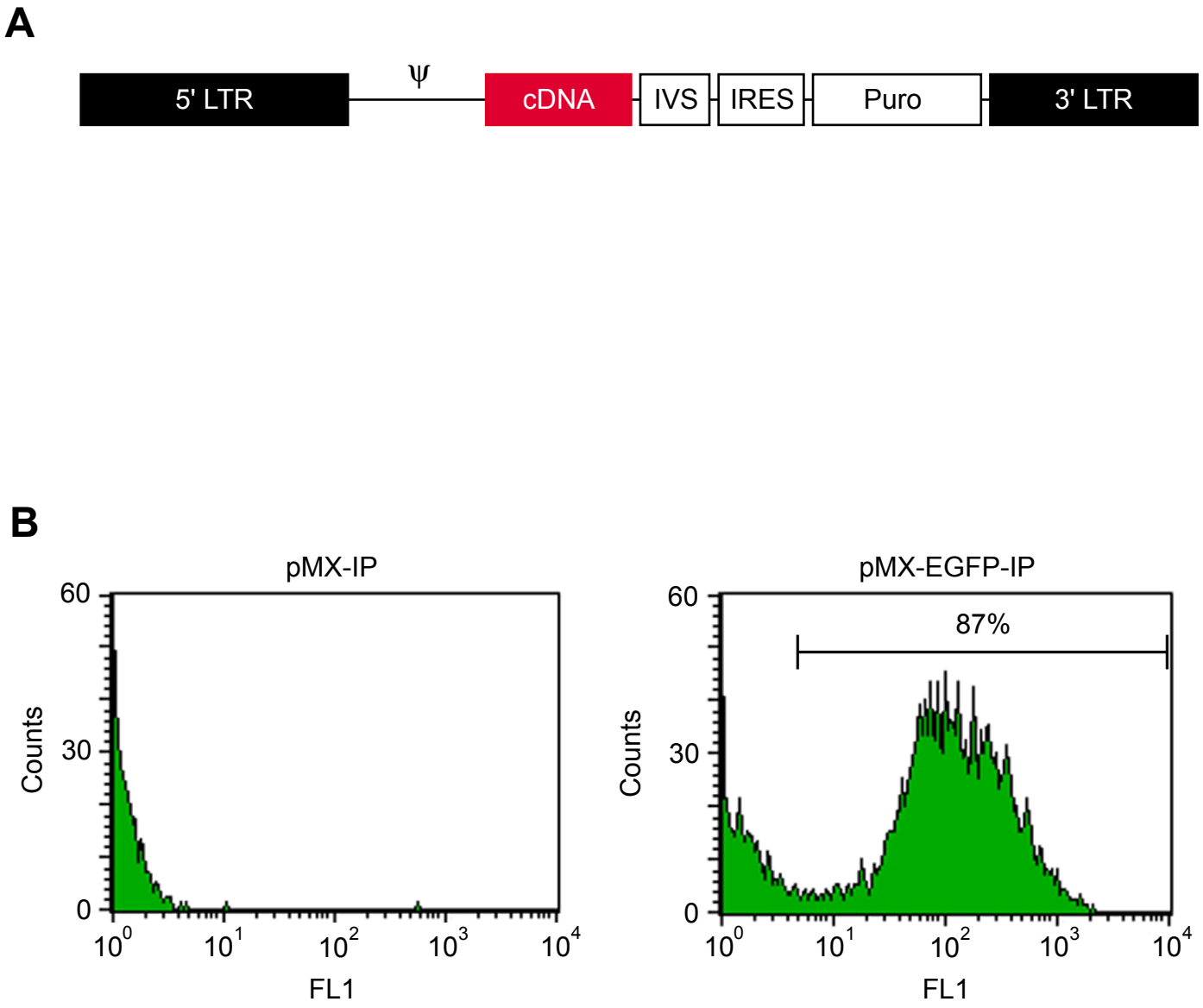

Figure 2. Retroviral infection system used in this study.
A. pMX-IP retroviral vector. LTR, long terminal repeat; ψ, packaging signal; IVS, intron; IRES, internal ribosome entry site; puro, puromycin resistant gene.
B. Flowcytometry analysis of cells infected with pMX-IP or pMX-EGFP-IP.

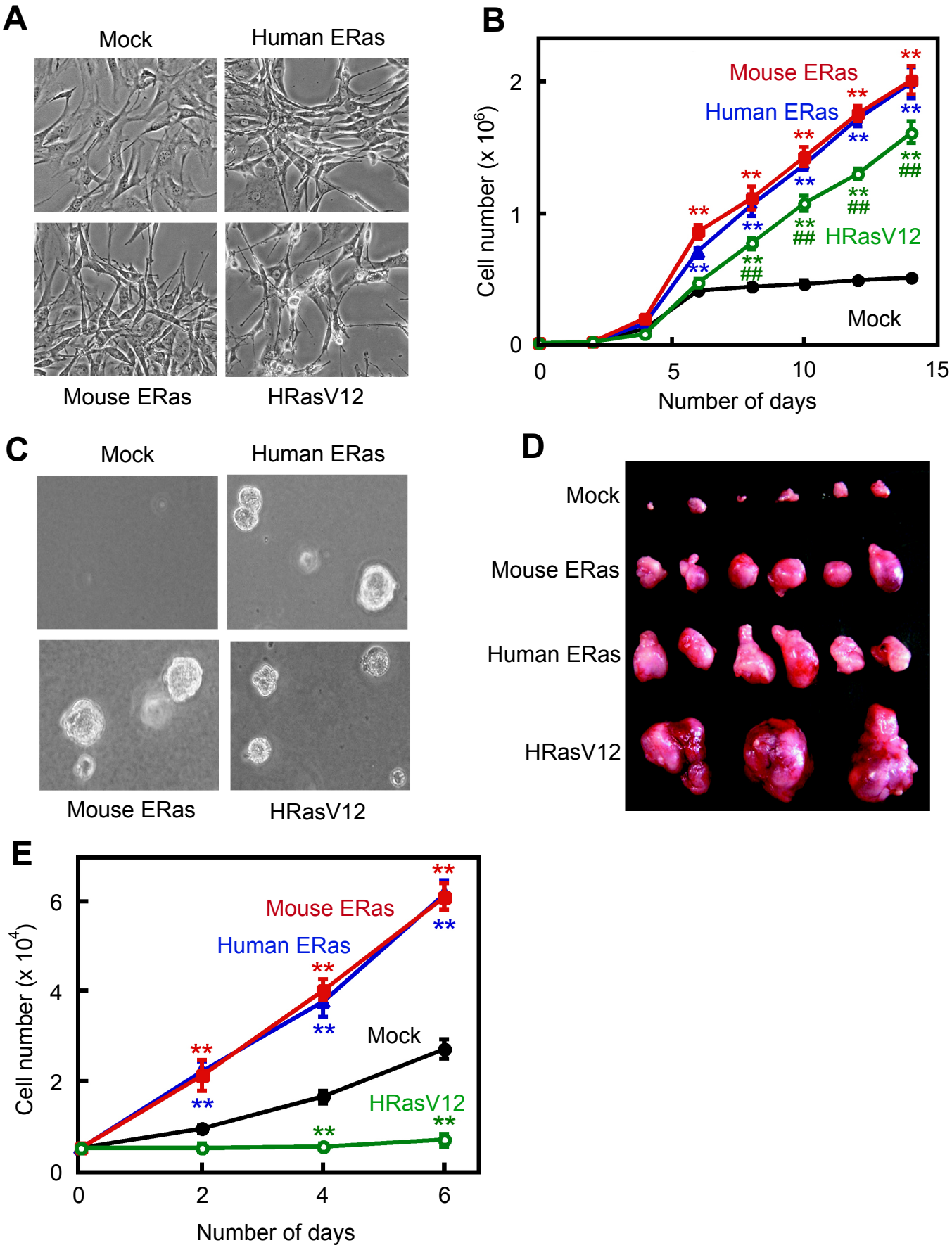

Figure 3. Transformation activity of ERas.

A. Morphologies of NIH3T3 expressing ERas or HRasV12.

B. NIH3T3 growth. Ten thousands cells were plated and counted every other day for 14 days. Double asterisks, $P < 0.01$ versus Mock transfected; double daggers, $P < 0.01$ versus ERas (n = 4).

C. Anchorage-independent growth in soft agar.

D. Tumors in nude mice.

E. MEF growth. Five thousands cells were plated and counted every other day for 6 days. Double asterisks, $P < 0.01$ versus Mock transfected (n = 5).

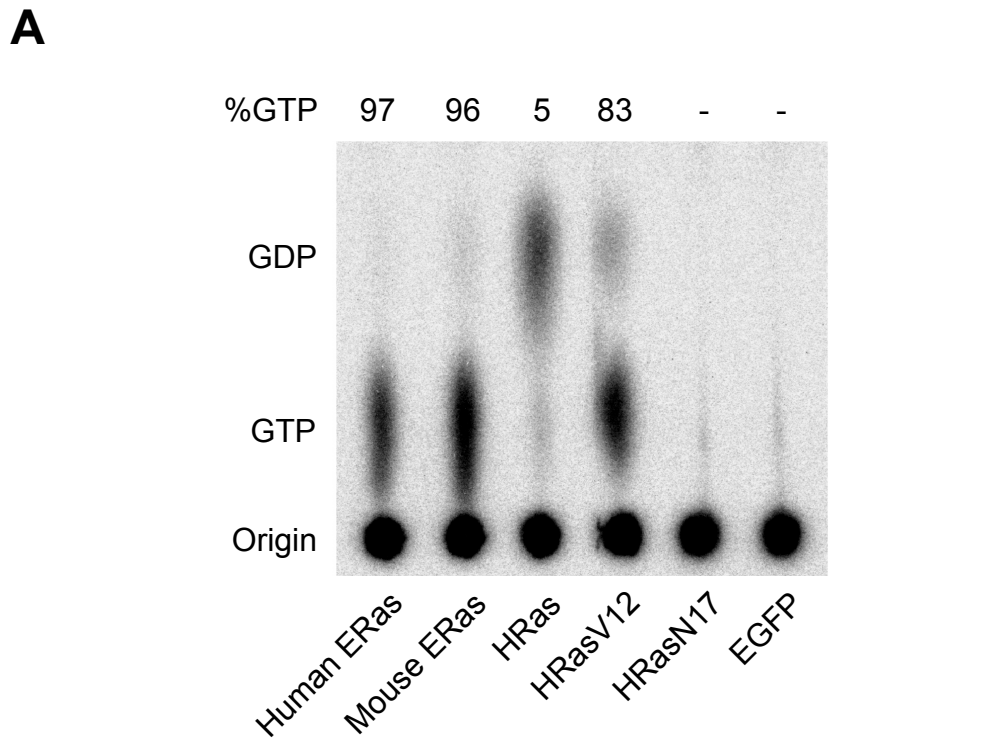

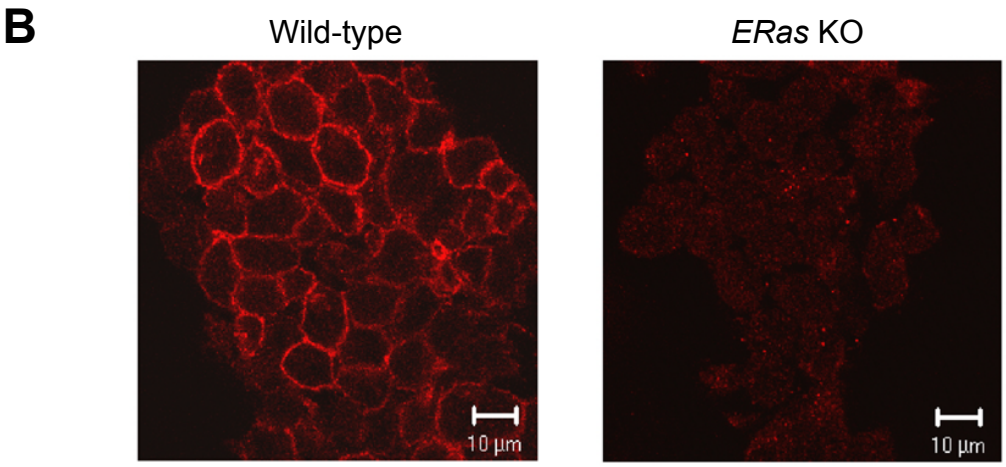

Figure 4. Post-translational modification of ERas.
A. Thin layer chromatography showing protein association with GDP and GTP.
B. Immunostaining of ERas in wild-type RF8 ES cells and *ERas*-knockout (KO) ES cells.

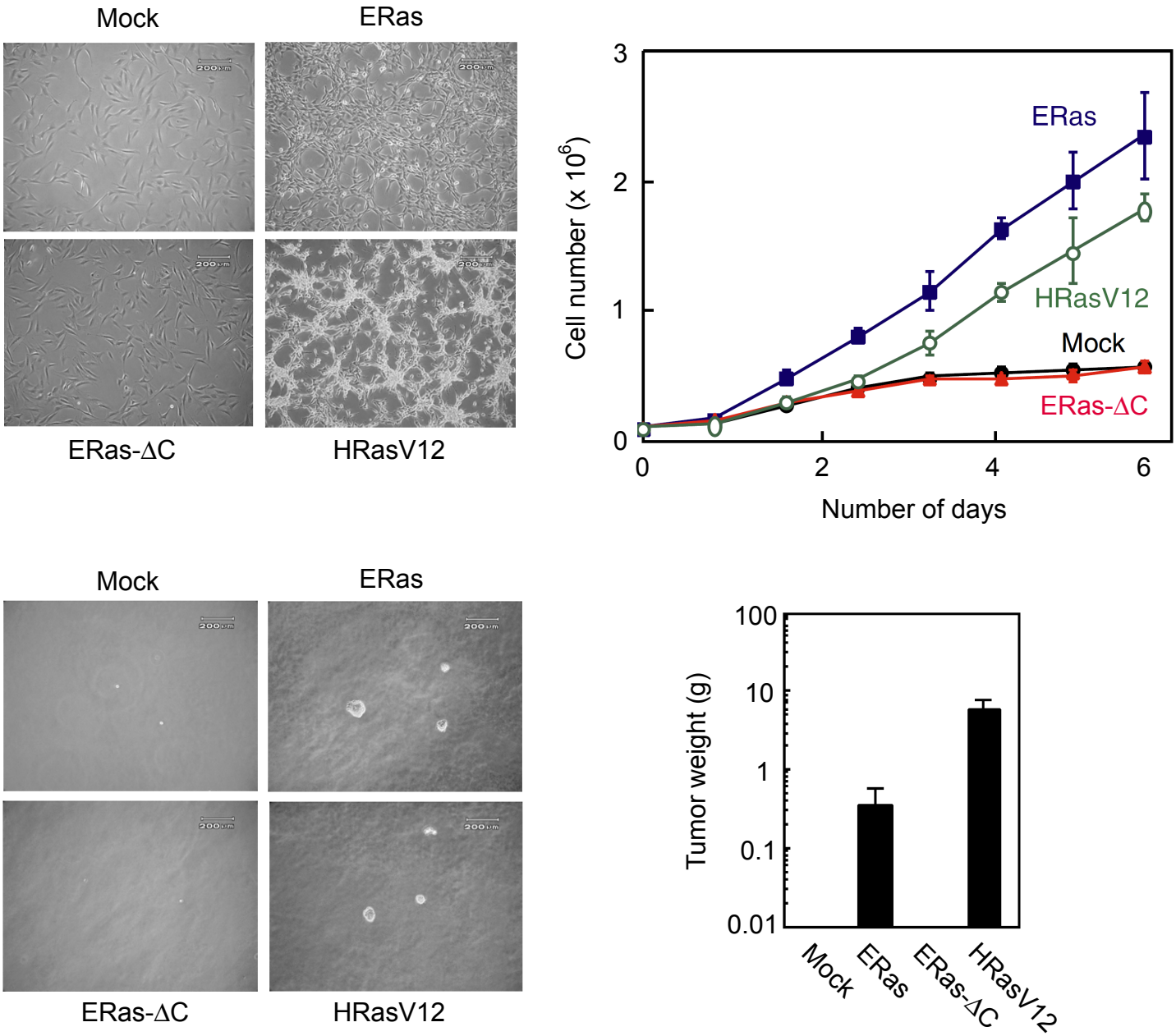

Figure 5. Carboxy-terminal region is required for the transformation activity of ERas.
A. Comparison carboxy-terminal sequence of ERas and other Ras-related proteins.
B. Morphologies of NIH3T3 expressing ERas, ERas-ΔC or HRasV12. NIH3T3 cells were infected with pMX-IP or pMX-IP encoding ERas, ERas-ΔC or HRasV12. Forty-eight hours after infection, cells were selected with 2 μg/ml of puromycin for 4 days.
C. Growth of NIH3T3 cells expressing ERas, ERas-ΔC or HRasV12. Cells used in B were plated at 1 x 10^4 cells per well of 24-well plates and counted every other day for 14 days.
D. Colony formation in soft agar. Cells used in B were cultured in the medium containing 0.33% agar for 21 days and then photographed.
E. Tumor formation in nude mice. One million cells were injected subsutaneously into nude mice. Two weeks after injection, tumors were dissected and weighted (n = 4).

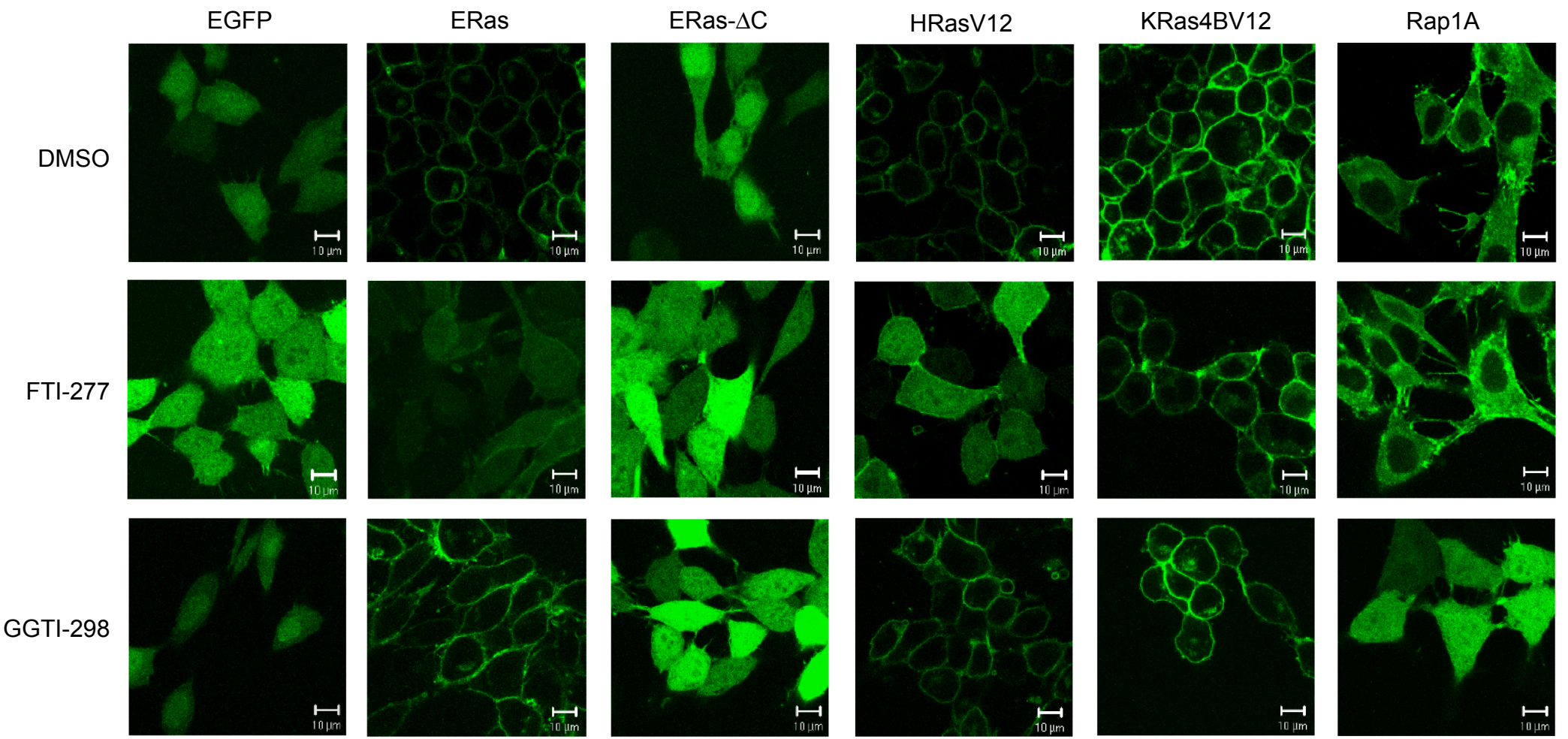

Figure 6. Effect of farnesyl transferase or geranyl geranyl transferase inhibitors on intracellular localization of various Ras-related proteins. MEFs expressing EGFP, EGFP-ERas, EGFP-ERas-ΔC, EGFP-HRasV12, EGFP-KRas4BV12 or EGFP-Rap1A were treated with DMSO, FTI-277 or GGTI-298 for 24 hours. After treatment, cells were fixed and observed with a confocal microscope (x 100).

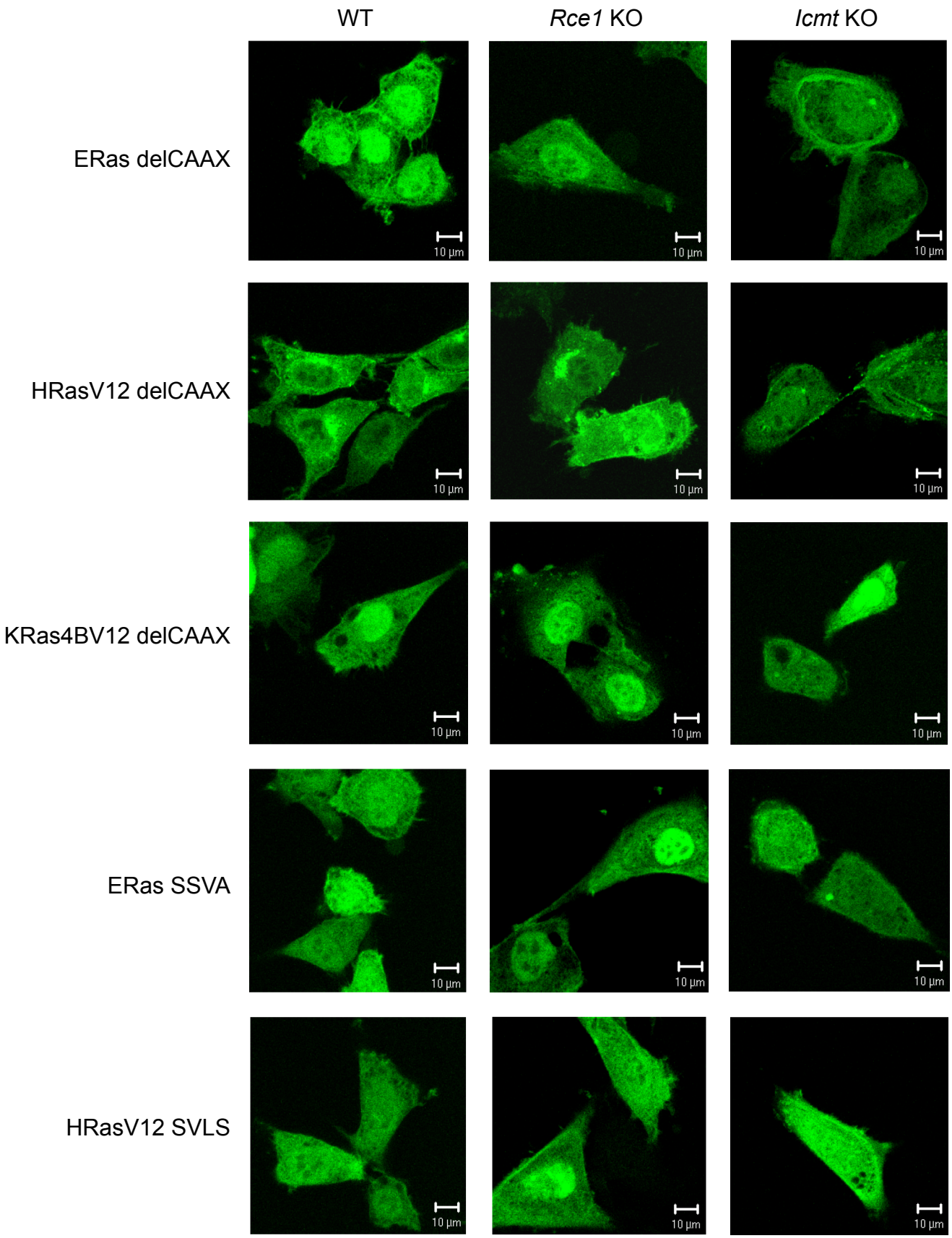

Figure 7. Intracellular localization of CAAX deletion mutants in wild-type, Rce1 KO or Icmt KO MEFs.
Wild-type, Rce1 KO or Icmt KO MEFs expressing EGFP-ERas delCAAX, EGFP-HRasV12 delCAAX, EGFP-KRas4BV12 delCAAX, EGFP-ERas SSVA or EGFP-HRasV12 SVLS were fixed and observed with a confocal microscope (x 100).

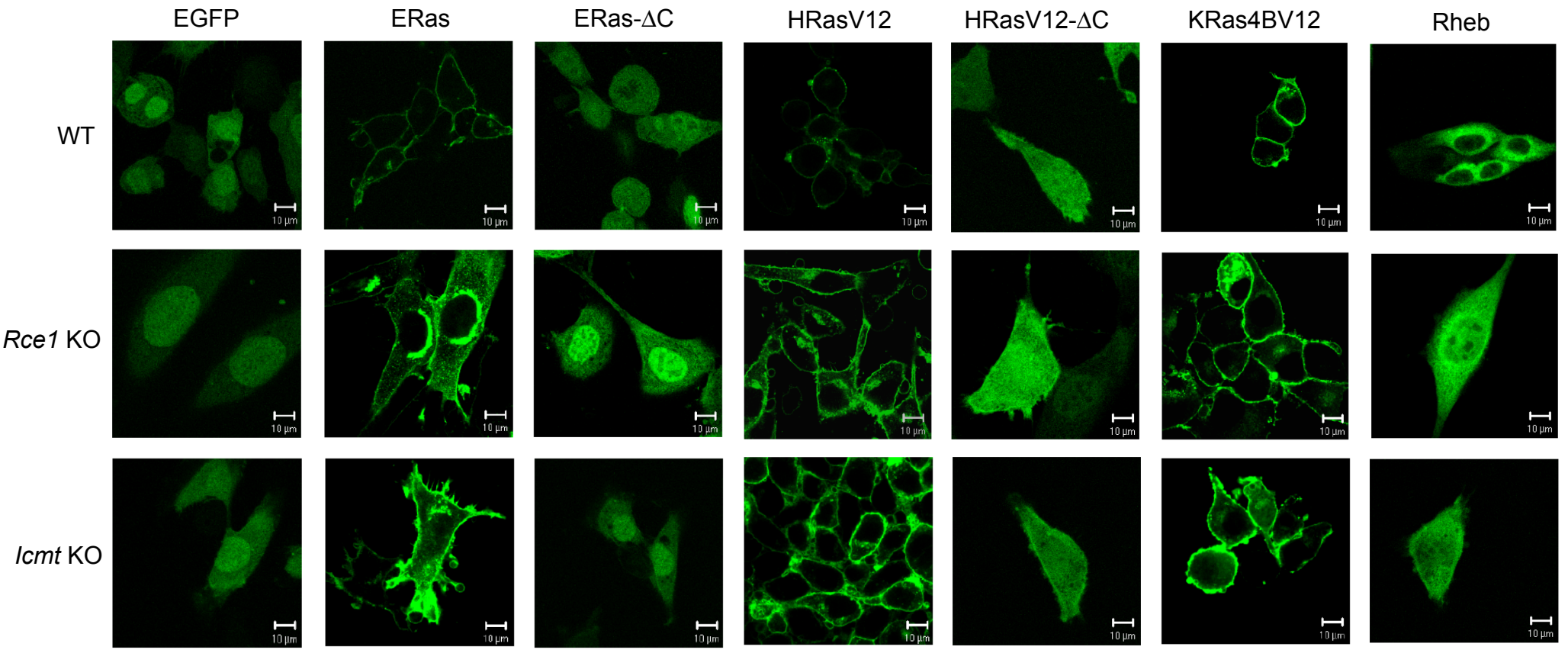

Figure 8. Intracellular localization of various Ras-related proteins in Wild-type, *Rce1* KO or *Icmt* KO MEFs.
Wild-type, *Rce1* KO or *Icmt* KO MEFs expressing EGFP, EGFP-ERas, EGFP-ERas-ΔC, EGFP-HRasV12, EGFP-HRasV12-ΔC, EGFP-KRas4BV12 or EGFP-Rheb were fixed and observed with a confocal microscope (x 100).

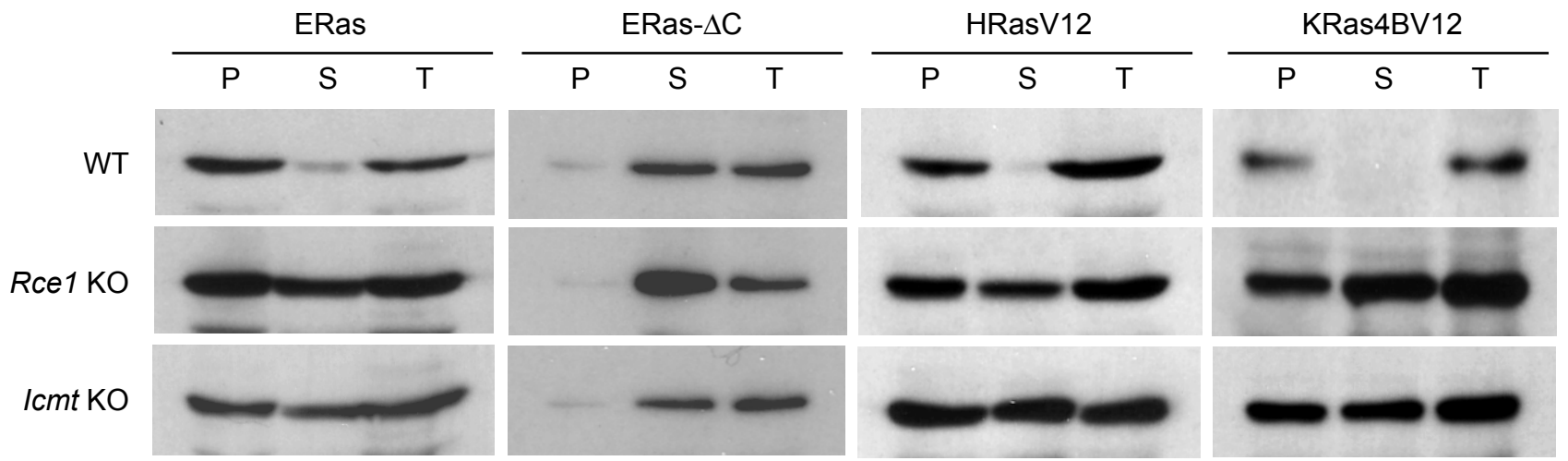

Figure 9. Subcellular fractionations of ERas, HRas and KRas4B.
Cells expressing EGFP-ERas, EGFP-ERas-ΔC, EGFP-HRasV12 or EGFP-KRas4BV12 were fractionated into cytosolic (S100; S) and membrane (P100; P) fractions. P100, S100 or Total lysate (T) were separated by SDS-PAGE and immunoblot was performed with anti-GFP polyclonal antibody.

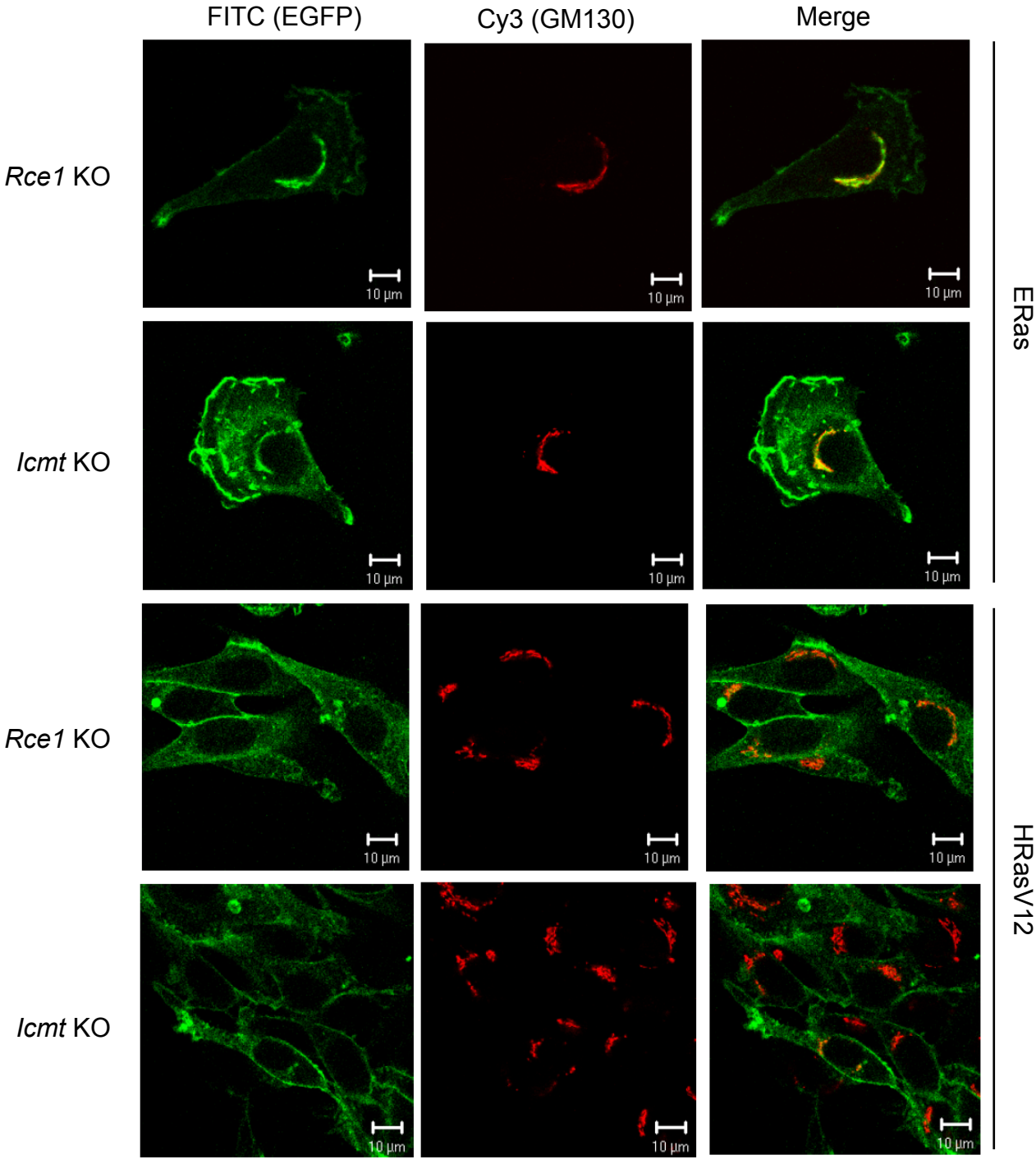

Figure 10. Co-localization of ERas and GM130 in *Rce1*- or *Icmt*-deficient MEFs.
Rce1 KO or *Icmt* KO MEFs expressing EGFP-ERas or EGFP-HRasV12 were fixed and incubated with anti-GM130 monoclonal antibody. After incubation, signals were visualized by using Cyanine3-labelled secondary antibody. These cells were observed with a confocal microscope (x 100).

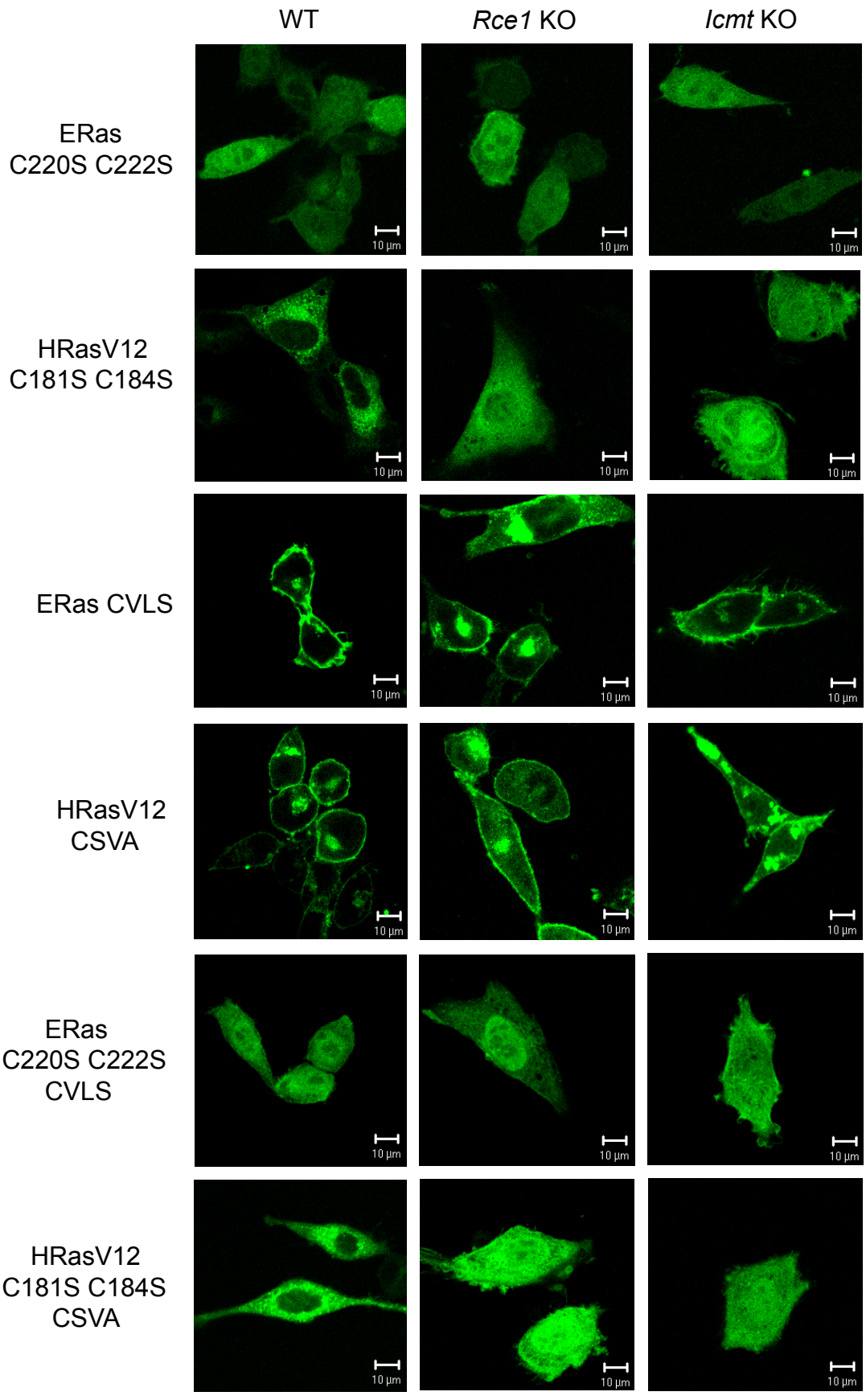

Figure 11. Intracellular localization of palmitoylation-deficient mutants of ERas and HRasV12. Wild-type, *Rce1* KO or *Icmt* KO MEFs expressing EGFP-ERas C220S C222S, EGFP-HRasV12 C181S C184S, EGFP-ERas CVLS, EGFP-HRasV12 CSVA, EGFP-ERas C220S C222S CVLS or EGFP-HRasV12 C181S C184S CSVA were fixed and observed with a confocal microscope (x 100).

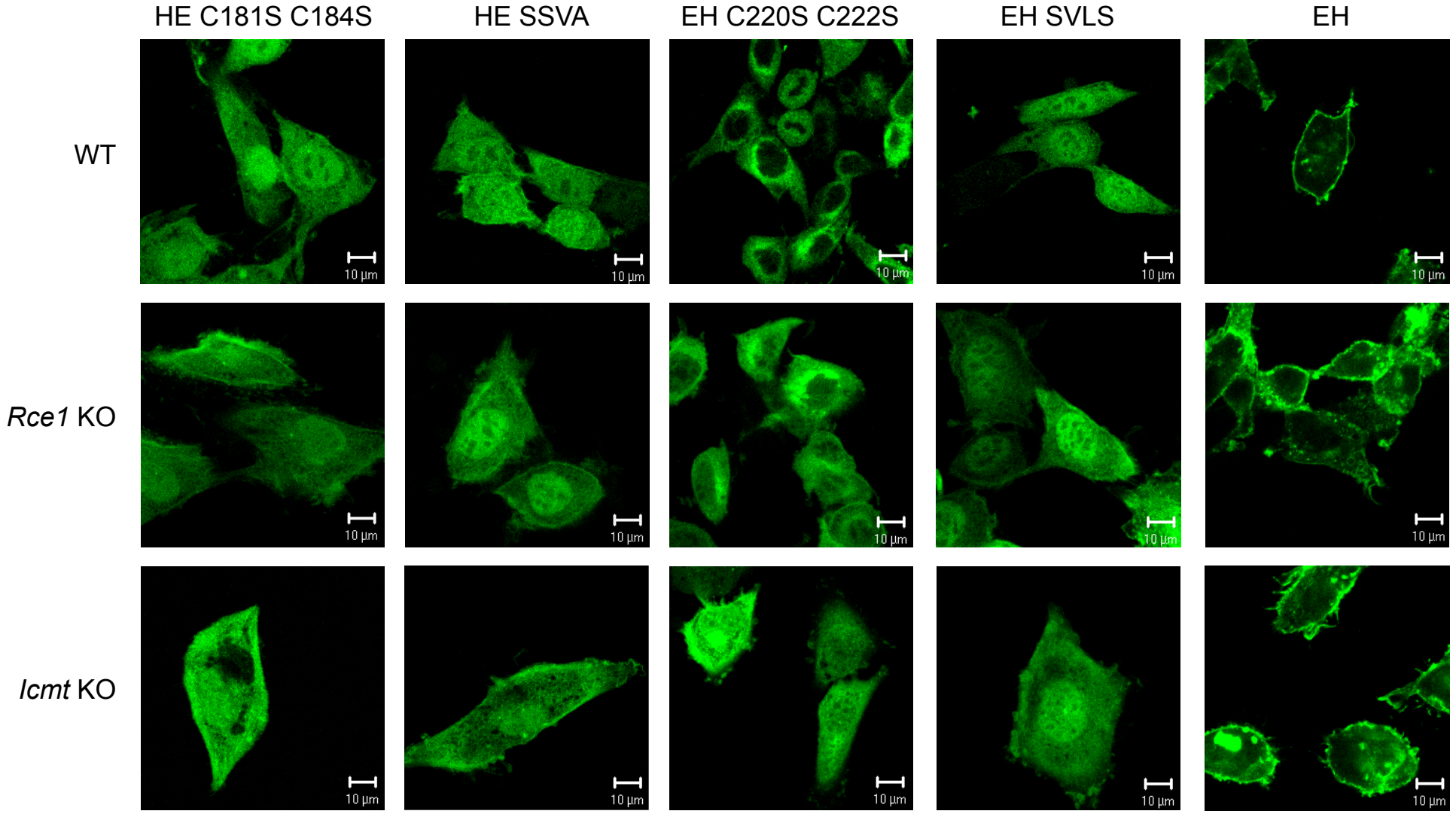

Figure 12. Intracellular localization of ERas-HRas chimeric proteins in wild-type, *Rce1* KO or *Icmt* KO MEFs.
Wild-type, *Rce1* KO or *Icmt* KO MEFs expressing EGFP-HE C181S C184S, EGFP-HE SSVA, EGFP-EH C220S C222S, EGFP-EH SVLS and EGFP-EH were fixed and observed with a confocal microscope (x 100).

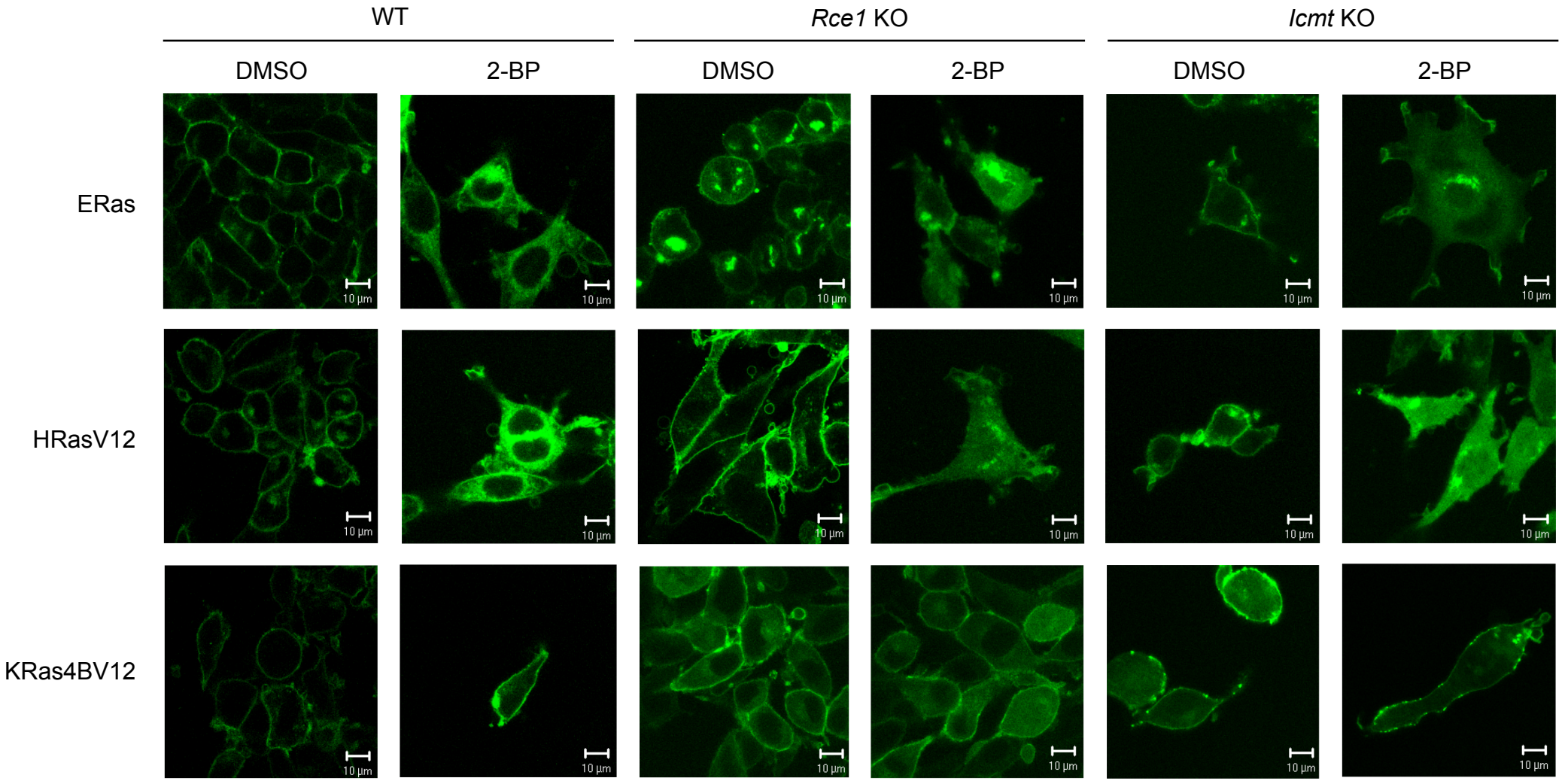

Figure 13. Palmitoylation inhibitor induced translocation of ERas to endomembrane.
Wild-type, *Rce1* KO or *Icmt* KO MEFs expressing EGFP-ERas, EGFP-HRasV12 or EGFP-KRas4BV12 were treated with DMSO or 25 µM of 2-bromopalmitate for 16 hours. Cells were fixed and observed with a confocal microscope (x 100).

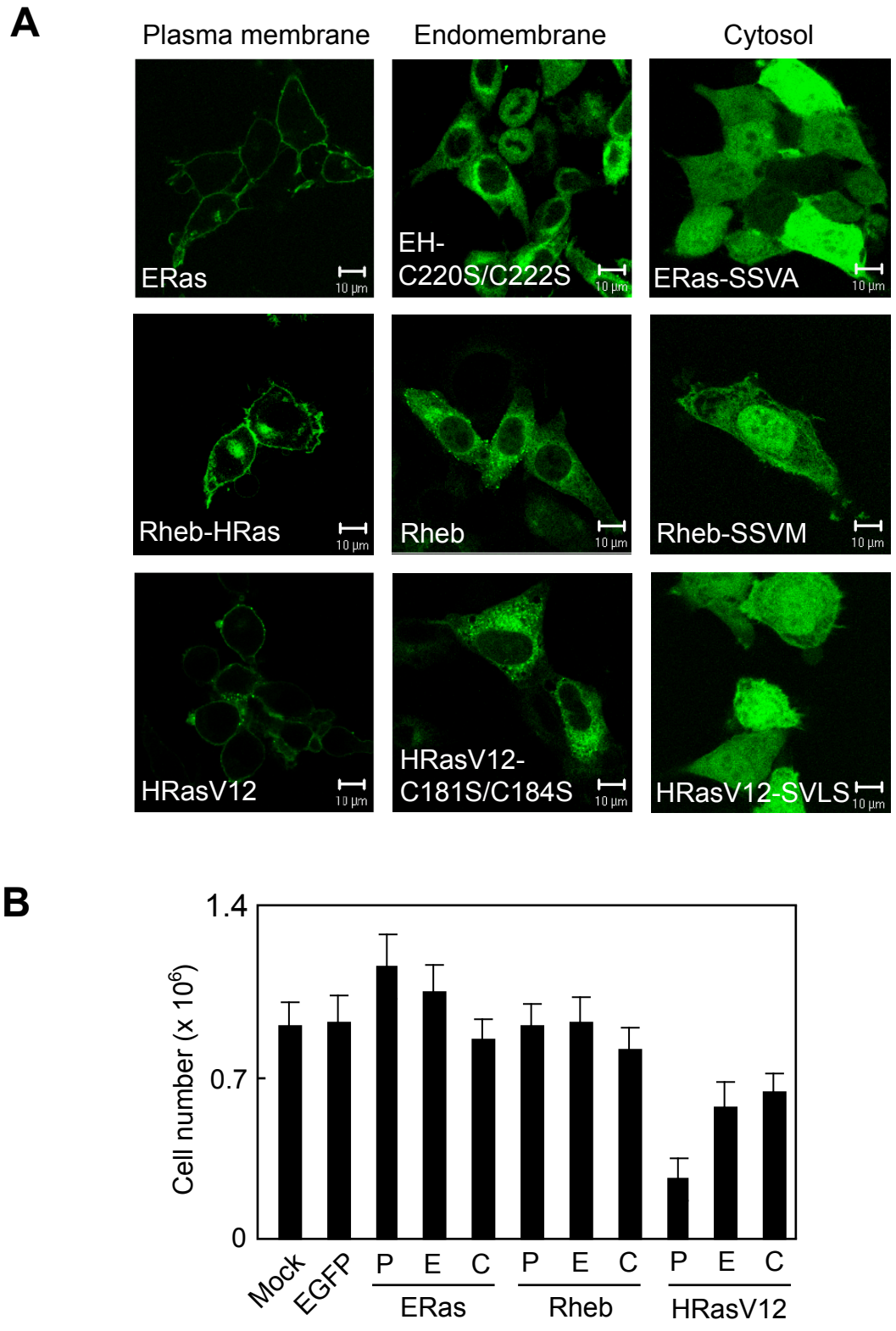

Figure 14. Effect of intracellular localization on functions of ERas, Rheb and HRas.
A. Intracellular localization of mutants of ERas, Rheb and HRasV12 in MEFs. EGFP-ERas, EGFP-Rheb-HRas and EGFP-HRasV12 were located at plasma membrane. EGFP-EH C220S C222S, EGFP-Rheb and EGFP-HRasV12 C181S C184S were located at endomembrane. EGFP-ERas SSVA, EGFP-Rheb SSVM and EGFP-HRasV12 SVLS were located in cytoplasm.
B. ES cell proliferation. MG1.19 ES cells introduced pPyCAG-IP or pPyCAG-IP encoding EGFP, Myc-ERas (ERas; P), Myc-EH-C220S/C222S (ERas; E), Myc-ERas-SSVA (ERas; C), Myc-Rheb-HRas (Rheb; P), Myc-Rheb (Rheb; E), Rheb-SSVM (Rheb; C), Myc-HRasV12 (HRasV12; P), Myc-HRasV12-C181S/C184S (HRasV12; E) or Myc-HRasV12-SVLS (HRasV12; C) were plated at 1 x 10^4 cells per well and counted at day 6 (n=3).

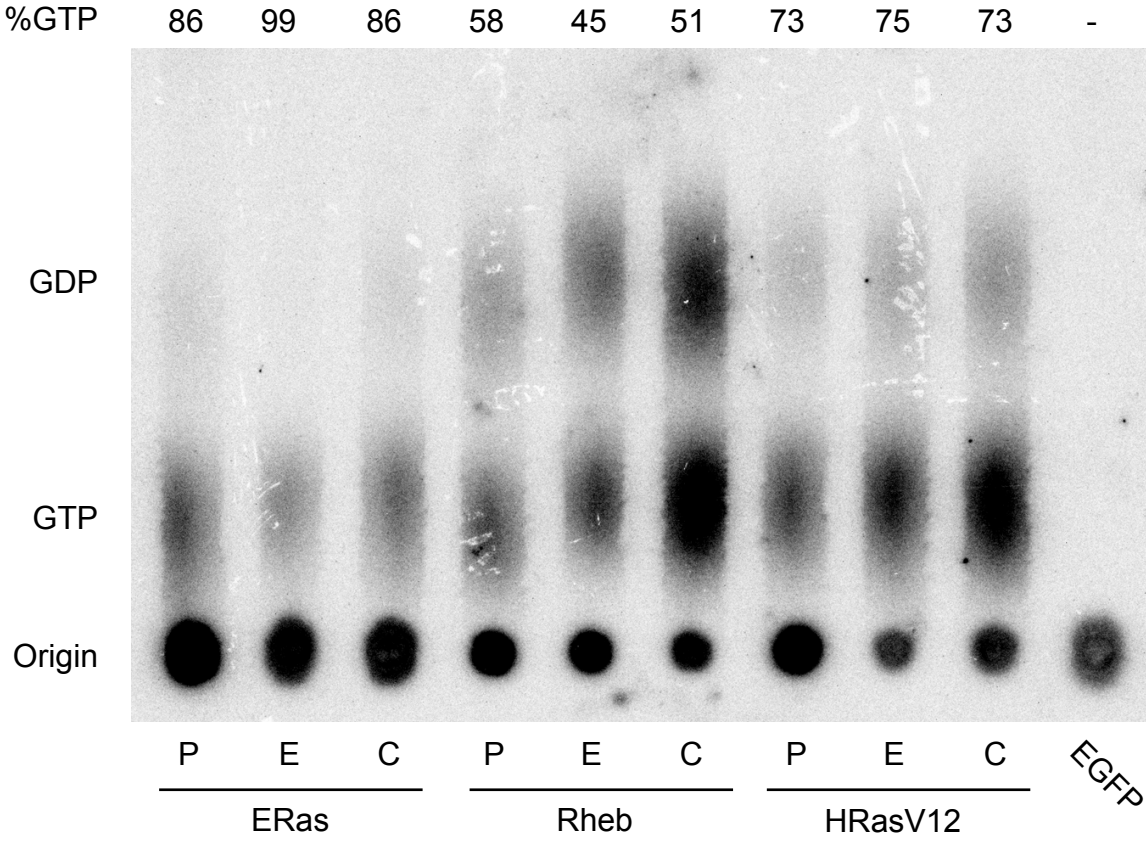

Figure 15. Effect of intracellular localization on GTP/GDP association of ERas, Rheb and HRasV12. MG1.19 ES cells were transfected pPyCAG-IP encoding Myc-ERas, Myc-ERas-HRas-C220S/C222S, Myc-ERas-SSVA, Myc-Rheb-HRas, Myc-Rheb, Myc-Rheb-SSVM, Myc-HRasV12, Myc-HRasV12-C181S/C184S or Myc-HRasV12-SVLS. Twenty-four hours after transfection, cells were labeled with 0.05 mCi/ml of ^{32}P for 4 hours. After incubation, cells were lysed and immunoprecipitated with agarose conjugated anti-Myc monoclonal antibody. Nucleotides were eluted by SDS-containing sample buffer and separated by Thin-layer chlomatography. P, plasma membrane; E, endomembrane; C, cytoplasm.

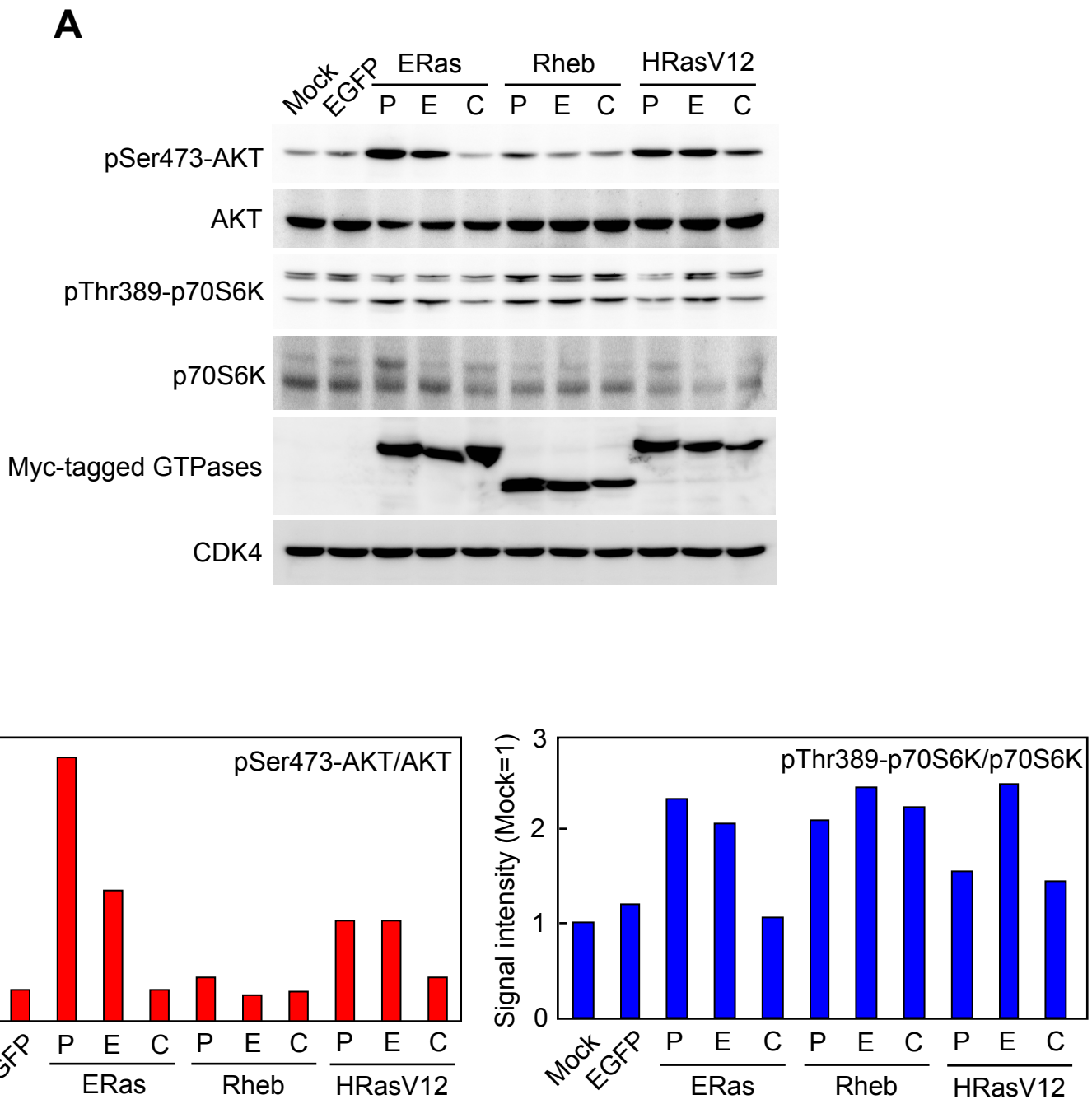

Figure 16. Phosphorylation status of AKT and p70S6K.
A. MG1.19 ES introduced with pPyCAG-IP or pPyCAG-IP encoding EGFP, Myc-ERas (ERas; P), Myc-EH-C220S/C222S (ERas; E), Myc-ERas-SSVA (ERas; C), Myc-Rheb-HRas (Rheb; P), Myc-Rheb (Rheb; E), Rheb-SSVM (Rheb; C), Myc-HRasV12 (HRasV12; P), Myc-HRasV12-C181S/C184S (HRasV12; E) or Myc-HRasV12-SVLS (HRasV12; C) were lysed, resolved on SDS-PAGE and transferred to PVDF membrane. Immunoblottings were performed with anti-phospho-Ser473-AKT, anti-AKT, anti-phospho-Thr389-p70S6K, anti-p70S6K, anti-Myc or anti-CDK4 antibodies.
B. Signals were quantified by LAS-3000 (n=3).

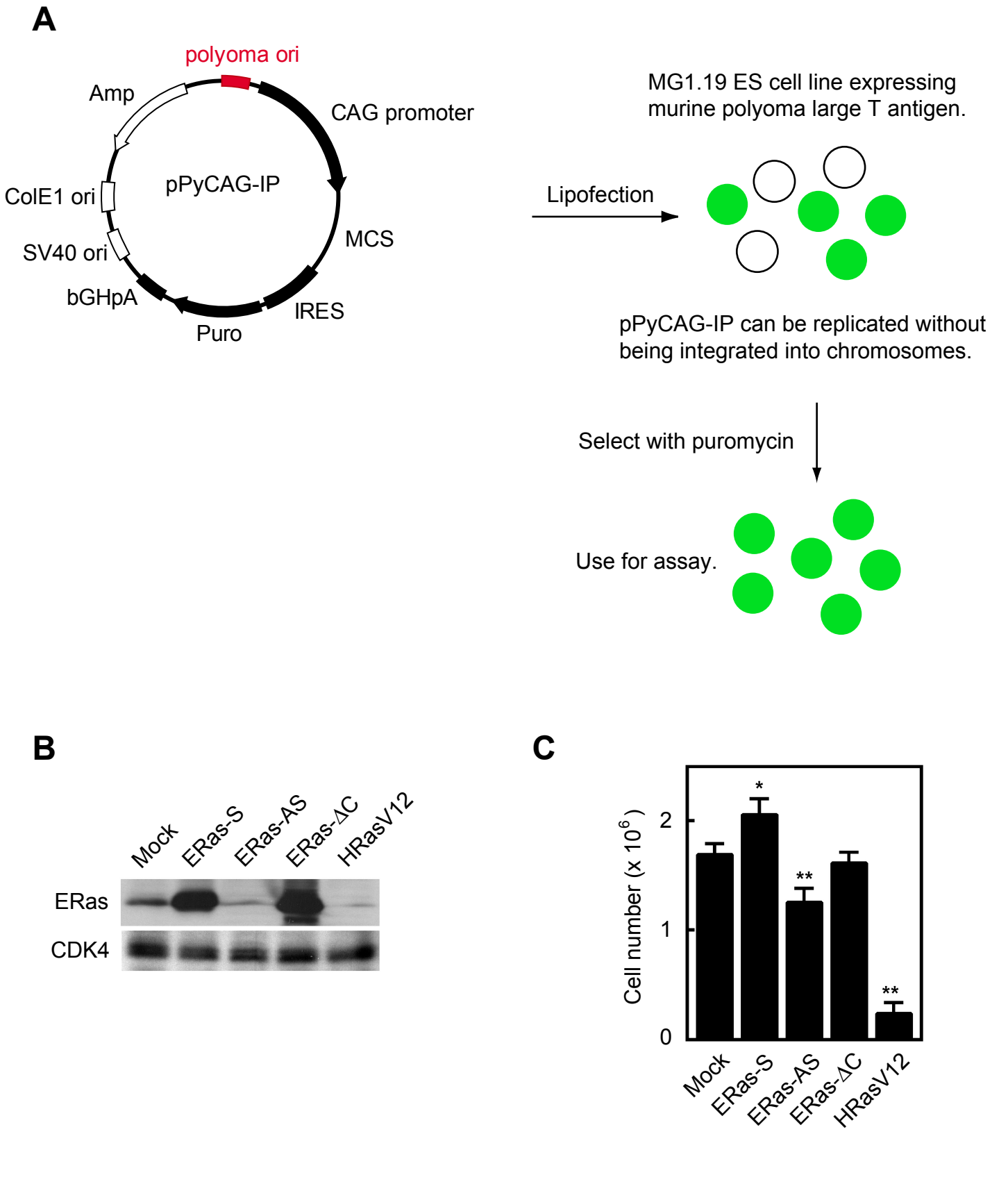

Figure 17. Forced expression of ERas in ES cells.
A. Forced expression strategy with pPyCAG-IP and MG1.19 ES cells. polyoma ori, murine polyoma virus replication origin; CAG promoter, chickin beta actin and rabbit beta globin intron chimeric promoter; MCS, multi cloning site; bGHpA, bovine growth hormone poly adenylation signal.
B. Expressin level of ERas. MG1.19 ES cells introduced pPyCAG-IP or pPyCAG-IP encoding ERas (ERas-S), antisense ERas (ERas-AS), ERas-ΔC or HRasV12 were lysed, separated by SDS-PAGE and transferred to a PVDF membrane. Immunoblots were performed with anti-ERas and anti-CDK4 antibodies.
C. ES cell proliferation. Cells used in B were plated at 1 x 10^4 cells per well and counted at day 6.

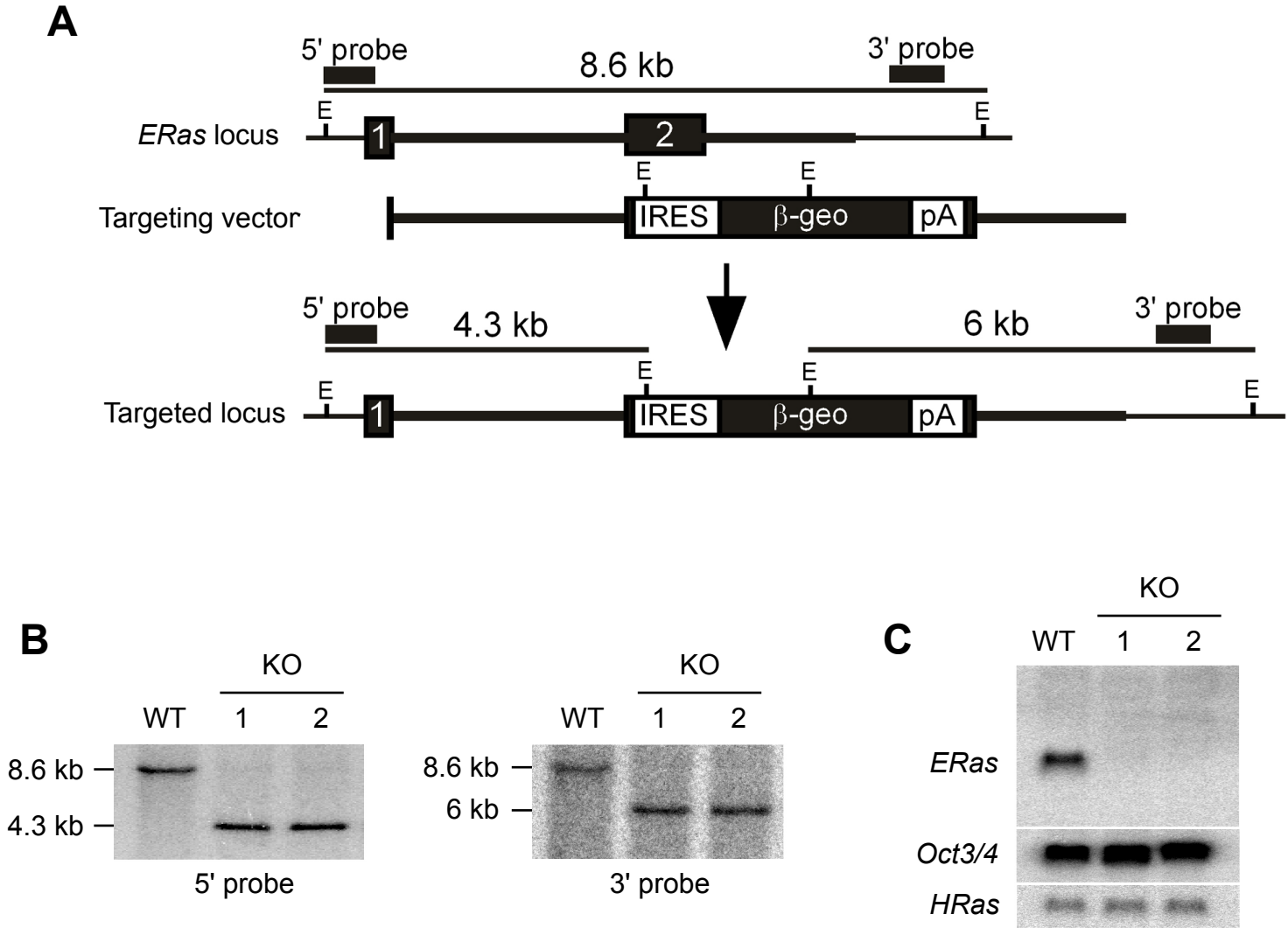

Figure 18. Targeted disruption of *ERas* gene.
A. Strategy for targeting of *ERas* gene. Filled boxes indicate exons. The length of diagnostic *Eco*RI (E) restriction fragments and location of the 5' and 3' flanking probes are shown.
B. Southern blotting to confirm homologous recombination. WT, wild-type ES cells; KO, *ERas* knockout ES cells.
C. Northen blotting.

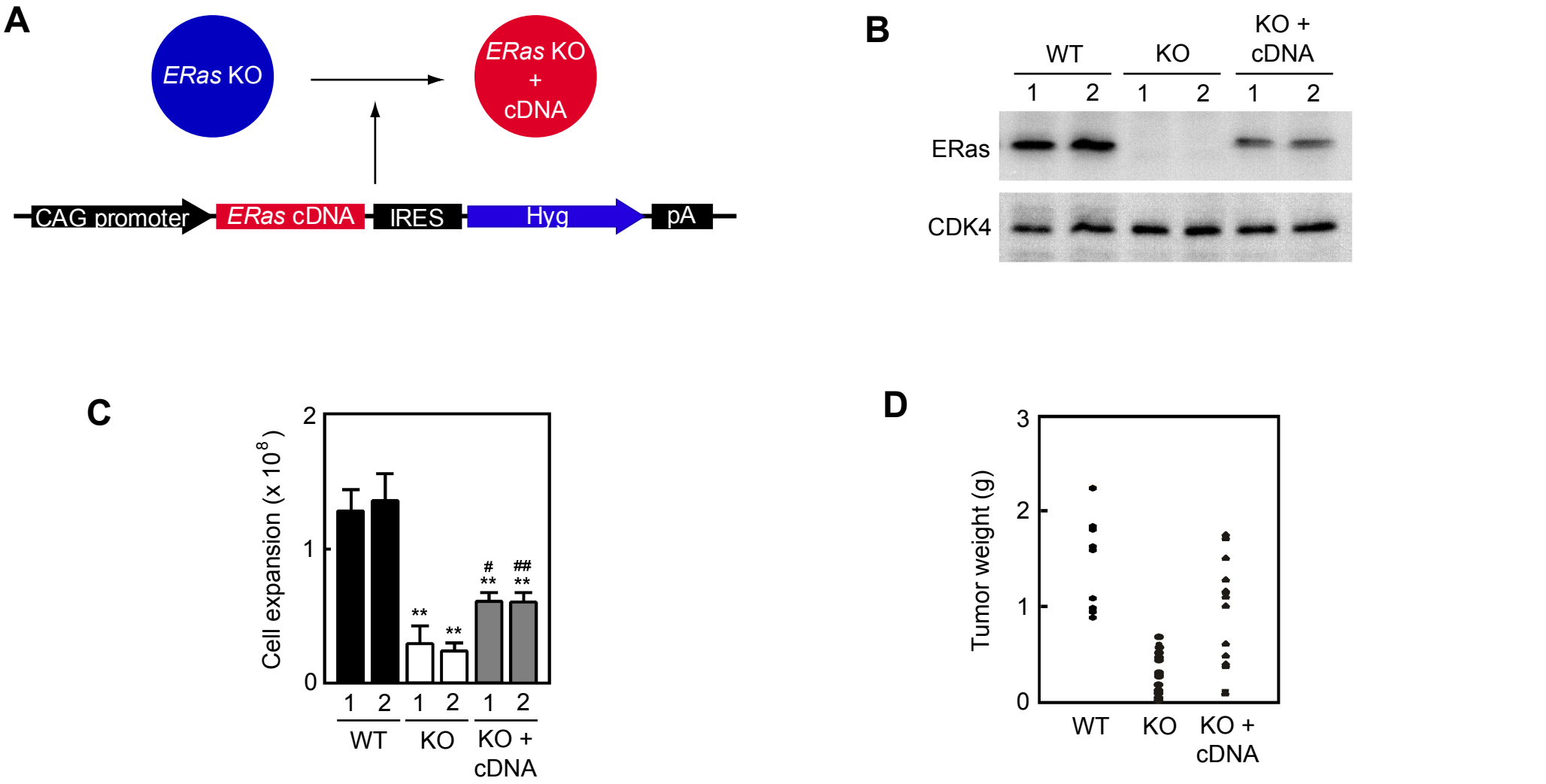

Figure 19. ERas promotes proliferation and tumorigenicity of ES cells.

A. Establishment of *ERas* KO + cDNA ES cells.

B. Immunoblotting. Wild-type ES cells (WT), *ERas* KO ES cells (KO) and *ERas* KO + cDNA ES cells (KO + cDNA) were lysed, separated by SDS-PAGE and transferred to PVDF membrane. Immunoblot was performed with anti-ERas and anti-CDK4 antibodies.

C. Cell expansion after 16 days of culture.

D. Teratoma formation. One million cells were subcutaneously injected into nude mice. Teratomas were dissected and weighted after 28 days.

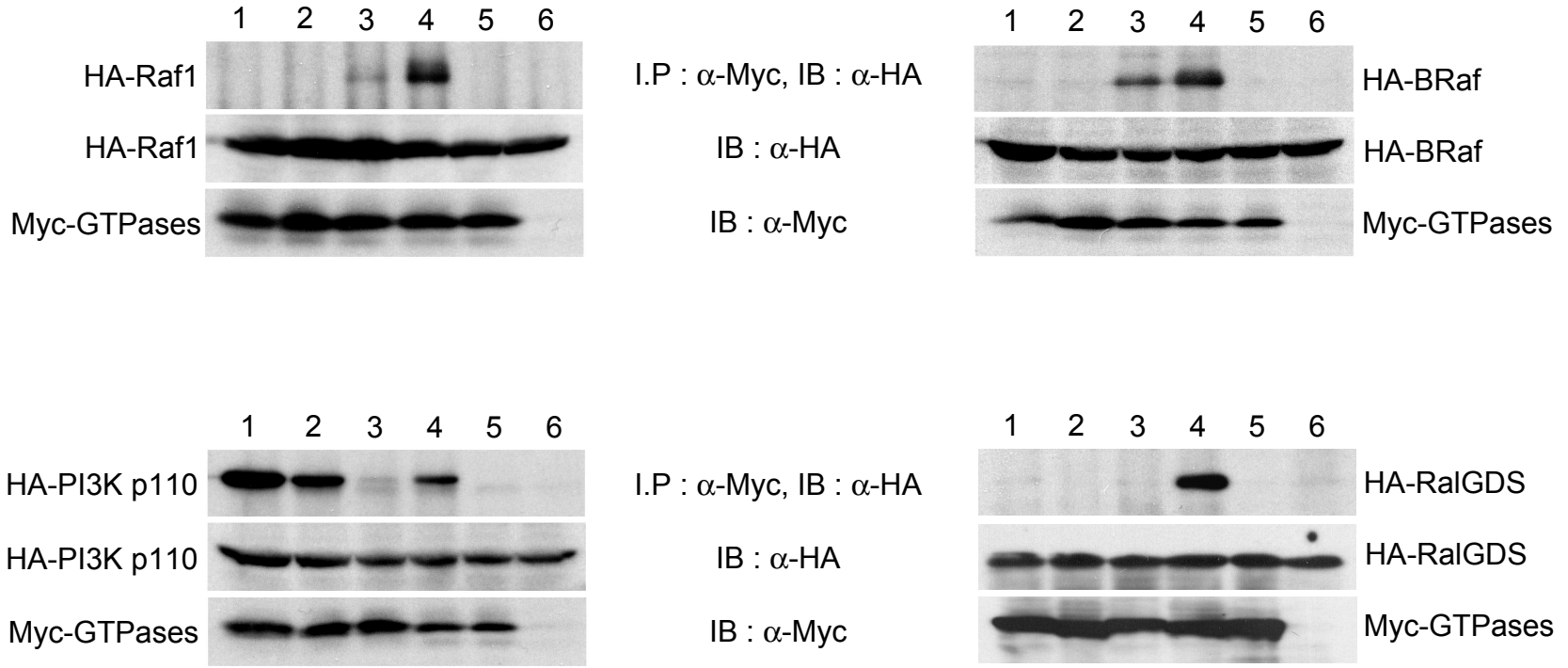

Figure 20. ERas interacts with p110.
MG1.19 ES cells were transfected with pPyCAG-IP encoding Myc-human ERas (lane 1), Myc-mouse ERas (lane 2), Myc-HRas (lane 3), Myc-HRasV12 (lane 4), Myc-HRasN17 (lane 5) or EGFP (lane 6) along with pPyCAG-IP encoding HA-Raf1, HA-BRaf, HA-p110 or HA-RalGDS. Twenty four hours after transfection, cells were lysed and incubated with agarose conjugated anti-Myc monoclonal antibody. Immunoprecipitants and total cell lysates were separated by SDS-PAGE and transferred to PVDF membranes. Immunoblot was performed with anti-HA and anti-Myc antibodies.

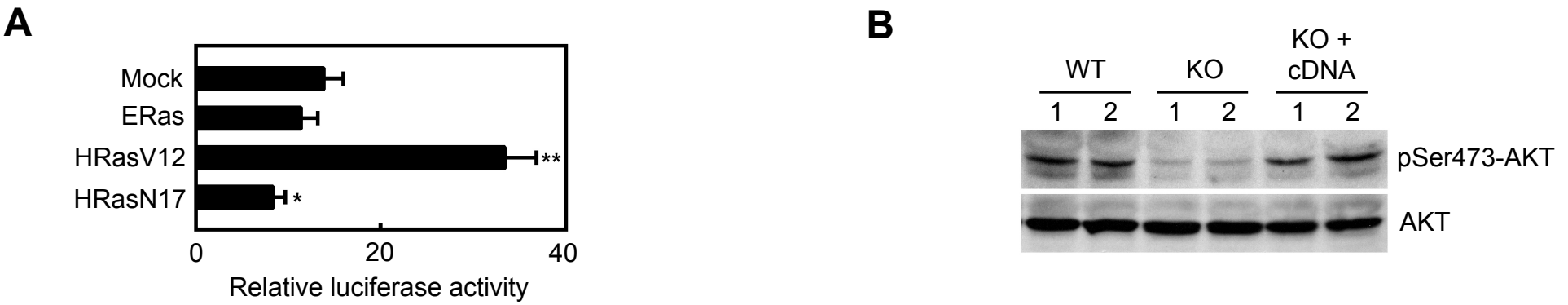

Figure 21. ERas activates PI3K but not MAPK.

A. AP1 reporter assay. MG1.19 ES cells were transfected 0.8 μg of pPyCAG-IP (Mock) or pPyCAG-IP encoding ERas, HRasV12 or HRasN17 along with 0.2 μg of pAP1-TAL-Luc and 0.025 μg of pRL-TK. Twenty four hours after transfection, cells were lysed and luciferase activities were measured.

B. Phosphorylation status of AKT. Wild-type ES cells (WT), *ERas* KO ES cells (KO) and *ERas* KO + cDNA ES cells (KO + cDNA) in log phase were lysed, separated by SDS-PAGE and transferred to a PVDF membrane. Immunoblot was performed with anti-phospho-Ser473-AKT and anti-AKT antibodies.

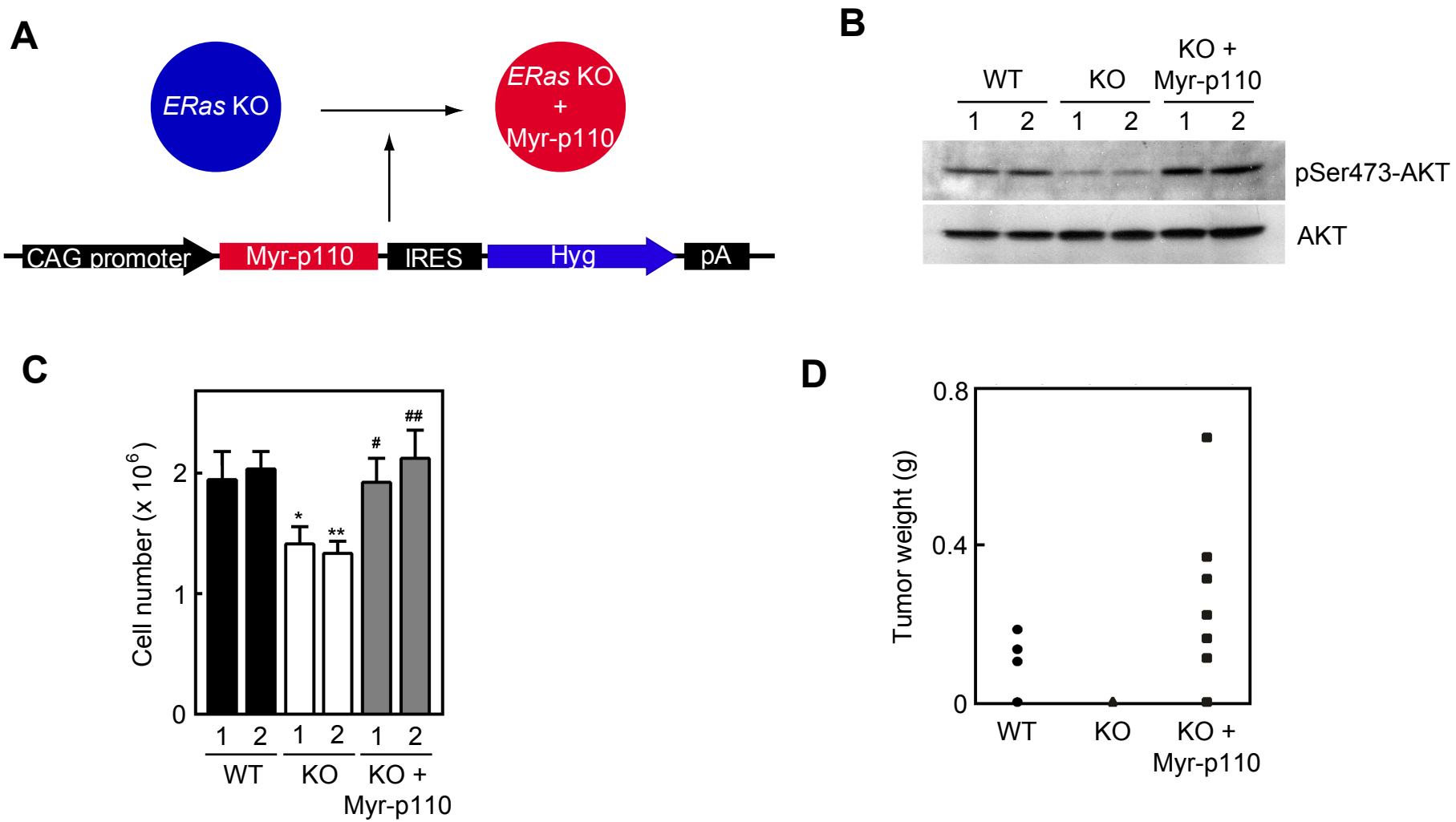

Figure 22. PI3K activation by ERas.

A. Establishment of *ERas* KO + Myr-p110 ES cells.

B. Phosphorylation status of AKT.

C. ES cell proliferation. Wild-type ES cells (WT), *ERas* KO ES cells (KO) and *ERas* KO + Myr-p110 ES cells (KO + Myr-p110) were plated 1 x 10^4 cells per well and countedat day 6. Asterisk, $P < 0.05$; double asterisks, $P < 0.01$ versus Mock transfected; dagger, $P < 0.05$; double daggers, $P < 0.01$ versus KO2 (n = 4).

D. Teratoma formation. One million cells were subcutaneously injected into nude mice. Teratomas were dissected and weighted after 16 days.

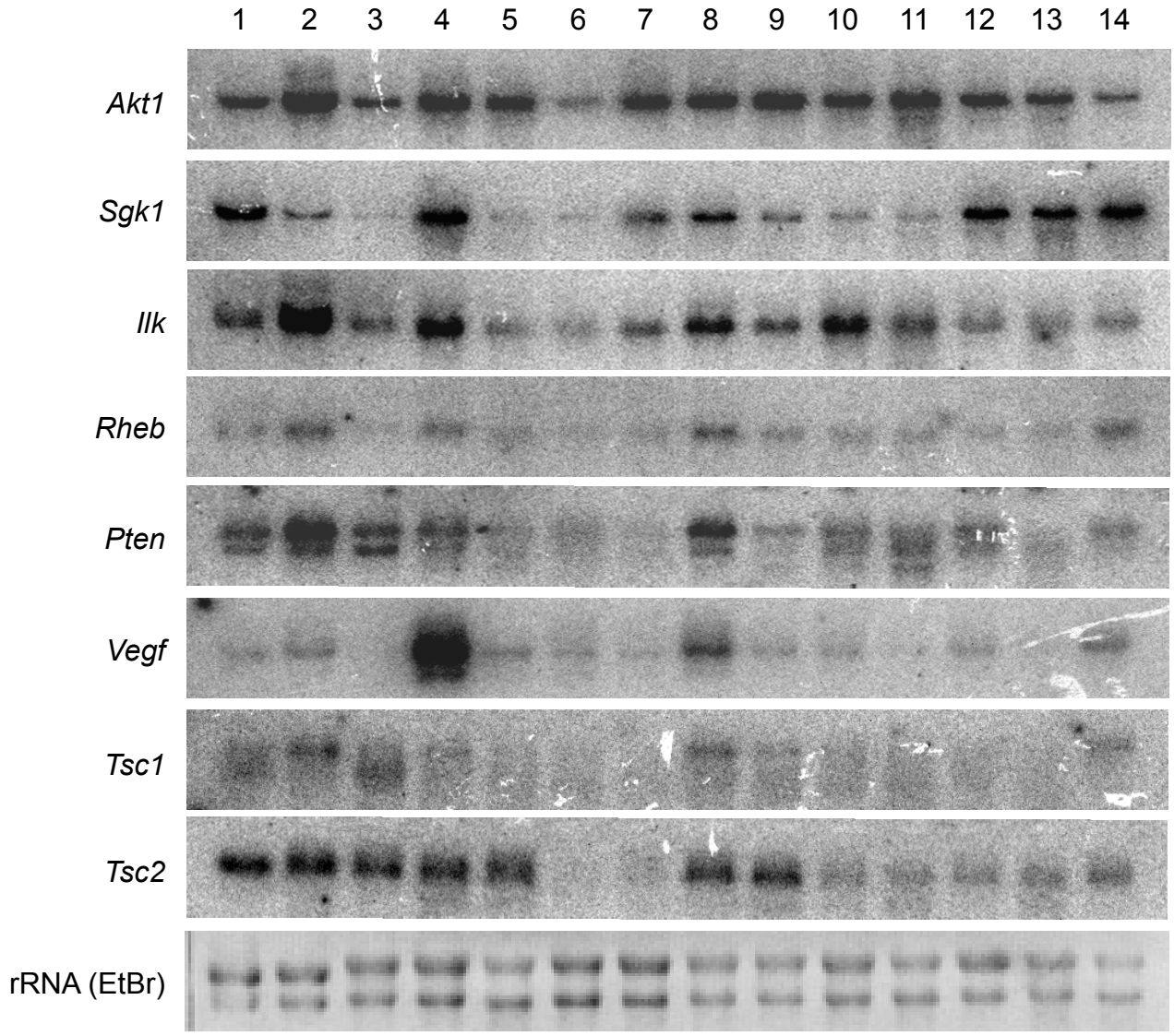

Figure 23. Expression pattern of PI3K related genes.
Northern blotting with *Akt1*, *Sgk1*, *Ilk*, *Rheb*, *Pten*, *Vegf*, *Tsc1* and *Tsc2* cDNA probes. 1, Undifferentiated ES cell; 2, Retinoic actid treated ES cells; 3, Tesitis; 4, Lung; 5, Heart; 6, Liver; 7, Stomach; 8, Kidney; 9, Brain; 10, Spleen; 11, Thymus; 12, Small intestine; 13, Skin; 14, Muscle.

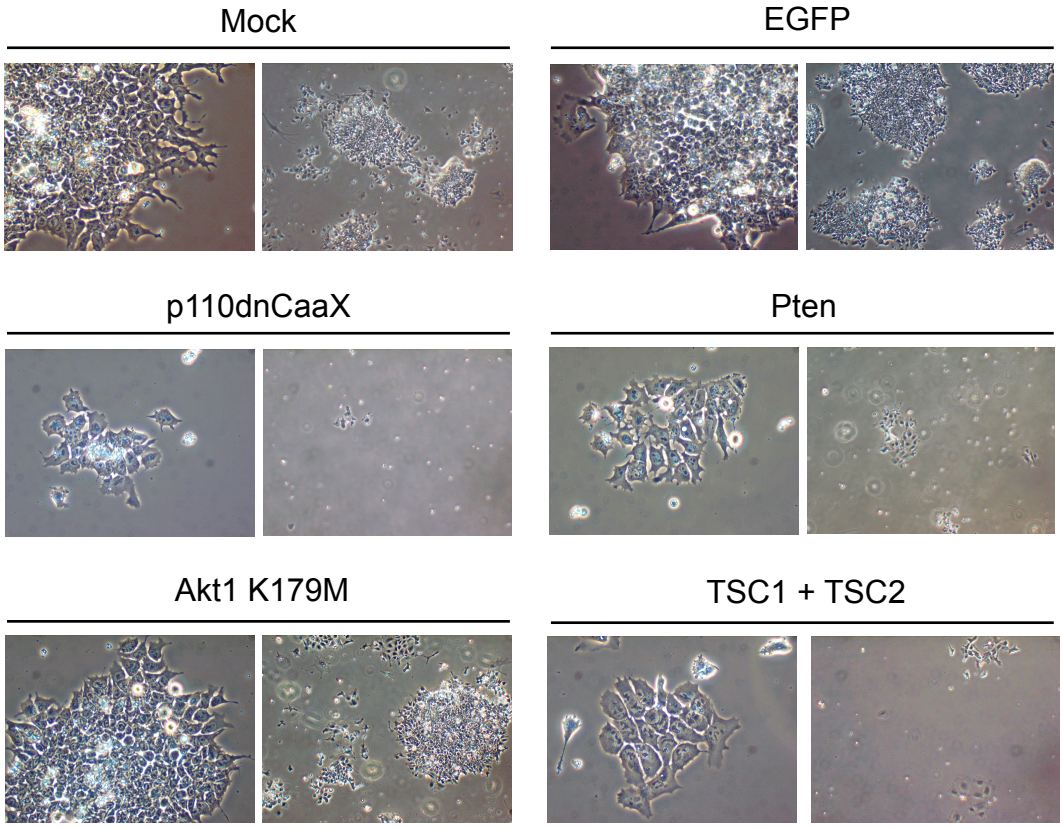

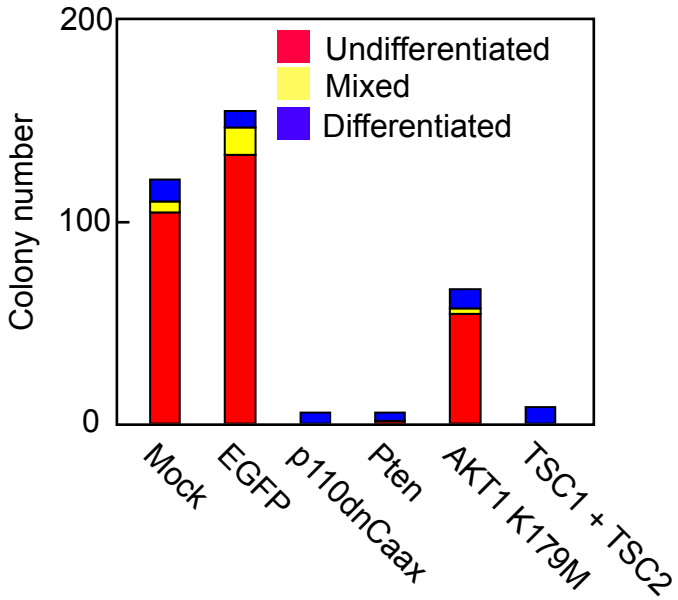

Figure 24. Effect on ES cell proliferation by forced-expression of PI3K related genes.
A. MG1.19 ES cells were transfected with pPyCAG-IP or pPyCAG-IP encoding EGFP, p110dnCaax, Pten, AKT K179M or TSC1 + TSC2. Cells were cultured with LIF and 2 μg/ml of puromycin for 6 days and photographed. Left panels, x 20; Right panels, x 4.
B. Colony number. Five hundreds of these cells were replated per well of 6-well plates. After 6 days, number of colonies were counted. Differentiation status of each colony was evaluated based on morphology.

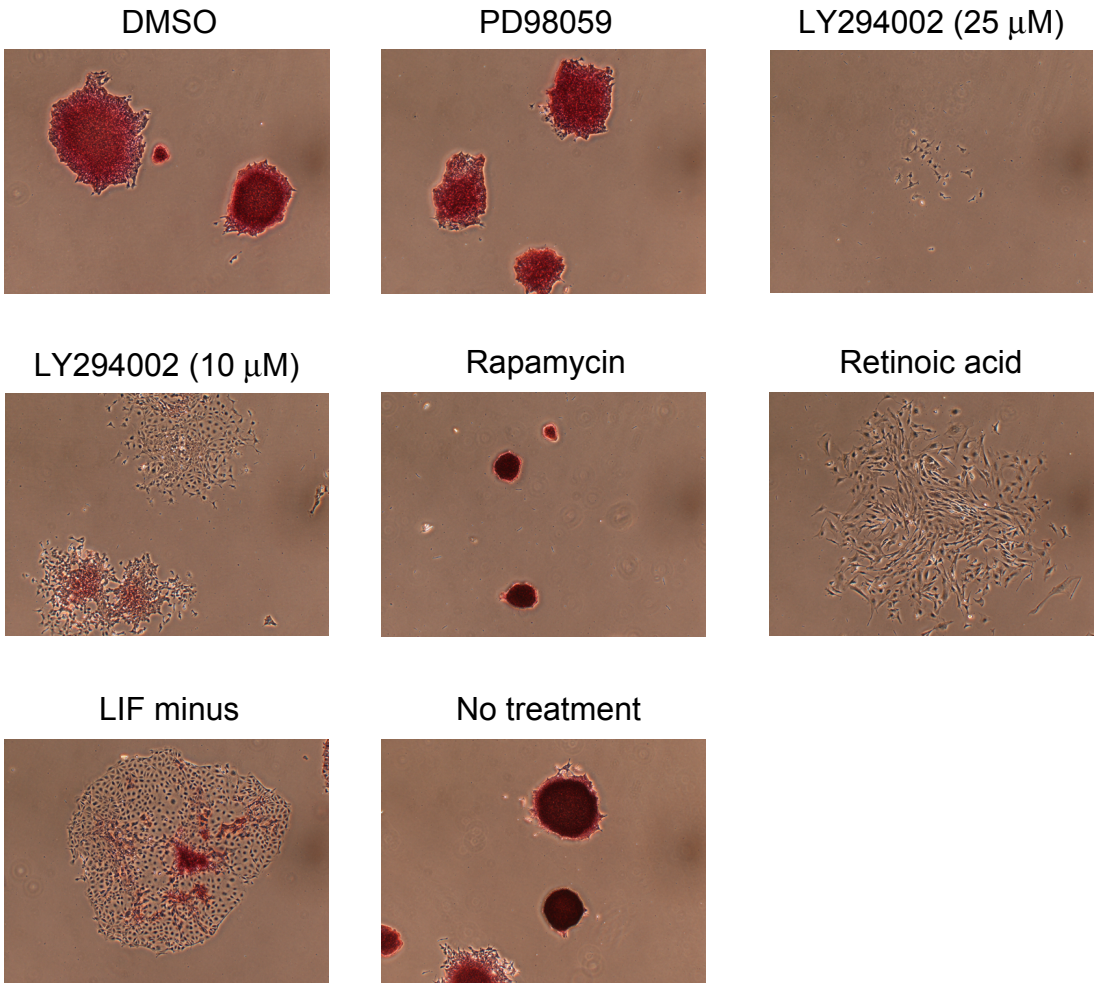

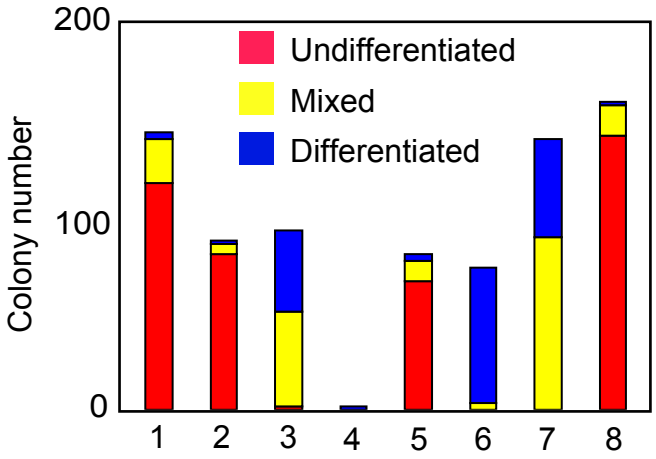

Figure 25. Effect of various inhibitors on colony formation.
A. MG1.19 ES cells were plated on gelatin-coated 6 well plates at 500 cells per well and incubated overnight. Next day, the cells were treated with DMSO (control), 25 μM of PD98059 (MEK inhibitor), 10 μM of LY294002 (PI3K inhibitor), 25 μM of LY294002, 20 nM of Rapamycin (TOR inhibitor), 3 x 10 M of Retinoic acid. The medium were changed every 2 days. After 5 days, cells were stained for alkaline phosphatase activitiy (AP) and photographed.
B. Colony number. Colonies conposing AP positive cells only were categorized as 'undifferentiated', AP positive and negative cells as 'mix' and AP negative cells only as 'differentiated'.

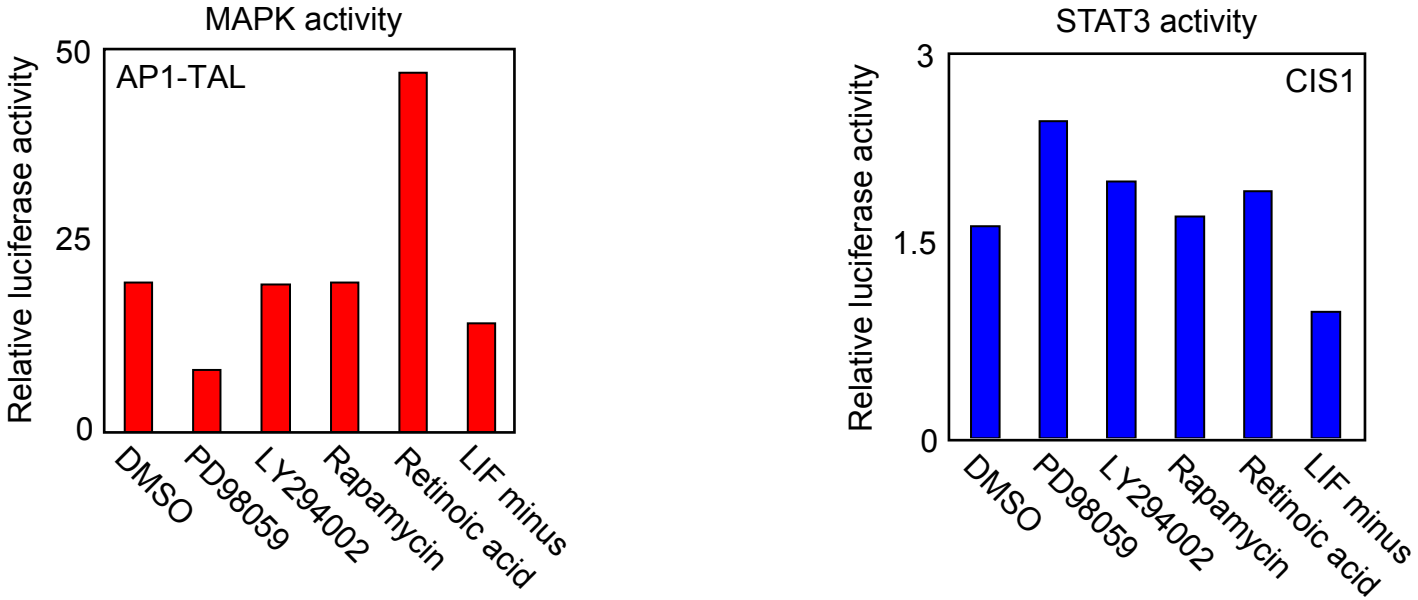

Figure 26. Effects of various inhibitors on MAPK and STAT3 activities in ES cells.
MG1.19 ES cells were transfected with 1 μg of pAP1-TAL-Luc or pCIS1-Luc along with 0.025 μg of pRL-TK. Twenty four hours after transfection, the cells were treated with DMSO, PD98059, LY294002, Rapamycin or Retinoic acid and incubated another 24 hours. Cells were lysed and luciferase activities were measured.

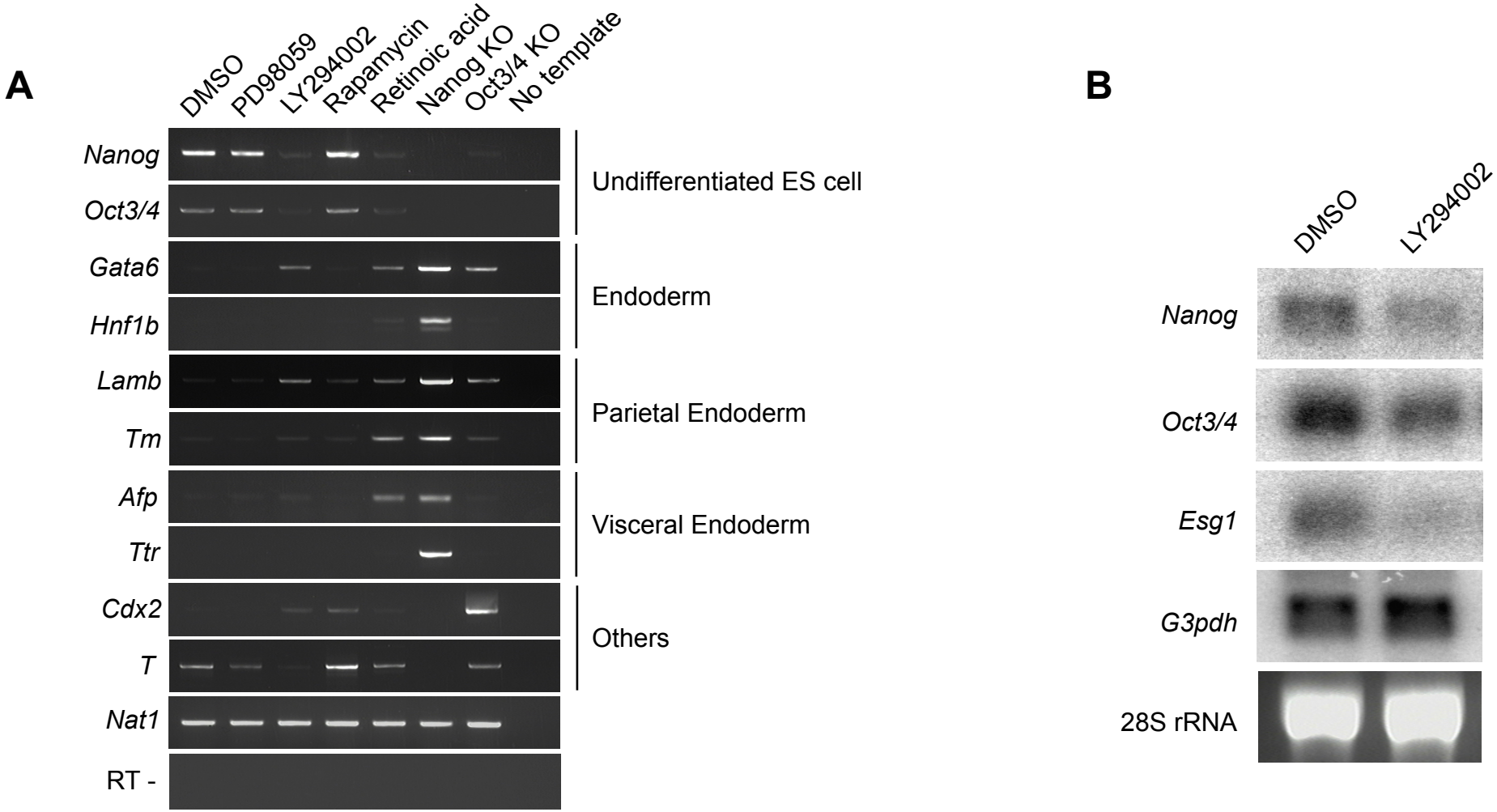

Figure 27. Expression patterns of marker genes.

A. MG1.19 ES cells were treated with DMSO, PD98059, LY294002, Rapamycin or Retinoic acid for 6 days. Total RNA of these cells were purified and used for templates of RT-PCR.

B. MG1.19 ES cells were treated with DMSO, PD98059, LY294002, Rapamycin or Retinoic acid for 16 hours. Total RNA of these cells were purified, separated on formardehyde-denaturing gel and transferred to nylon membranes. Northern blotting analyses were performed with *Nanog*, *Oct3/4*, *Esg1* and *G3pdh* cDNA probes.

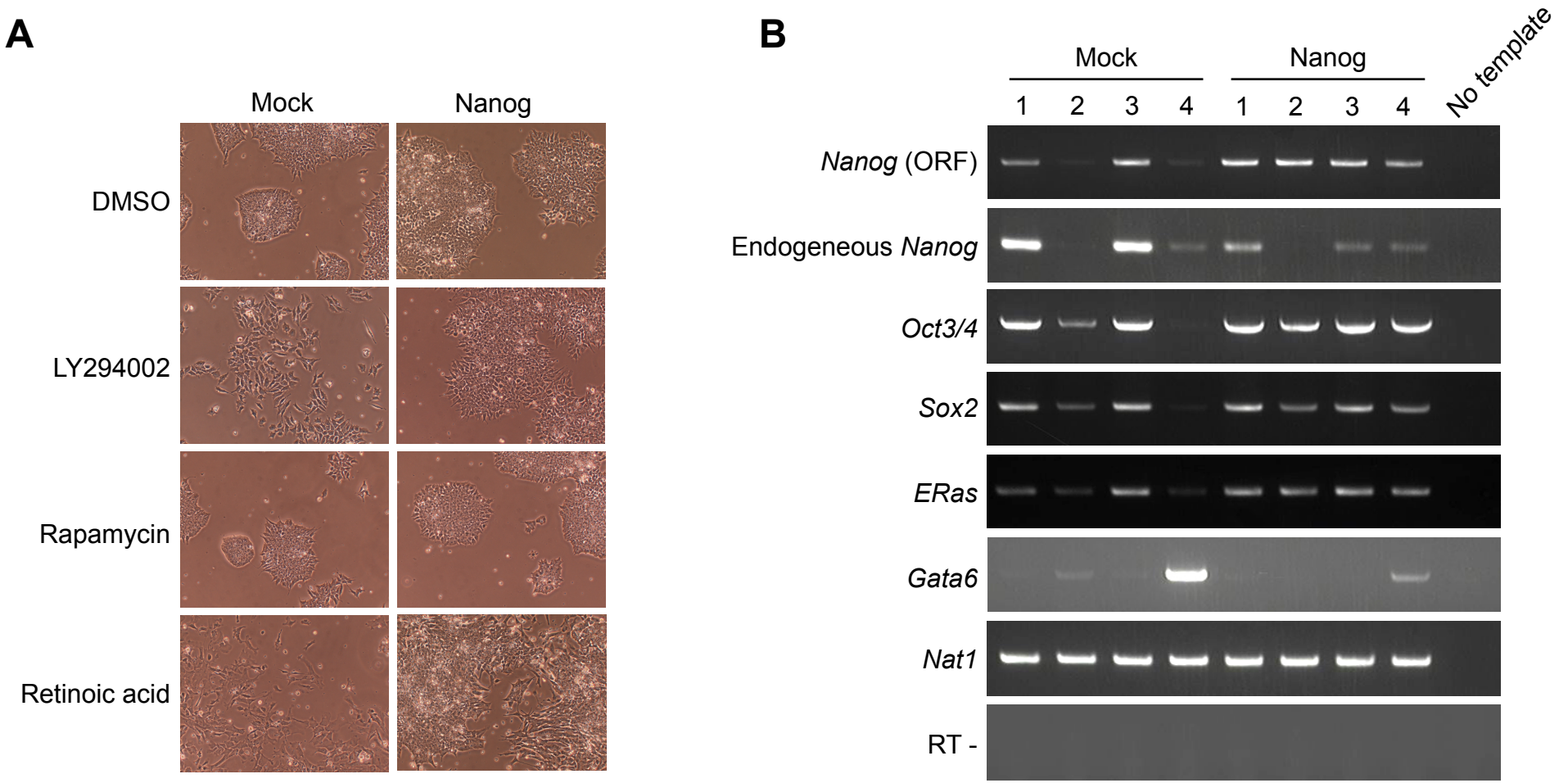

Figure 28. Transgenic expression of Nanog inhibits ES cell differentiation by LY294002-treatment.
A. MG1.19 ES cells were introduced with pPyCAG-IP or pPyCAG-IP encoding Flag-Nanog by lipofection. Cells were selected with 2 μg/ml of puromycin for 5 days. After selection, cells were plated at 1 x 10^5 cells per well of 6-well plates, cultured in the medium supplemented with DMSO, 10 μM of LY294002, 20 nM of Rapamycin or 300 nM of retinoic acid for 6 days and photographed.
B. Total RNA derived from the cells indicated A were used for first-strand cDNA synthesis. RT-PCR was performed with *Nanog* open reading frame, *Nanog* 3' untranslated region, *Oct3/4, Sox2, ERas, Gata6* or *Nat1* specific primers.

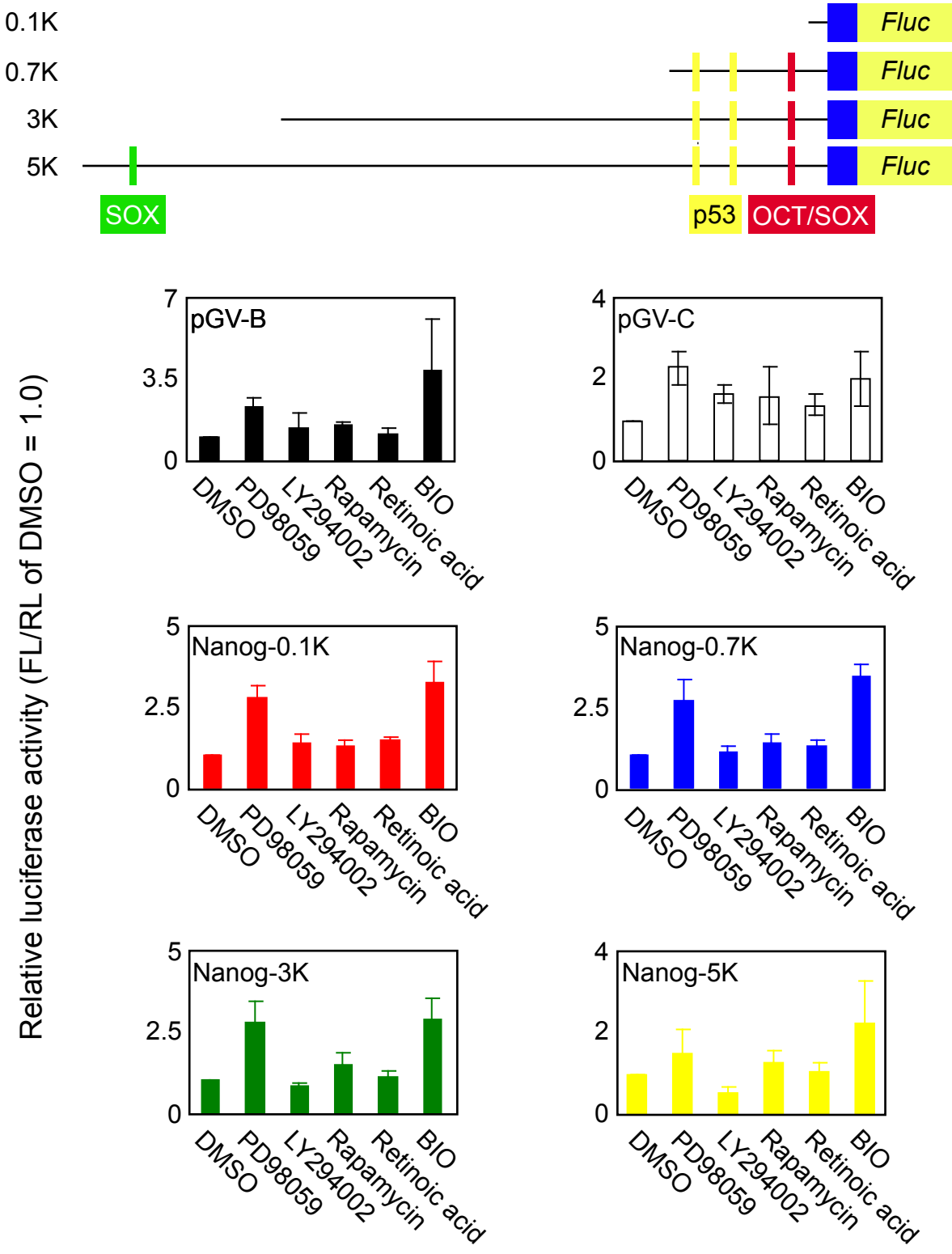

Figure 29. Effect of LY294002 on Nanog endogenous promoter.
MG1.19 ES cells expressing Nanog were seeded at 1 x 10^5 cells per well and incubated overnight. Next day, cells were transfected 1 μg of pGV-C, pGV-B or pGV-B containing fragments upstream region of Nanog gene (0.1, 0.7, 3 or 5 K) along with 0.025 μg of pRL-TK by using Lipofectamine 2000. Twenty-four hours after transfection, the medium was removed and add new one supplemented with DMSO, 25 μM of PD98059, 25 μM of LY294002, 20 nM of Rapamycin, 300 nM of retinoic acid or 2 μM of BIO and cells were cultured for 24 hours.

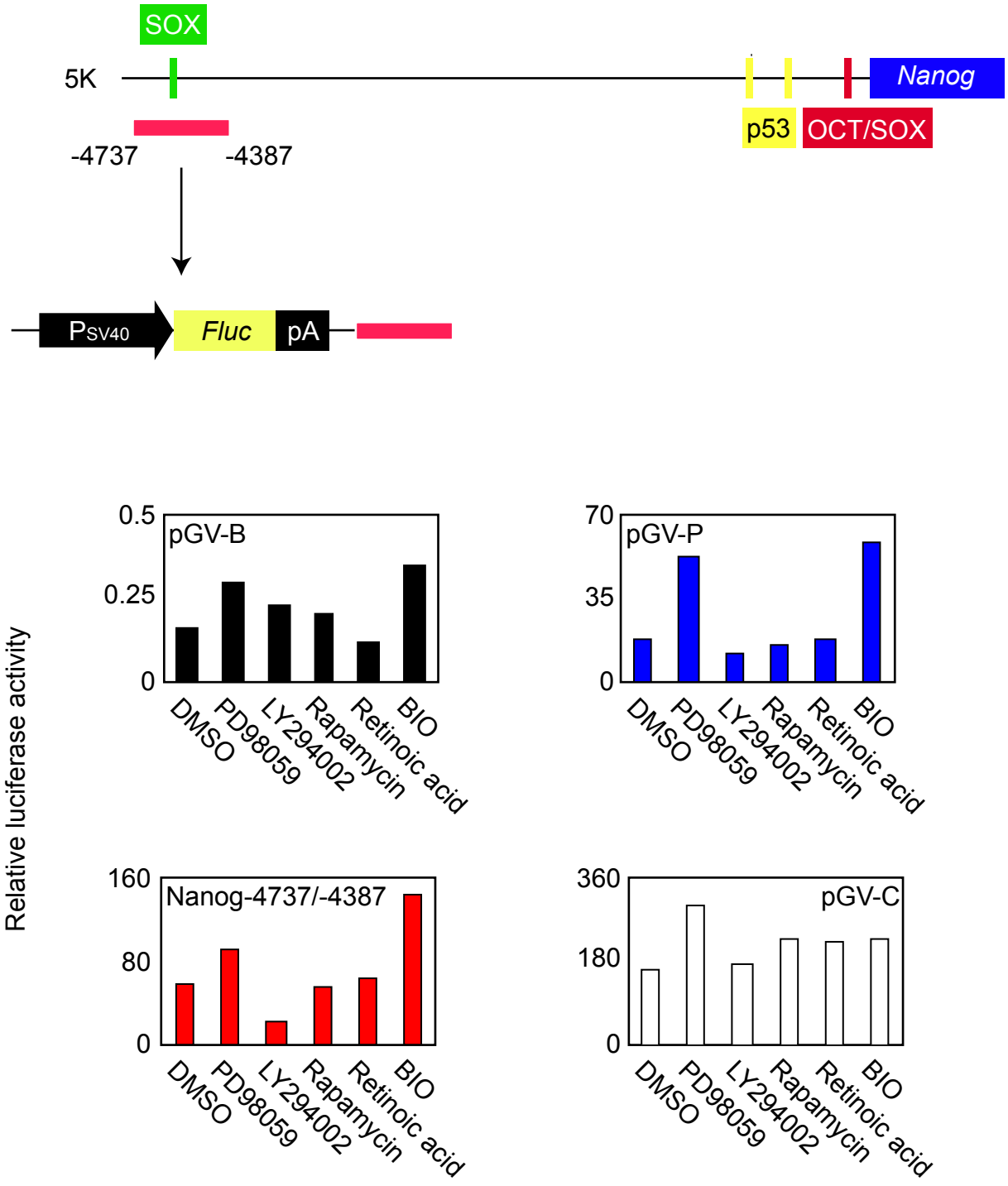

Figure 30. Effect of LY294002 on Nanog distal enhancer activity.
MG1.19 ES cells expressing Nanog were seeded at 1 x 10^5 cells per well and incubated overnight. Next day, cells were transfected 1 μg of pGV-B, pGV-C, pGV-P or pGV-P containing a fragment upstream region of Nanog gene (-4737/-4387) along with 0.025 μg of pRL-TK by using Lipofectamine 2000. Twenty-four hours after transfection, the medium was removed and add new one supplemented with DMSO, 25 μM of PD98059, 25 μM of LY294002, 20 nM of Rapamycin, 300 nM of retinoic acid or 2 μM of BIO and cells were cultured for 24 hours.

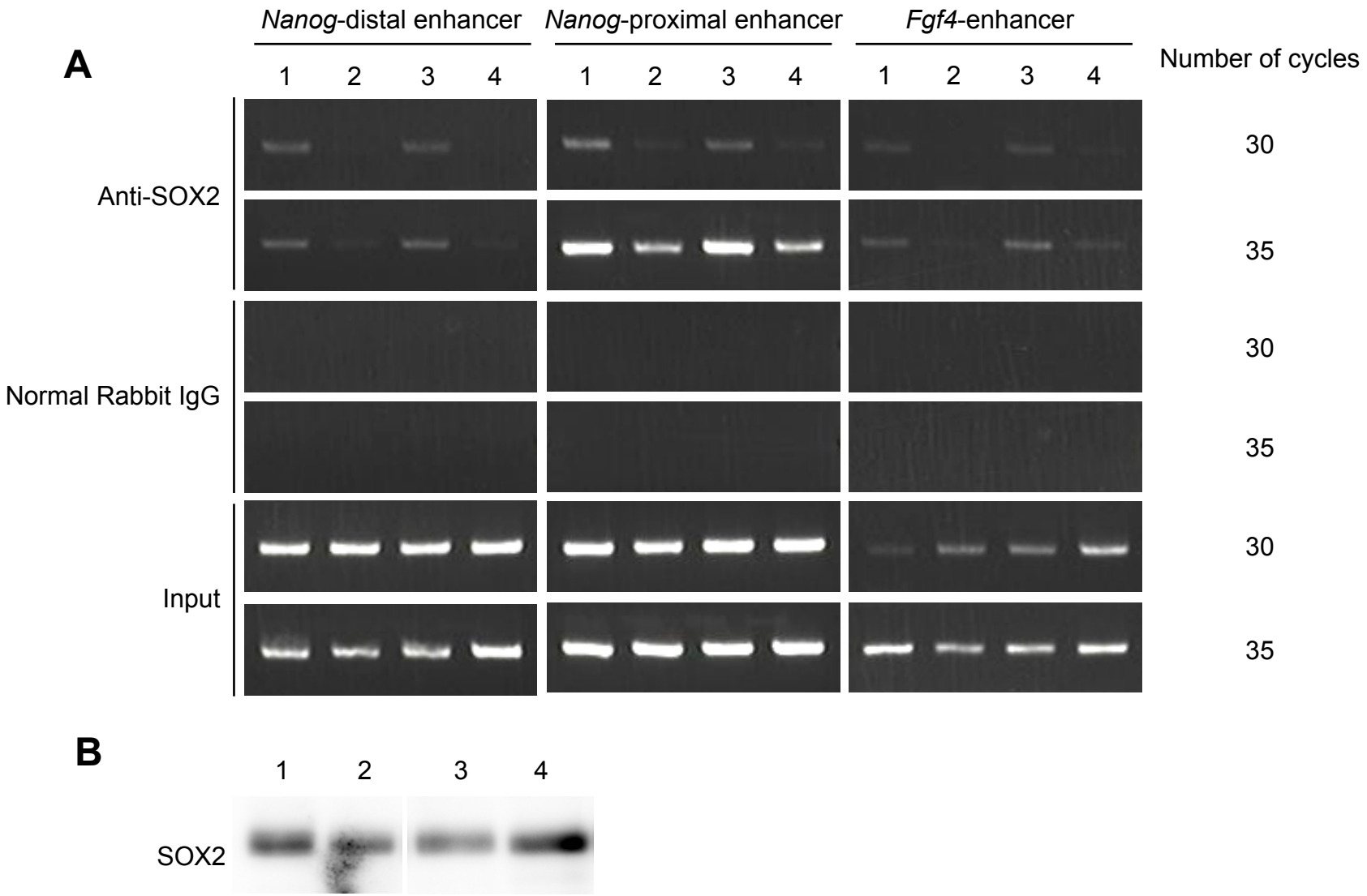

Figure 31. ChIP assay suggests that LY294002 prevents DNA binding activity of SOX2.
A. MG1.19 introduced with pPyCAG-IP or pPyCAG-Flag-Nanog-IP were seeded at 1 x 10^5 cells on gelatinized 100-mm dishes and incubated overnight. Cells were treated with DMSO or 10 μM of LY294002 for 6 days. After treatment, chromatin immunoprecipitation with anti-SOX2 antibody was performed. PCR was performed with the distal enhancer of *Nanog* gene (Nanog-ChIP-S/Nanog-ChIP-AS), the proximal enhancer of *Nanog* gene (Nanog-exon-ChIP-S/Nanog-exon-ChIP-AS) or the enhancer of *Fgf4* gene (Fgf4-ChIP-S/Fgf4-ChIP-AS)specific primers. 1, Mock/DMSO; 2, Mock/LY294002; 3, Flag-Nanog/DMSO; 4, Flag-Nanog/LY294002.
B. Seven-point five microliters of the 'Input' samples were separated by SDS-PAGE and transferred to a PVDF membrane. Immunoblot was performed with anti-SOX2 antibody.

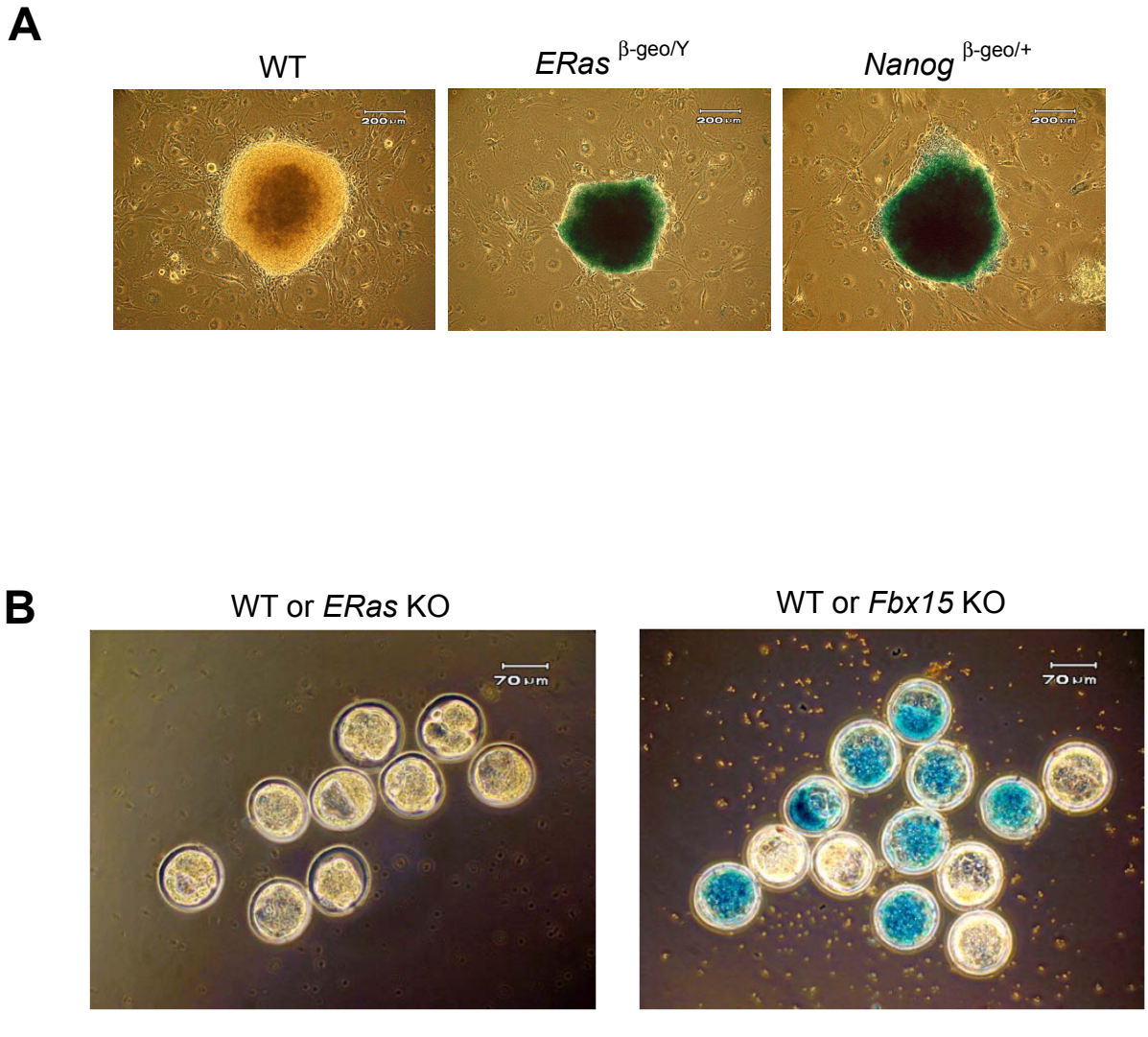

Figure 32. *ERas* is expressed in ES cells but not in blastocysts.
A. Two hundreds of wild-type (WT), *ERas* $^{\beta\text{-geo/Y}}$ or *Nanog* $^{\beta\text{-geo/+}}$ ES cells were plated on mitomycin C-treated STO cells on 6-well plates and cultured for 10 days. Colonies were fixed with 4% glutaraldehyde, permeadized with 1% Triton-X100 and stained with X-gal.
B. X-gal staining of blastocysts. Blastocysts from *ERas* $^{\beta\text{-geo/Y}}$ x *ERas* $^{\beta\text{-geo/+}}$ intercross (left) and *Fbx15* $^{\beta\text{-geo/+}}$ intercross (right) were stained with X-gal.

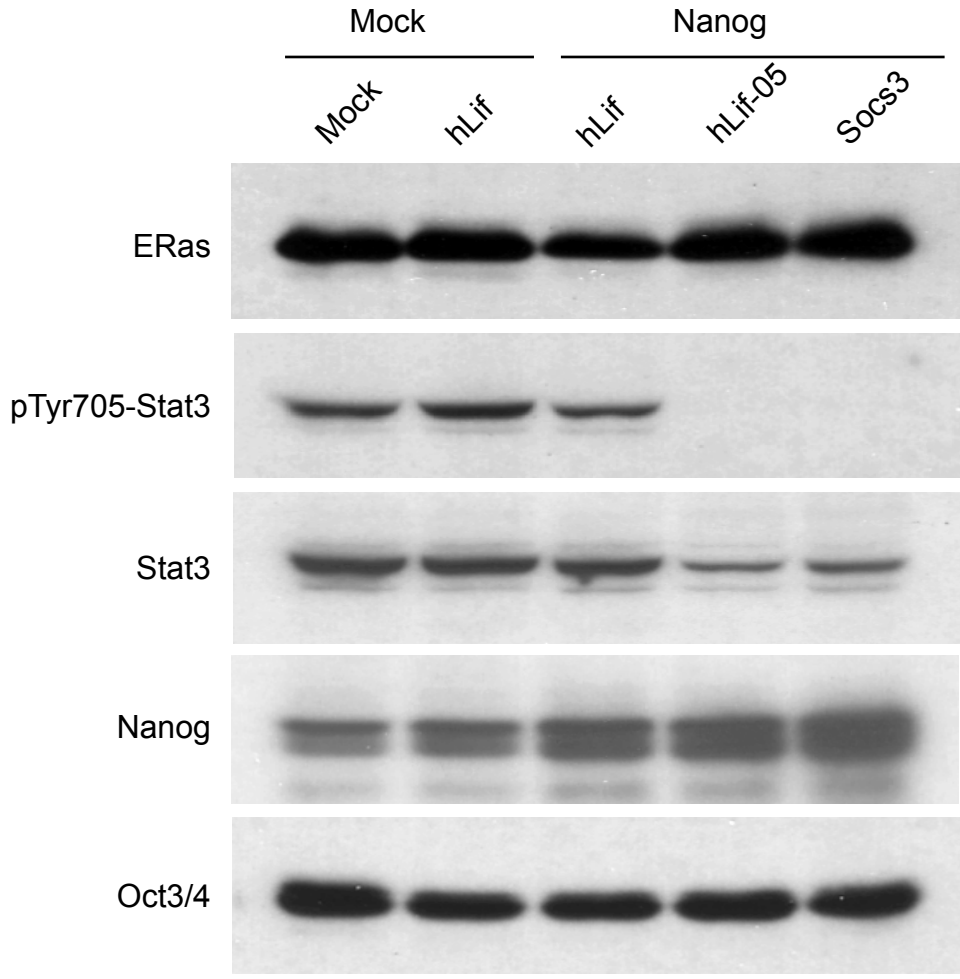

Figure 33. The LIF/STAT3 activity does not regulated expression of ERas.
MG1.19 ES cells were transfected with expression vectors for hLIF, Nanog + hLif, Nanog + hLif-05 or Nanog + SCOS3 and selected with 2 mg/ml of puromycin and 100 mg/ml of hygromycin B Cell lysates from these cells were separated bySDS-PAGE and transferred to PVDF membranes. Immunoblotting was performed with anti-ERas, anti-Nanog, anti-phospho-Tyr705-Stat3, anti-Stat3 and anti-Oct3/4 antibodies.

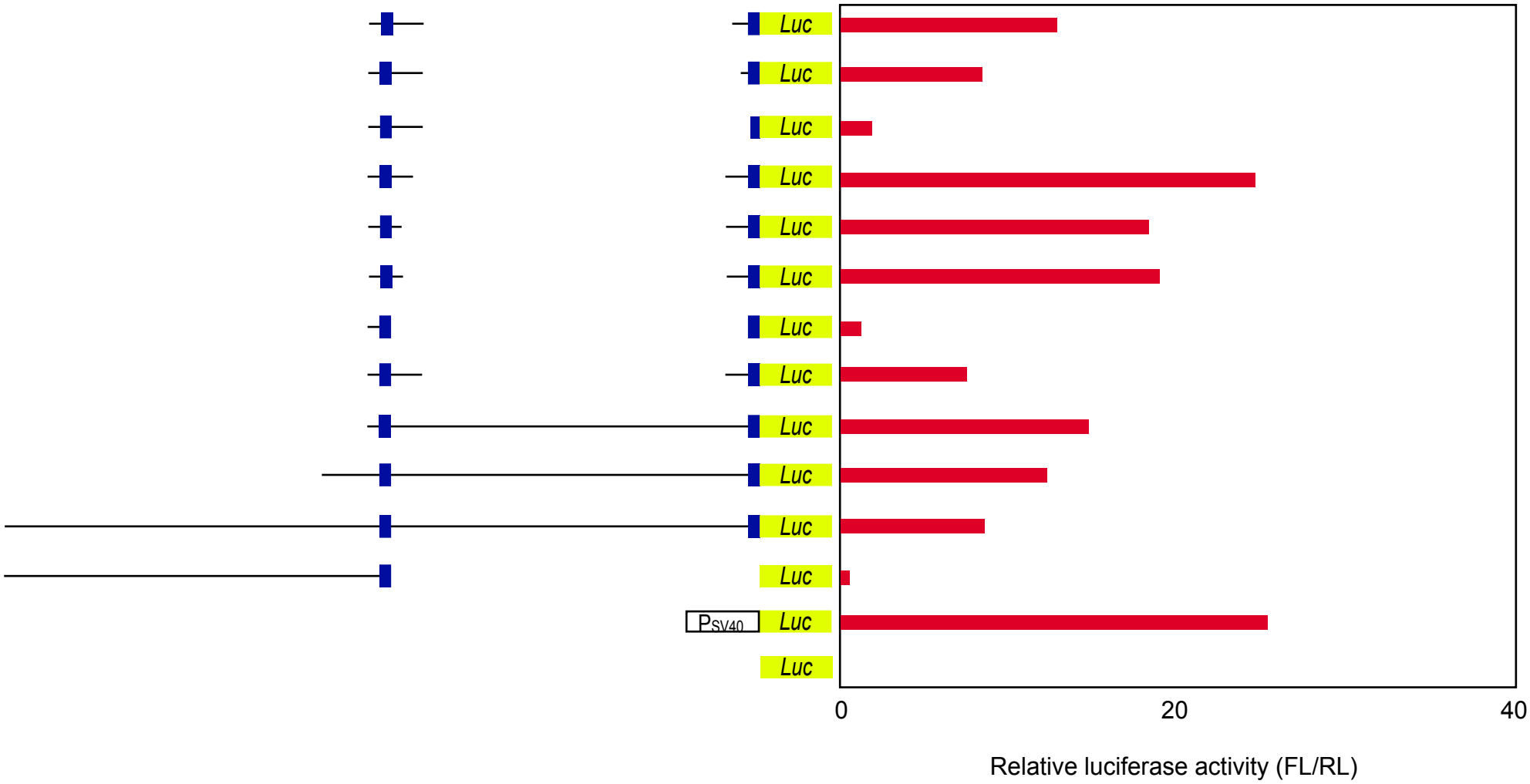

Figure 34. Luciferase reporter assay to identify regulatory regions of the mouse ERas gene (1).
Each reporter construct was transfected into undifferentiated ES cells along with pRL-TK. Twenty-four hours after transfection, cells were lysed and luciferase activities were measured.

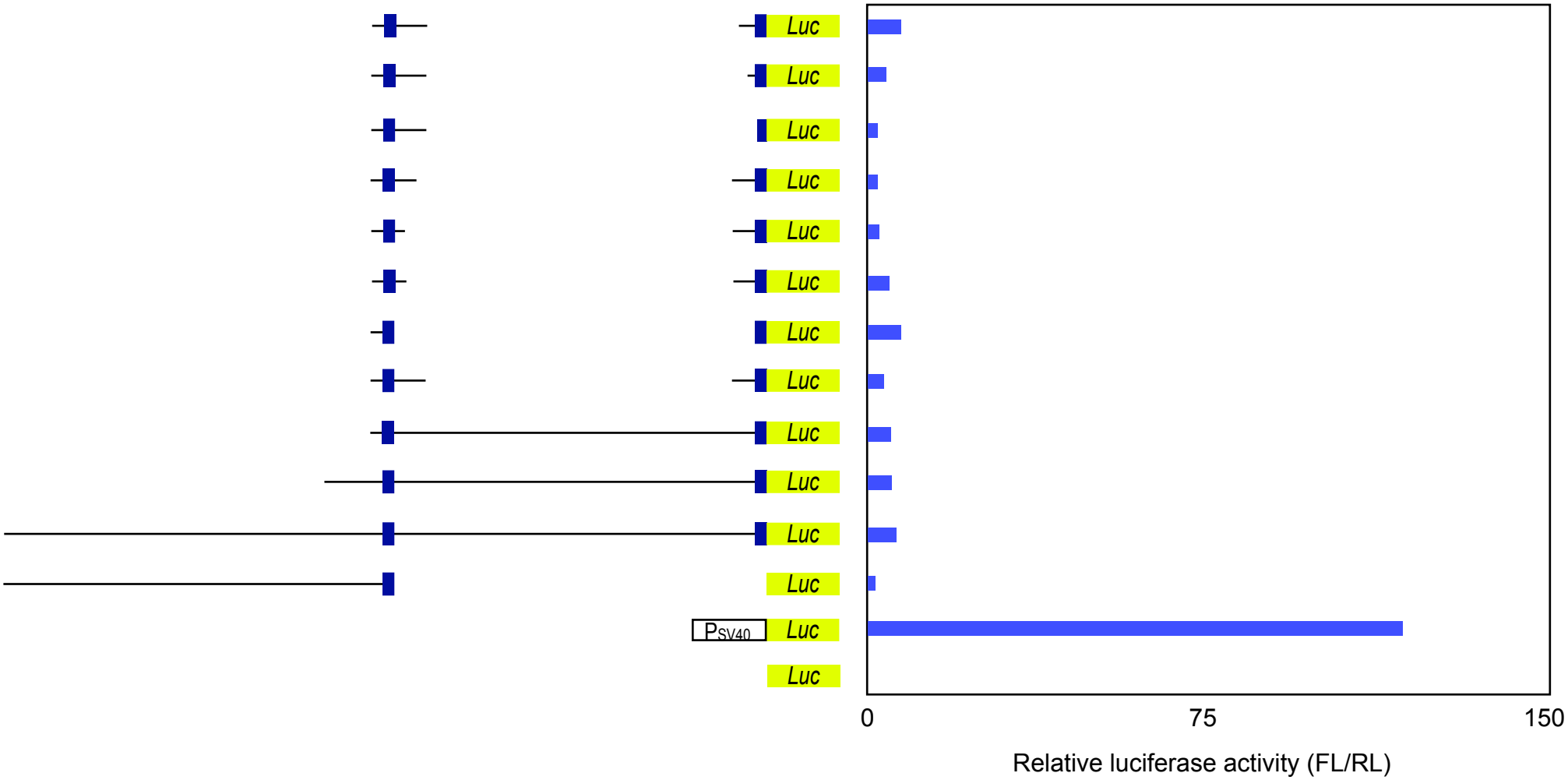

Figure 35. Luciferase reporter assay to identify regulatory regions of the mouse ERas gene (2).
Each reporter construct was transfected into NIH3T3 cells along with pRL-TK. Twenty-four hours after transfection, cells were lysed and luciferase activities were measured.

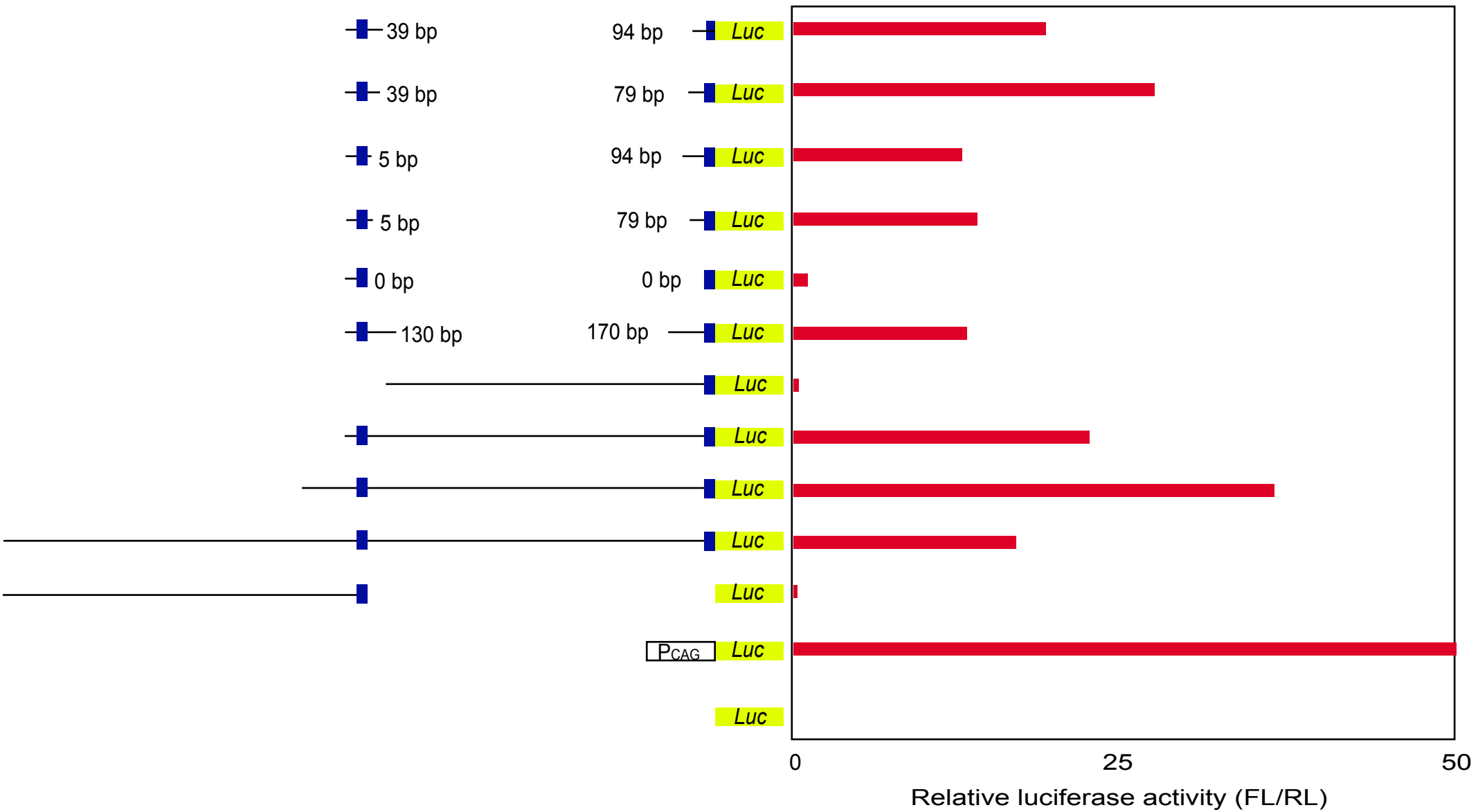

Figure 36. Luciferase reporter assay to identify regulatory regions of the mouse ERas gene (3).
RF8 ES cells were introduced with 1 μg of each reporter constructs along with 0.025 μg of pRL-TK by using Lipofectamine 2000. Twenty-four hours after transfection, cells were lysed and luciferase activities were measured.

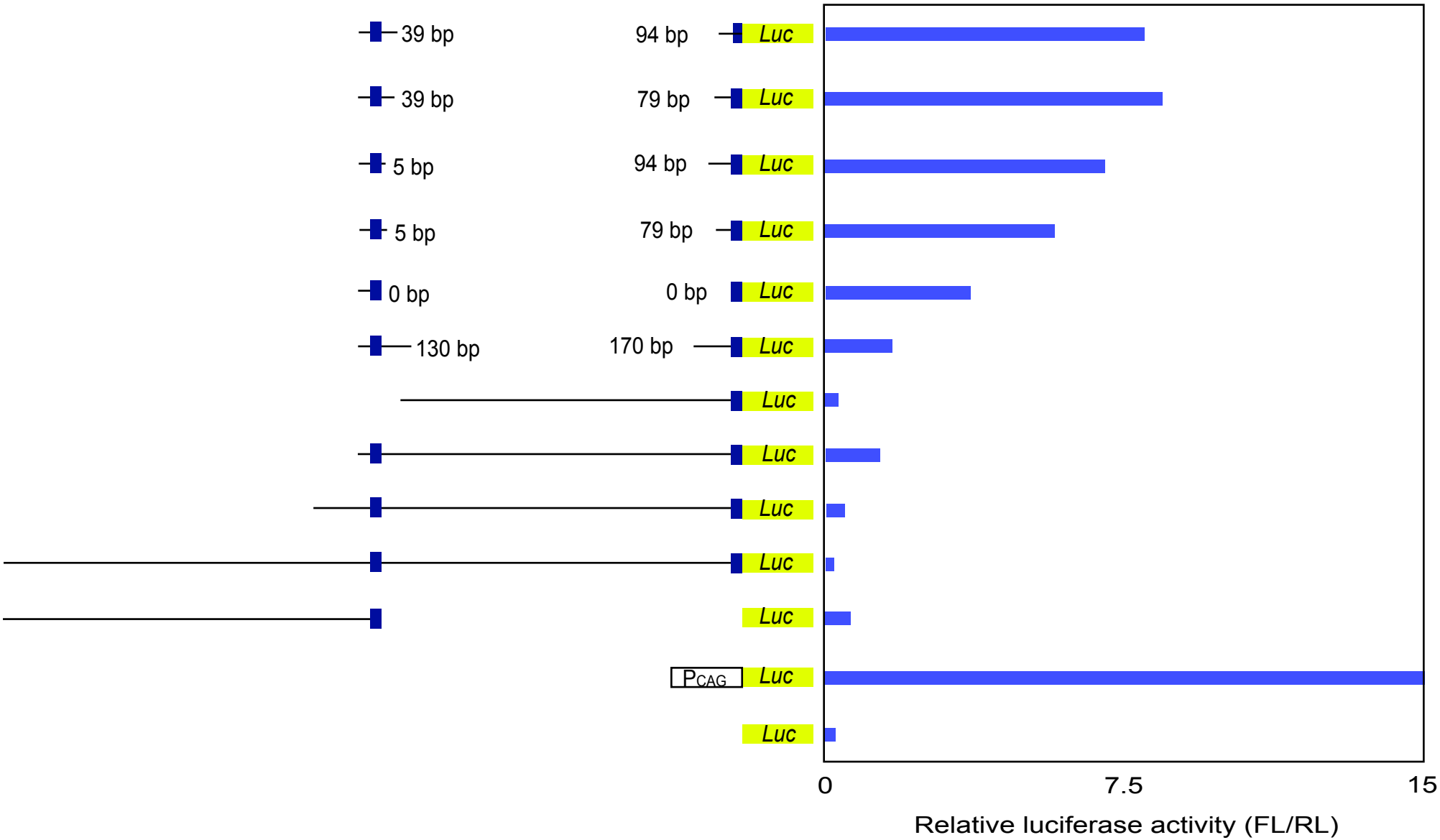

Figure 37. Luciferase reporter assay to identify regulatory regions of the mouse ERas gene (4).
NIH3T3 cells were introduced with 1 μg of each reporter construct along with 0.025 μg of pRL-TK by using Lipofectamine 2000. Twenty-four hours after transfection, cells were lysed and luciferase activities were measured.

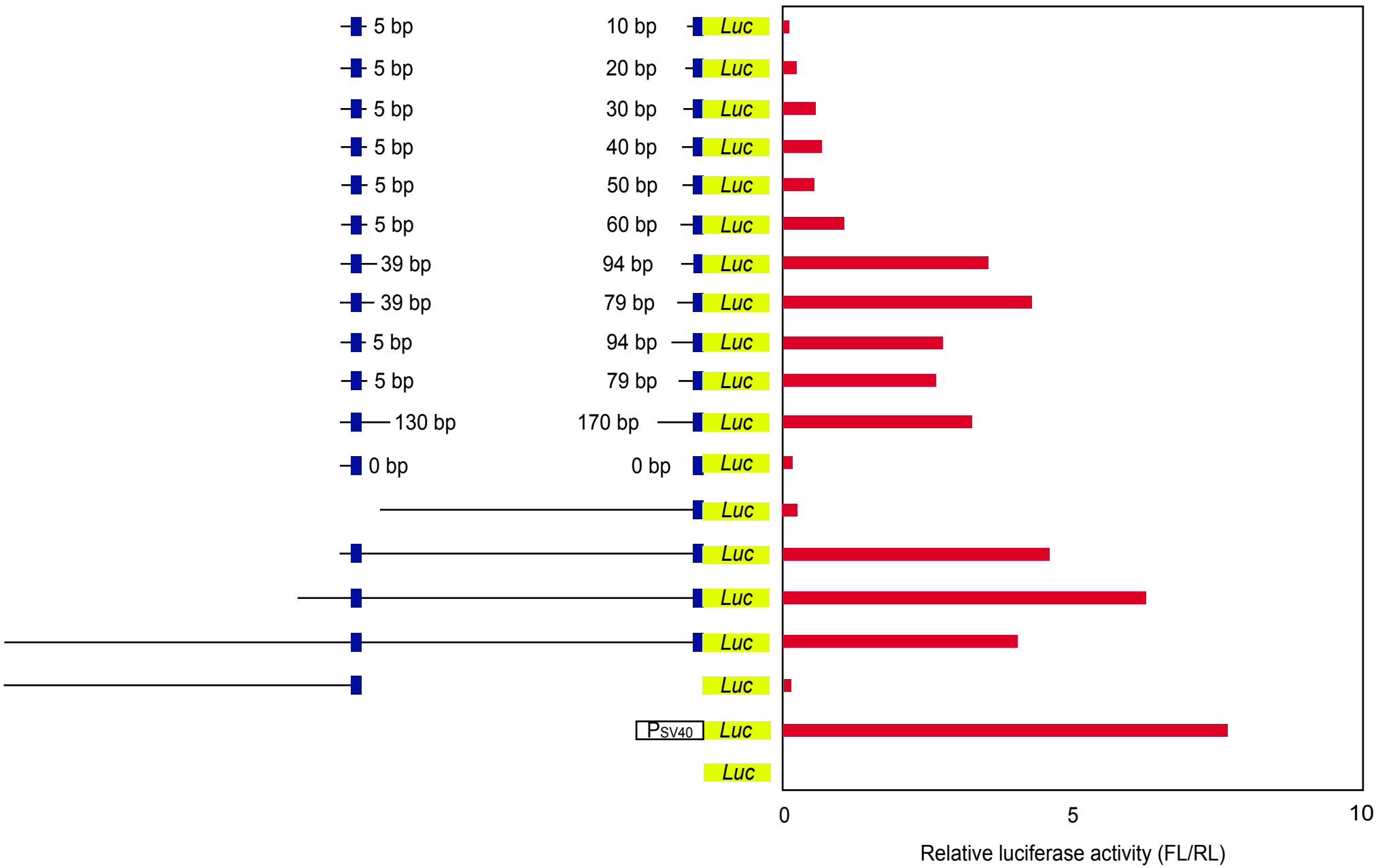

Figure 38. Luciferase reporter assay to identify regulatory regions of the mouse ERas gene (5).
One microgram of each reporter construct was introduced into RF8 ES cells by using Lipofectamine 2000. Twenty four hours after transfection, cells were lysed and luciferase activities were measured.

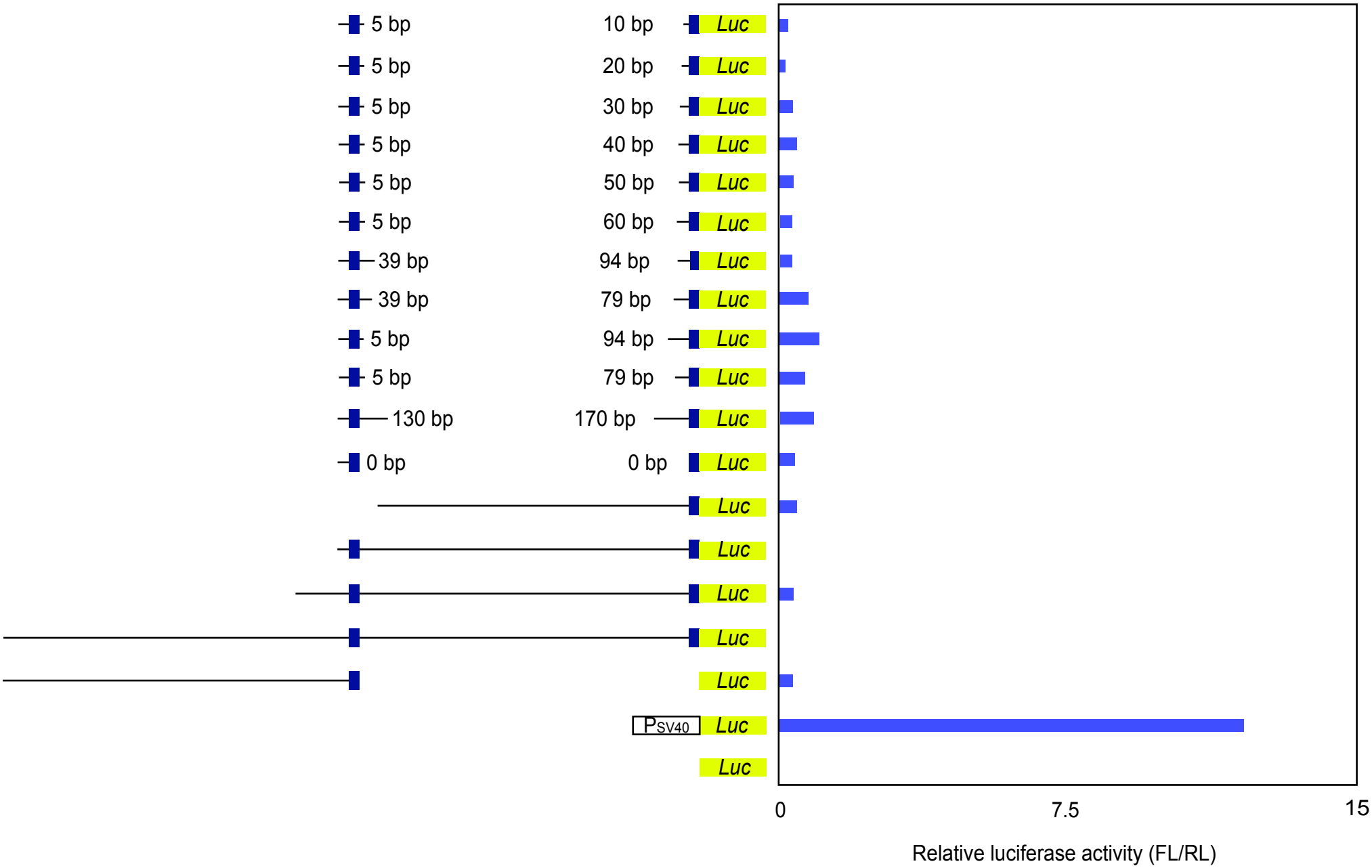

Figure 39. Luciferase reporter assay to identify regulatory regions of the mouse ERas gene (6).
One microgram of each reporter construct was introduced into NIH3T3 cells by using Lipofectamine 2000. Twenty four hours after transfection, cells were lysed and luciferase activities were measured.

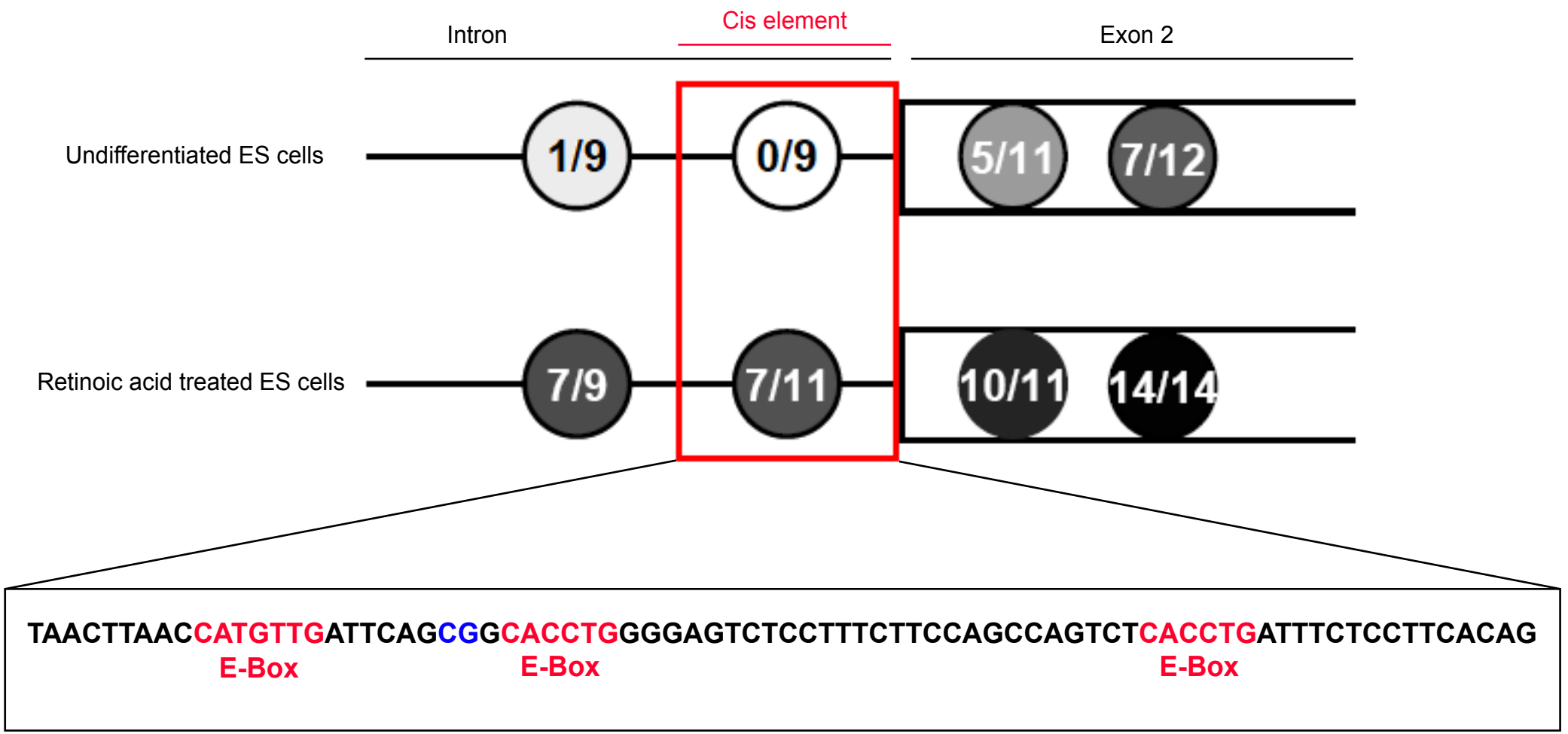

Figure 40. CpG in cis element of ERas gene is demethylated in undifferentiated ES cells.
Genomic DNA was isolated from undifferentiated ES cells or retinoic acid-treated ES cells and treated with bisulfite. PCR was performed with primers specific for the ERas cis element. Amplified 388-base pairs products were subcloned into pCR2.1. Their sequences were confirmed with the M13 reverse primer. The cis element of the ERas gene containss three E-Box sequences.

Appendix 1 (Plasmid List)

Name			Stock No.
pUSEamp-myr-PI3K-p110	Commercial (Upstate bio)	Myr-p110 alpha ORF	B31-45
pCMV-Ras dominant negative set	Commercial (Clonetech)	Hras, HRasV12 and HRasN17 ORF	
pCMV-Raf dominant negative set	Commercial (Clonetech)	Raf1 ORF	
pBluescript SK	Commercial (Stratagene)	Cloning	
pCR2.1-TOPO	Commercial (Invitrogen)	Cloning	
pCR-XL-TOPO	Commercial (Invitrogen)	Cloning	
pGEM-T-Easy	Commercial (Promega)	Cloning	
pDONR201	Commercial (Invitrogen)	Entry vector for Gateway system	
pENTR-1A	Commercial (Invitrogen)	Entry vector for Gateway system	
pENTR-D-TOPO	Commercial (Invitrogen)	Entry vector for Gateway system	
pDEST17	Commercial (Invitrogen)	E. coli expression vector	
pEGFP-N1	Commercial (Clonetech)	C-terminal EGFP fusion	
pEGFP-C1	Commercial (Clonetech)	N-termanal EGFP fusion	
pUSEamp-myr-PI3K-p110	Commercial (Upstate bio)	Myr-p110 alpha ORF	
pCMV-Ras dominant negative set	Commercial (Clonetech)	Hras, HRasV12 and HRasN17 ORF	
pCMV-Raf dominant negative set	Commercial (Clonetech)	Raf1 ORF	
pBluescript SK	Commercial (Stratagene)	Cloning	
pCR2.1-TOPO	Commercial (Invitrogen)	Cloning	
pCR-XL-TOPO	Commercial (Invitrogen)	Cloning	
pGEM-T-Easy	Commercial (Promega)	Cloning	
pDONR201	Commercial (Invitrogen)	Entry vector for Gateway system	
pENTR-1A	Commercial (Invitrogen)	Entry vector for Gateway system	
pENTR-D-TOPO	Commercial (Invitrogen)	Entry vector for Gateway system	
pDEST17	Commercial (Invitrogen)	E. coli expression vector	
pEGFP-N1	Commercial (Clonetech)	C-terminal EGFP fusion	
pEGFP-C1	Commercial (Clonetech)	N-termanal EGFP fusion	
pEGFP-C2	Commercial (Clonetech)	N-termanal EGFP fusion	
pCX-EGFP	Kind gift from Dr. Masaru Okabe	CAG promoter and EGFP subcloning	B4-52
278N24	BAC clone containing mouse ERas locus screened by PCR and southern blotting.	PCR template or Transgenic vector	BAC1-32
pPyCAG-IP	Kind gift from Dr. Hitoshi Niwa	Forced expression in MG1.19 ES cells	
pBIKS(-)IresBgeopA	Kind gift from Dr. Hitoshi Niwa	Gene targeting	
pCIG		Nuclear localization tagged EGFP	B31-30
pGV-BM2	Commertial	Reporter assay	B19-4
pRL-TK	Commercial (Promega)	Reporter assay	B1-57
pCS2+MT		6 x Myc tag	
pFlag-CMV2	Commercial (Kodak)	Flag tag	
pMX	Kind gift from Dr. Toshio Kitamura	Retroviral vector	B31-38
pMX-IP	An EcoRV/XbaI (Blunted) fragment of pIRESpuro was introduced into the BamHI (Blunted) site of pMX.	Retroviral vector (puromycin resistance)	B31-44
pMX-gw-IP	The gateway cassette rfB was introduced into the EcoRI (Blunted) site of pMX-IP.	Retroviral vector (puromycin resistance)	
pMX-IH	An EcoRV/XbaI (Blunted) fragment of pIRES-hyg was introduced into the BamHI (Blunted)/SalI (Blunted) site of pMX.	Retroviral vector (hygromycin resistance)	B31-42
pIRESneo	Commercial (Clonetech)	Expression vector for mammalian cells	
pIRESpuro	Commercial (Clonetech)	Expression vector for mammalian cells	
pCAG-IRESneo	An NdeI/EcoRI fragment of pCX-EGFP was introduced into the NdeI/EcoRI site of pIRESneo.	Expression vector for mammalian cells	B10-1
pCAG-HA-IRESneo	HA-oligo-S and HA-oligo-AS were annealed and introduced into the EcoRI/BamHI site of pCAG-IRESneo.	Expression vector for mammalian cells	B1-61
pCAG-HA-gw-IRESneo	The gateway cassette rfB was introduced into the BamHI site (Blunted) site of pCAG-HA-IRESneo.	Expression vector for mammalian cells	B10-29
pPyCAG-HA-gw-IP	An SpeI/XhoI fragment of pCAG-HA-gw-IRESneo was introduced into the SpeI/XhoI site of pPyCAG-IP.	Expression vector for mammalian cells	B10-31
pMX-EGFP-gw-IP	An Eco47III/HindIII (Blunted) fragment of pEGFP-gw was introduced into the EcoRI (Blunted)/BamHI (Blunted) site of pMX-IP.	Retroviral vector (N-termanal EGFP fusion)	B20-58
pCR2.1-HaRas2 (hERas)	The PCR product amplified with hHRas2-S and hHRas2-AS primers was subcloned into pCR2.1-TOPO.	Confirm the sequence of human ERas	B10-5, 6
pDONR-ERas	Mouse ERas ORF amplified by PCR with 45328-gw-S and 45328-gw-AS primers was inserted into pDONR201 by BP reaction.	Entry vector for Gateway system	**B10-7**
pDONR-ERas delC	Mouse ERas ORF amplified by PCR with 45328-gw-S and 45328-gw-AS2 primers was inserted into pDONR201 by BP reaction.	Entry vector for Gateway system	B10-8
pENTR-hERas	Human ERas ORF amplified by PCR with HaRas2-gw-S and HaRas2-gw-AS primers was subcloned into pENTR-D-TOPO.	Entry vector for Gateway system	B10-9
pENTR-Hras	An XhoI (Blunted)/BamHI fragment of pCMV-Hras was introduced into the BamHI (Blunted)/EcoRV site of pENTR-1A.	Entry vector for Gateway system	B10-10
pENTR-HRasV12	An XhoI (Blunted)/BamHI fragment of pCMV-HrasV12 was introduced into the BamHI (Blunted)/EcoRV site of pENTR-1A.	Entry vector for Gateway system	B10-11
pENTR-HRasN17	An XhoI (Blunted)/BamHI fragment of pCMV-HrasN17 was introduced into the BamHI (Blunted)/EcoRV site of pENTR-1A.	Entry vector for Gateway system	B10-12
pENTR-HRasV12 delC	HRasV12 delC mutant was amplified by PCR with mHRas-TOPO-gw-S and mHRas-delC primers and subcloned into pENTR-D-TOPO.	Entry vector for Gateway system	B10-14

pENTR-Raf1	An XhoI (Blunted)/BamHI (Blunted) fragment of pCMV-Raf1 was introduced into the XnmI/EcoRV site of pENTR-1A.	Entry vector for Gateway system	B10-20
pDONR-PI3K p110 delta	Mouse PI3K catalitic subunit p110 delta ORF amplified by PCR with mPI3K-gw-U and mPI3K-gw-L was inserted into pDONR201 by BP reaction.	Entry vector for Gateway system	B10-22
pDONR-RalGDS	Mouse RalGDS ORF amplified by PCR with RalGDS-gw-U and RalGDS-gw-L was inserted into pDONR201 by BP reaction.	Entry vector for Gateway system	B10-23
pCR2.1-Myr-p110 alpha	An HindIII (partially digested)/EcoRV fragment of pUSEamp-myr-PI3K-p110 was subcloned into pCR2.1-TOPO.	Subcloning dominant active form of p110 to various expression vectors	B10-32, 33
pCAG-ERas-IH	Mouse ERas ORF from pDONR-ERas was inserted into pCAG-gw-IH by LR reaction.	Expression vector of ERas in ES cells (hygromycin B resistance)	B10-50
pCAG-Myr-p110-IH	A BamHI fragment of pCR2.1-Myr-p110 alpha was introduced into the BamHI site of pCAG-IH.	Expression vector of dominant active form of p110 in ES cells	B10-34
pMX-Myr-p110-IP	A BamHI fragment of pCR2.1-Myr-p110 alpha was introduced into the BamHI site of pMX-IP.	Retroviral vector (dominant active form of p110 expression)	B10-35
pENTR-Braf	Human BRaf ORF amplified by PCR with Braf-gw-S and Braf-gw-AS primers was subcloned into pENTR-D-TOPO.	Entry vector for Gateway system	B10-39
pDEST17-ERas	Mouse ERas ORF from pDONR-ERas was inserted into pDEST17 by LR reaction.	E. coli expression vector of HIS-ERas protein	B10-43
pGEM-ERas-LA	The PCR product amplified with ERas-S118 and ERas-AS264 was subcloned into pGEM-T-Easy.	Subcloning 5' homologous arm of ERas targeting vector	B10-59
pCR2.1-U51	The PCR product amplified from NsiI digested BAC clone (278N24) with ERas-S812 and TOPO-linker primers was subcloned into pCR2.1-TOPO.	Subcloning 3' homologous arm of ERas targeting vector	B10-60
ERas TV-Bgeo	An SacII/NotI fragment of pGEM-ERas-LA and an EcoRI (Blunted) fragment of pCR2.1-U51 were introduced into the SacII/NotI site and the SalI (Blunted) site of pBIKS(-)IresBgeopA, respectively.	Beta-geo knockin vector to mouse ERas locus	B10-58
pCR2.1-ERas CV-SA	The PCR product amplified with ERas-S812 and ERas-CVSA primers was subcloned into pCR2.1-TOPO.	Subcloning 5' homologous arm of ERas Control vector	B10-61
ERas CV-Bgeo	An EcoRI (Blunted) fragment of pCR2.1-ERas CV-SA was introduced into SalI (Blunted) site of pBIKS(-)IresBgeopA.	Positive control of PCR screening	
pCR2.1-ERas-5'TW-NsiI	The PCR product amplified from NsiI digested BAC clone (278N24) with ERas-AS45 and TOPO-linker primers was subcloned into pCR2.1-TOPO.	Confirm the sequence of upstream region of ERas gene	B10-63
pCR2.1-ERas 5'probe	An EcoRI fragment of pCR2.1-ERas-5'TW-NsiI was inserted into the EcoRI site of pCR2.1.	ERas 5' probe for southern blotting	B10-62
pCR2.1-ERas 3'probe	The PCR product amplified with ERas-3'probe-S and ERas-3'probe-AS primers was subcloned into pCR2.1-TOPO.	ERas 3' probe for southern blotting	B10-65
pENTR-Akt1	Mouse Akt1 ORF amplified by PCR with Akt1-S and Akt1-AS primers was subcloned into pENTR-D-TOPO.	Entry vector for Gateway system	B10-66
pENTR-Pten	Mouse Pten ORF amplified by PCR with Pten-S andPten-AS primers was subcloned into pENTR-D-TOPO.	Entry vector for Gateway system	B10-67
pENTR-p27kip1	Mouse p27kip1 ORF amplified by PCR with p27kip1-S and p27kip1-AS primers was subcloned into pENTR-D-TOPO.	Entry vector for Gateway system	B10-68
pENTR-Gab1	Mouse Gab1 ORF amplified by PCR with Gab1-S and Gab1-AS primers was subcloned into pENTR-D-TOPO.	Entry vector for Gateway system	B10-69
pENTR-Gab1 beta	Mouse Gab1 beta ORF amplified by PCR with Gab1-delPH-S and Gab1-AS primers was subcloned into pENTR-D-TOPO.	Entry vector for Gateway system	B10-71
pENTR-Ship	Mouse Ship ORF amplified by PCR with Ship-S and Ship-AS primers was subcloned into pENTR-D-TOPO.	Entry vector for Gateway system	B10-72
pENTR-s-Ship	Mouse s-Ship ORF amplified by PCR with s-Ship-S and Ship-AS primers was subcloned into pENTR-D-TOPO.	Entry vector for Gateway system	B10-73
pENTR-hLif	Human Lif ORF amplified by PCR with hLif-S and hLif-AS primers was subcloned into pENTR-D-TOPO.	Entry vector for Gateway system	B10-75
pENTR-hLif05	Three PCR products amplified with M13 and hLifmut1-AS primers, hLifmut1-S and hLifmut2-AS primers, or hLifmut2-S and M13rev primers were mixed, then were used as templates in second PCR with hLif-S and hLif-AS primers and subcloned into pENTR-D-TOPO.	Entry vector for Gateway system	B10-76
pENTR-KRas4B	Human KRas4B ORF amplified by PCR with KRas-S and KRas4B-AS was subcloned into pENTR-D-TOPO.	Entry vector for Gateway system	B11-75
pENTR-KRas4BV12	Dominant active mutant of human KRas4B amplified by PCR with KRasV12-S and KRas4B-AS primers was subcloned into pENTR-D-TOPO.	Entry vector for Gateway system	B11-76
pENTR-Nras	Human NRas ORF amplified by PCR with NRas-S and NRas-AS was subcloned into pENTR-D-TOPO.	Entry vector for Gateway system	B11-73
pENTR-NRasV12	Dominant active mutant of human NRas amplified by PCR with NRasV12-S and NRas-AS primers was subcloned into pENTR-D-TOPO.	Entry vector for Gateway system	B11-74
pPyCAG-EGFP-IP	A BamHI (Blunted)/NotI (Blunted) fragment of pEGFP-N1 was introduced into the XhoI (Blunted) site of pPyCAG-IP.	EGFP expression vector in MG1.19 ES cells	
pPyCAG-Myr-p110-IP	A BamHI (Blunted) fragment of pCR2.1-Myr-p110 alpha was introduced into the XhoI (Blunted) site of pPyCAG-IP.	Dominant active form of p110 expression vector in MG1.19 ES cells	B11-49
pMX-EGFP-IP	An EcoRI fragment of pCX-EGFP was introduced into the EcoRI site of pMX-IP.	Entry vector for Gateway system	B11-50
pENTR-Rac1	Mouse Rac1 ORF amplified by PCR with Rac1-S and Rac1-AS primers was subcloned into pENTR-D-TOPO.	Entry vector for Gateway system	B11-77
pENTR-Rac1V12	Dominant active mutant of mouse Rac1 amplified by PCR with Rac1V12-S and Rac1-AS was subcloned into pENTR-D-TOPO.	Entry vector for Gateway system	B11-78
pEGFP-gw	The gateway cassette rfB was introduced into the XhoI (Blunted) site of pEGFP-C2.	EGFP and gateway casette fusion construct	B20-1
pPyCAG-EGFP-gw-IP	An Eco47III/HindIII (Blunted) fragment of pEGFP-gw was introduced into the XhoI (Blunted) site of pPyCAG-IP.	EGFP fusion protein expression vector in MG1.19 ES cells	B20-2
pFlag-gw-CMV2	The gateway cassette rfB was introduced into the HindIII (blunted)/BglII (Blunted) site of pFlag-CMV2.	Flag tag and gateway casette fusion construct	B20-3
pPyCAG-Flag-gw-IP	An SacI (Blunted)/EcoRV fragment of pFlag-gw-CMV2 was introduced into the XhoI (Blunted) site of pPyCAG-IP.	Flag tagged protein expression vector in MG1.19 ES cells	B20-4
pCS2+MT-gw	The gateway cassette rfC was introduced into the EcoRI (Blunted) site of pCS2+MT.	Myc tag and gateway casette fusion construct	B20-5
pPyCAG-Myc-gw-IP	A ClaI (Blunted)/XhoI (Blunted) fragment of pCS2+MT-gw was introduced into the XhoI (Blunted) site of pPyCAG-IP.	Myc tagged protein expression vector in MG1.19 ES cells	B20-6
pENTR-Rap1A	Mouse Rap1A ORF amplified by PCR with Rap1A-S and Rap1A-AS primers was subcloned into pENTR-D-TOPO.	Entry vector for Gateway system	B20-19
pENTR-HE	Two PCR products amplified with mHRas-topo-gw-S and HRas-chimera-AS primers or H-E-chimera-S and 45328-gw-AS primers were mixed, then used as templates in second PCR with mHRas-topo-gw-S and 45328-gw-AS primers and subcloned into pENTR-D-TOPO.	Entry vector for Gateway system	B20-27
pENTR-EH	Two PCR products amplified with ERas-topo-gw-S and ERas-chimera-AS primers or E-H-chimera-S and mHRas-gw-AS primers were mixed, then used as templates in second PCR with ERas-topo-gw-S and mHRas-gw-AS primers and subcloned into pENTR-D-TOPO.	Entry vector for Gateway system	B20-29
pENTR-EK	Two PCR products amplified with ERas-topo-gw-S and ERas-chimera-AS primers or E-K-chimera-S and KRas4B-AS primers were mixed, then used as templates in second PCR with ERas-topo-gw-S and KRas4B-AS primers and subcloned into pENTR-D-TOPO.	Entry vector for Gateway system	B20-31
pENTR-HrasV12 C181S C184S	Site derected mutagenesis on pENTR-HRasV12 with Hras-C2S-S and Hras-C2S-AS primers.	Entry vector for Gateway system	B20-52
pENTR-ERas C220S C222S	The PCR product amplified with ERas-topo-gw-S and ERas-CtoS-AS primers was subcloned into pENTR-D-TOPO.	Entry vector for Gateway system	B20-33
pENTR-ERas delCAAX	The PCR product amplified with ERas-topo-gw-S and ERas-delCAAX-AS primers was subcloned into pENTR-D-TOPO.	Entry vector for Gateway system	B20-50
pENTR-HRasV12 delCAAX	The PCR product amplified with mHRas-topo-gw-S and HRas-delCAAX-AS primers was subcloned into pENTR-D-TOPO.	Entry vector for Gateway system	B20-51
pENTR-Akt1 K179M	Site derected mutagenesis on pENTR-Akt1 with Akt1 K179M-S and Akt1 K179M-AS primers.	Entry vector for Gateway system	B20-53
pENTR-Rheb	Mouse Rheb ORF amplified by PCR with Rheb-S and Rheb-AS primers was subcloned into pENTR-D-TOPO.	Entry vector for Gateway system	B20-56
pENTR-Rheb D60V	Two PCR products amplified with Rheb-S and Rheb D60V-AS primers or Rheb D60V-S and Rheb-AS primers were mixed, then used as templates in second PCR with Rheb-S and Rheb-AS primers and subcloned into pENTR-D-TOPO.	Entry vector for Gateway system	B20-57
pENTR-ERas CVLS	The PCR product amplified with ERas-topo-gw-S and ERas-CVLS-AS primers was subcloned into pENTR-D-TOPO.	Entry vector for Gateway system	B20-59
pENTR-ERas SSVA	The PCR product amplified with ERas-topo-gw-S and ERas-SSVA-AS primers was subcloned into pENTR-D-TOPO.	Entry vector for Gateway system	B20-60
pENTR-ERas C220S C222S CVLS	The PCR product amplified with ERas-topo-gw-S and ERas-C2S-CVLS-AS primers was subcloned into pENTR-D-TOPO.	Entry vector for Gateway system	B20-61

pENTR-HRasV12 CSVA	The PCR product amplified with mHRas-topo-gw-S and HRas-CSVA-AS primers was subcloned into pENTR-D-TOPO.	Entry vector for Gateway system	B20-65
pENTR-HRasV12 SVLS	The PCR product amplified with mHRas-topo-gw-S and HRas-SVLS-AS primers was subcloned into pENTR-D-TOPO.	Entry vector for Gateway system	B20-66
pENTR-HRasV12 C181S C184S CSVA	Site derected mutagenesis on pENTR-HRasV12 CSVA with Hras-C2S-CSVA-U and Hras-C2S-CSVA-L primers.	Entry vector for Gateway system	B20-67
pENTR-ILK	Mouse ILK ORF amplified by PCR with ILK-S and ILK-AS primers was subcloned into pENTR-D-TOPO.	Entry vector for Gateway system	B20-62
pENTR-SGK	Mouse SGK ORF amplified by PCR with SGK-S and SGK-AS primers was subcloned into pENTR-D-TOPO.	Entry vector for Gateway system	B20-63
pENTR-VEGF	Mouse VEGF ORF amplified by PCR with VEGF-S and VEGF-AS primers was subcloned into pENTR-D-TOPO.	Entry vector for Gateway system	B20-64
pENTR-KRas4BV12 delCAAX	The PCR product amplified with KRas-S and KRas4B-delCAAX-AS primers was subcloned into pENTR-D-TOPO.	Entry vector for Gateway system	B20-68
pENTR-Rap1A CVLS	The PCR product amplified with Rap1A-S and Rap1A-CVLS-AS primers was subcloned into pENTR-D-TOPO.	Entry vector for Gateway system	B20-69
pCR2.1-ERas promoter	The PCR product amplified with ERas-ES1 and ERas-EAS1 primers was subcloned into pCR2.1-TOPO.	Subcloning mouse ERas promoter region	B24-24
pCR2.1-polyoma ori	An ScaI (Blunted)/EcoRV fragment of pPyCAG-IP was subcloned into pCR2.1-TOPO.	Subcloning murine polyoma virus replication origin	B24-26
pENTR-p110dnCAAX	Two PCR products amplified with p110a-S and p110dnCAAX-AS primers or p110dnCAAX-S and mHRas-gw-AS primers were mixed, then used as templates in second PCR with p110a-S and mHRas-gw-AS primers and subcloned into pENTR-D-TOPO.	Entry vector for Gateway system	B24-27
pENTR-Hamartin (TSC1)	Three PCR products amplified with TSC1-S and TSC1-AS1293 primers, TSC1-S1154 and TSC1-AS2400 primers or TSC1-S2296 and TSC1-AS primers were mixed, then used as templates in second PCR with TSC1-S and TSC1-AS primers and subcloned into pENTR-D-TOPO.	Entry vector for Gateway system	B24-33
pENTR-Tuberin (TSC2)	Four PCR products amplified with TSC2-S and TSC2-AS1332 primers, TSC2-S1175 and TSC2-AS2600 primers, TSC2-S2485 and TSC2-AS4120 primers or TSC2-S4001 and TSC2-AS primers were mixed, then used as templates in second PCR with TSC2-S and TSC2-AS primers and subcloned into pENTR-D-TOPO.	Entry vector for Gateway system	B24-34
pENTR-HE C181S C184S	C181 and C184 of HE were mutated to serine residues by PCR with mHRas-topo-gw-S and ERas-C2S-AS, and subcloned into pENTR-D-TOPO.	Entry vector for Gateway system	B24-35
pENTR-HE SSVA	C186 of HE was mutated to serine by PCR with mHRas-topo-gw-S and ERas-SSVA-AS, and subcloned into pENTR-D-TOPO.	Entry vector for Gateway system	B24-36
pENTR-EH C220S C222S	C220 and C222 of EH were mutated to serine residues by PCR with ERas-topo-gw-S and HRas-C2S-AS, and subcloned into pENTR-D-TOPO.	Entry vector for Gateway system	B24-37
pENTR-EH SVLS	C224 of EH was mutated to serine by PCR with ERas-topo-gw-S and HRas-SVLS-AS, and subcloned into pENTR-D-TOPO.	Entry vector for Gateway system	B24-38
pENTR-Rheb SSVM	PCR product amplified by PCR with Rheb-S and Rheb-SSVM-AS was subcloned into pENTR-D-TOPO.	Entry vector for Gateway system	B24-42

Appendix 2 (Primer List)

Name	Sequence (5'-3')	Application
45328-S1	TCAAGCAAGAAGACCCGACA	5' RACE and BAC screening
45328-AS1	CCCATGTTACCACGTAACTT	5' RACE and BAC screening
45328-RACE1	GGATGTCCCATGTTACCACGTAACTT	5' RACE
45328-RACE2	TGGTGTCGGGTCTTCTTGCTTGATTC	5' RACE
45328-RACE11	GGTAACTTGGTCGGAAAGGGAAAT	5' RACE
mHRas2-gw-S	AAAAAGCAGGCTGGGGAATGGCTTTGCCTA	Mouse ERas ORF cloning to pDONR201
mHRas2-gw-AS	AGAAAGCTGGGTCAAAGATCTTCAGGCTACAG	Mouse ERas ORF cloning to pDONR201
hHRas2-S	GATCAGCACACAATAGGCAT	Human ERas cloning
hHRas2-AS	ACTCCCACCCACACAACACT	Human ERas cloning
ERas-U527	CTGGTGATGGTGTGCTGGGCGTCT	Topowalker, Genotyping etc.
ERas-L826	CACGGCTTTCTGGTGTCGGGTCTT	Topowalker, Genotyping etc.
bgeo-screening1	AATGGGCTGACCGCTTCCTCGTGCTT	Genotyping
EGFP-N	CGTCGCCGTCCAGCTCGACCAG	Sequencing
ERas-S812	CGAATCAAGCAAGAAGACCCGACA	3' arm of targeting vector
ERas-AS264	ACTGTGCCCAAGCCTCGTGACTTT	
ERas-AS304	CACTGCCTTGTACTCGGGTAGCTG	
ERas-screening1	GGG AGG GAG GGC AAG GGC AGA GGG CT	Genotyping
ERAS-5'TW1	CTC AAG AAA GTC CGC TTC CCG CTC AG	Topowalker
ERAS-5'TW2	GGA ACG CCA GAG CCC TGC TTA CCT GT	Topowalker
CAG-1	TCG GCT TCT GGC GTG TGA CC	Sequencing
SeqL-A	TCG CGT TAA CGC TAG CAT GGA TCT C	Sequencing
SeqL-B	GTA ACA TCA GAG ATT TTG AGA CAC	Sequencing
SeqL-C	GGA TAA CCG TAT TAC CGC TAG	Sequencing
HAtag-oligo-s	AAT TCA CCA TGG GGT ACC CAT ACG ATG TTC CGG ATT ACG CTG GAT CCC TCG AGC	HA-Tag sequence
HAtag-oligo-as	GAT CGC TCG AGG GAT CCA GCG TAA TCC GGA ACA TCG TAT GGG TAC CCC ATG GTG	HA-Tag sequence
pGV-2U	ACT AAC ATA CGC TCT CCA TCA A	Sequencing
ERAS-pro-4K-U	GAT CTG TAC TGC CAT TGT TAC CTT GC	4 kbps upstream region of mouse ERas gene
ERAS-AS167	CCC CAG CAG CTC AAG GAA GAG GTG TA	Reporter assay
RalGDS-gw-U	AAA AAG CAG GCT TGC CGA GGC TGA GGA TGA TGG	Mouse RalGDS ORF cloning to pDONR201
RalGDS-gw-L	AGA AAG CTG GGT TAG TCT CCA GCC AGT CAG CCC G	Mouse RalGDS ORF cloning to pDONR201
PI3K deita-gw-U	AAA AAG CAG GCT CCA TGC CCC CTG GGG TGG ACT GCC	Mouse PI3K p110 delta ORF cloning to pDONR201
PI3K deita-gw-L	AGA AAG CTG GGT CTA CTG TCG GTT ATC CTT GGA C	Mouse PI3K p110 delta ORF cloning to pDONR201
ERAS-5'UTR-S646	GAA TGC ACC CAA TCT ACC CCG TAG	300 bps upstream region of mouse ERas gene
ERAS-5'UTR-S919	CCG CCC ACA TTT GCT CTT ACA TTG	50 bps upstream region of mouse ERas gene
ERAS-intron-S31	GAC ATC TTT CTC AGC GCG GGA TTC	Reporter assay
ERAS-intron-S385	GTG CCC AGC CTG CTT CTG TGT GCC	Reporter assay
ERAS-intron-mid-S1	GAT GGT GCG TGT GCC CTT TAT CCC	Reporter assay
ERAS-intron-mid-S2	CCA ATC ACC AGA CAG GCG CTA CTG	Reporter assay
RalGDS-S635	CAT CTC CTC CAT CCT GGG CAC CTG	Sequencing
RalGDS-S1045	CCG CCG TCT CAC AGA GCC TGG AAC	Sequencing
RalGDS-S1495	AGA GCA ATG CCA TCC ACC GCC TAA	Sequencing
RalGDS-AS2287	AAG AGG AGG TGC TGC TGG AGG CGG	Sequencing
PI3K-delta-S227	CGG CGG AGC AGC AGG AGT TGG AGG	Sequencing
PI3K-delta-S675	CAC AGT GTT CCG GCA GCC TCT GGT	Sequencing
PI3K-delta-S917	TCC CTG CCA AGA AGC CCT CCT CTG	Sequencing
PI3K-delta-S1256	CTT GGG CCA ACC TCA TGC TAT TCG	Sequencing

PI3K-delta-AS2766	GGG ACG CGC TCT CGG TTG ATT CCA	Sequencing
PI3K-delta-AS2308	AAA GAT GAT GCC CAC GTT GCC AGC	Sequencing
PI3K-delta-AS1955	TGA GAC CAA ACC GCA GAG CCA CTG	Sequencing
mHRAS-topo-gw-s	CAC CAT GAC GGA ATA TAA GCT TGT TG	Mouse HRas ORF cloning to pENTR-D-TOPO
mHRAS-del-C	TCA GCC GGG GCC ACT CTC ATC AGG AG	Deletion of Hras c-terminal region
E-Ras3'probe-s	AGC TGG AGC GTC CGG GTC ATC GTC	3' probe for southern blotting
E-Ras3'probe-as	AGG CTG GGA ATT AAA GGC GTG AAC	3' probe for southern blotting
pMX-S1811	GAC GGC ATC GCA GCT TGG ATA CAC	Sequencing
A-raf-s	GCA CCA TGG AAC CAC CAC GAG GCC	Mouse Araf ORF cloning to pDONR201
A-raf-as	CTA AGG CAC AAG ACG GGC TGC GCT	Mouse Araf ORF cloning to pDONR201
B-raf-s	GCA GGA CCA TGG AGG GTG GCT GTG	Mouse Braf ORF cloning to pDONR201
B-raf-as	ACT CAG GGT GTT TCA GTG GAC TGG	Mouse Braf ORF cloning to pDONR201
Akt1-S	CAC CAT GAA CGA CGT AGC CAT TGT GAA GGA	Mouse Akt1 ORF cloning to pENTR-D-TOPO
Akt1-AS	TCA GGC TGT GCC ACT GGC TGA GTA GGA GAA	Mouse Akt1 ORF cloning to pENTR-D-TOPO
Pten-S	CAC CAT GAC AGC CAT CAT CAA AGA GAT CGT	Mouse Pten ORF cloning to pENTR-D-TOPO
Pten-AS	TCA GAC TTT TGT AAT TTG TGA ATG CTG ATC	Mouse Pten ORF cloning to pENTR-D-TOPO
Gab1-S	CAC CAT GAG CGG CGG CGA AGT GGT TTG CTC	Mouse Gab1 ORF cloning to pENTR-D-TOPO
Gab1-AS	TCA CTT CAC ATT CTT TGT GGG TGT CTC GGA	Mouse Gab1 ORF cloning to pENTR-D-TOPO
Gab1-S800	TGA CGT GTT GCC AAA GGA ATC CCC	Sequencing
Gab1-S1292	AAA GCG TGT TGA CAG CGG GAG GTG	Sequencing
Gab1-AS1838	TGG GTT TAT TCA TCG GGC TGC TTC	Sequencing
Gab1-delPH-S	CAC CAT GAA CAA GTG GGT CCG TTG TAT CTG	Mouse Gab1 beta ORF cloning to pENTR-D-TOPO
Akt1-S420	GCC CAA GCA CCG TGT GAC CAT GAA	Sequencing
Akt1-AS1134	TTC TTG AGC AGC CCG GAG AGC AGG	Sequencing
p27kip1-S	CAC CAT GTC AAA CGT GAG AGT GTC TAA CGG	Mouse p27kip1 ORF cloning to pENTR-D-TOPO
p27kip1-AS	TTA CGT CTG GCG TCG AAG GCC GGG CTT CTT	Mouse p27kip1 ORF cloning to pENTR-D-TOPO
hLIF-S	CAC CAT GAA GGT CTT GGC GGC AGG AGT TGT	Human Lif ORF cloning to pENTR-D-TOPO
hLIF-AS	CTA GAA GGC CTG GGC CAA CAC GGC GAT GAT	Human Lif ORF cloning to pENTR-D-TOPO
Pten-S499	ACA ATT CCC AGT CAG AGG CGC TAT	Sequencing
hLif-mut-S1	CTG ATC AGG GAA CAA CTG GCA GCG CTC AAT GGC AAA GCC AAT GCC CTC TT	Mutagenesis for hLif05
hLif-mut-AS1	CTT TGC CAT TGA GCG CTG CCA GTT GTT CCC TGA TCA GGT TCA TGA GGT TG	Mutagenesis for hLif05
hLif-mut-S2	GAG ACC GCC CGC AAG CTG CGA AAC CTC CTT CTC AAC GTG CTG TGC CGC CT	Mutagenesis for hLif05
hLif-mut-AS2	GAG AAG GAG GTT TCG CAG CTT GCG GGC GGT CTC GTT GAG CTT GCT GTG GA	Mutagenesis for hLif05
SHIP-S1439	TTA AAA CAG TTG CCA TCC ACA CCC	Sequencing
SHIP-S1820	AGA AGA TCA AGC AAC AGC AGT ATT	Sequencing
SHIP-S2285	GTT TTG TCA AGA GTC AGG AAG GAG	Sequencing
SHIP-S3028	CTC AAA CAT CTC GGG CTT CGT CAG	Sequencing
SHIP-AS888	AAG GTG ACC GGA GGG ATA AGG GAA	Sequencing
Rac1V12-S	CAC CAT GCA GGC CAT CAA GTG TGT GGT GGT GGG AGA CGT AGC T	Dominant active mutant of Rac1
Rac1-S	CAC CAT GCA GGC CAT CAA GTG TGT GGT GGT	Mouse Rac1 ORF cloning to pENTR-D-TOPO
Rac1-AS	TTA CAA CAG CAG GCA TTT TCT CTT CCT CTT	Mouse Rac1 ORF cloning to pENTR-D-TOPO
ERas-AS113	CTC CCA GGA GTA GCA GTC TGA TGA	
Akt1-K179M-S	CCG CTA CTA TGC CAT GAT GAT CCT CAA GAA	Kinase dead mutant of Akt1
Akt1-K179M-AS	TTC TTG AGG ATC ATC ATG GCA TAG TAG CGG	Kinase dead mutant of Akt1
Rap1A-S	CAC CAT GCG TGA GTA CAA GCT AGT AGT CCT	Mouse Rap1A ORF cloning to pENTR-D-TOPO
Rap1A-AS	CTA GAG CAG CAA ACA TGA TTT CTT TTT AGG	Mouse Rap1A ORF cloning to pENTR-D-TOPO
Myr-S	CAC CAT GGG GAG CAG CAA GAG CAA	
p110-S706-S	ATC AGG AAA AAG ACT CGG AGC ATG	Sequencing
H-E-chimera-S	GTG CGT GAG ATC CGA CAG AGG GCC CAG GAG	C-terminal region of Hras-Eras chimeric gene
ERas-chimera-AS	AAT CTC ATG GAC AAG CAG GGC AAA	N-terminal region of ERas chimeric gene

HRas-chimera-AS	CCG GAT CTC ACG CAC CAA CGT	N-terminal region of HRas chimeric gene
E-H-chimera-S	TGT CCA TGA GAT TCA ACA CAA GCT GCG GAA GC	C-terminal region of Eras-Hras chimeric gene
E-K-chimera-S	GTC CAT GAG ATT AAA CAT AAA GAA AAG ATG AGC	C-terminal region of Eras-Kras chimeric gene
HRas-gw-AS	TCA GGA GAG CAC ACA CTT GCA GCT	Mouse Hras ORF cloning to pENTR-D-TOPO
Eras-CtoS-AS	TCA GGC TAC AGA GCA GCC ACT GCT ACT CAC	Mutation in palmitoylation sites of ERas
ERas-ES1	GGA ATT CCC GCC CAC ATT TGC TCT TAC ATT GTG CGA T	Reporter assay
ERas-EAS1	GGC CAT GGT CCC CAG CAG CTC AAG GAA GAG GTG TAA AG	Reporter assay
ERas-ESA	GGG AGC ACA GGT AAG TAA CTT AAC CAT GTT GAT TCA GCG	Reporter assay
ERas-ESB	AGA TCA GAC ATC TTT TAA CTT AAC CAT GTT GAT TCA GCG	Reporter assay
ERas-EASA	AAC ATG GTT AAG TTA GCT TAC CTG TGC TCC CAG GAG TAG	Reporter assay
ERas-EASB	AAC ATG GTT AAG TTA AAA GAT GTC TGA TCT AAG GAA CGC	Reporter assay
ERas-S2A	GGG AGC ACA GGT AAG AAG TAA GGA GAG AAG AGT TTT TA	Reporter assay
ERas-ES2B	AGA TCA GAC ATC TTT AAG TAA GGA GAG AAG AGT TTT TA	Reporter assay
ERas-EAS2A	CTC TTC TCT CCT TAC TTC TTA CCT GTG CTC CCA GGA GTA G	Reporter assay
ERas-EAS2B	CTC TTC TCT CCT TAC TTA AAG ATG TCT GAT CTA AGG AAC GC	Reporter assay
ERas-ES3	GCT ACT CCT GGG AGC ACA GGT AAG GAT TCA GCG GCA CCT GGG GA	Reporter assay
ERas-ES4	GCT ACT CCT GGG AGC ACA GGT AAG CAC CTG GGG AGT CTC CTT TC	Reporter assay
ERas-ES5	GCT ACT CCT GGG AGC ACA GGT AAG GTC TCC TTT CTT CCA GCC AG	Reporter assay
ERas-ES6	GCT ACT CCT GGG AGC ACA GGT AAG TTC CAG CCA GTC TCA CCT GA	Reporter assay
ERas-ES7	GCT ACT CCT GGG AGC ACA GGT AAG TCT CAC CTG ATT TCT CCT TCA C	Reporter assay
ERas-ES8	GCT ACT CCT GGG AGC ACA GGT AAG TTT CTC CTT CAC AGC ACC TG	Reporter assay
ERas-EAS3	GCT CCC AGG AGT AGC AGT CTG ATG AGG GGC	Reporter assay
HRas-C2S-S	GTG GCC CCG GCA GCA TGA GCA GCA AGT GTG	Mutation in palmitoylation sites of HRas
HRas-C2S-AS	CAC ACT TGC TGC TCA TGC TGC CGG GGC CAC	Mutation in palmitoylation sites of HRas
HRas-delCAAX-AS	TCA CTT GCA GCT CAT ACA GCC GGG GCC ACT	CAAX deletion mutant of Hras
ERas-delCAAX-AS	TCA TCC ACA GCT ACA CAC GGC TTT CTG GTG	CAAX deletion mutant of Eras
Rheb-S	CAC CAT GCC TCA GTC CAA GTC CCG GAA GAT	Mouse Rheb ORF cloning to pENTR-D-TOPO
Rheb-AS	TCA CAT CAC CGA GCA CGA AGA CTT TCC TTG	Mouse Rheb ORF cloning to pENTR-D-TOPO
RhebD60V-S	CAT CTT CAG CTT GTA GTC ACA GCG GGG CAG	Dominant negative mutant of Rheb
RhebD60V-AS	CTG CCC CGC TGT GAC TAC AAG CTG AAG ATG	Dominant negative mutant of Rheb
ERas-CVLS-AS	TCA GGA GAG CAC ACA GCC ACA GCT ACA CAC	CSVA (ERas) to CVLS (Hras)
ERas-C2S-CVLS-AS	TCA GGA GAG CAC ACA GCC ACT ACT ACT CAC	Mutation in palmitoylation sites of ERas and CSVA (ERas) to CVLS (Hras)
ERas-SSVA-AS	TCA AGC TAC AGA GGA GCC ACA GCT ACA CAC	CSVA to SSVA
HRas-SVLS-AS	TCA GGA GAG CAC AGA CTT GCA GCT	CVLS to SVLS
VEGF-S	CAC CAT GAA CTT TCT GCT CTC TTG GGT GC	Mouse Vegf ORF cloning to pENTR-D-TOPO
VEGF-AS	TCA CCG CCT TGG CTT GTC ACA TCT GCA A	Mouse Vegf ORF cloning to pENTR-D-TOPO
ILK-S	CAC CAT GGA CGA CAT TTT CAC TCA GTG CCG	Mouse ILK ORF cloning to pENTR-D-TOPO
ILK-AS	CTA CTT GTC CTG CAT CTT CTC CAA GA	Mouse ILK ORF cloning to pENTR-D-TOPO
SGK-S	CAC CAT GAC CGT CAA AGC CGA GGC TGC TC	Mouse SGK ORF cloning to pENTR-D-TOPO
SGK-AS	TCA GAG GAA GGA ATC CAC AGG AGG TGC ATA	Mouse SGK ORF cloning to pENTR-D-TOPO
HRas-C2S-CSVA-U	GTG GCC CCG GCA GCA TGA GCA GCA AGT GTT	Mutation in palmitoylation sites of HRas and CVLS (Hras) to CSVA (ERas)
HRas-C2S-CSVA-L	AAC ACT TGC TGC TCA TGC TGC CGG GGC CAC	Mutation in palmitoylation sites of HRas and CVLS (Hras) to CSVA (ERas)
HRas-CSVA-L	TCA GGC TAC AGA ACA CTT GCA GCT CAT G	CVLS (Hras) to CSVA (ERas)
KRas4B-delCAAX-AS	TCA CTT TGT CTT TGA CTT CTT TTT CTT CTT	CAAX deletion mutant of Kras
Rap1A-CVLS-AS	CTA GGA CAG CAC ACA TGA TTT CTT TTT AGG	CLLL (Rap1A) to CVLS (Hras)
TSC1-S	CAC CAT GGC ACA GTT AGC AAA CAT TGG GGA	Mouse TSC1 ORF cloning to pENTR-D-TOPO
TSC1-AS	TCA GCT GTG TTC AGG ATG AGT CTC ATT GTA	Mouse TSC1 ORF cloning to pENTR-D-TOPO
TSC2-S	CAC CAT GGC CAA ACC AAC AAG CAA AGA TTC	Mouse TSC2 ORF cloning to pENTR-D-TOPO
TSC2-AS	TTA CAC AAA CTC TGT GAA GTC ATC CAC GGA	Mouse TSC2 ORF cloning to pENTR-D-TOPO
TSC1-S1154	GAA CTC CTT CAG GAA CCC CAG CGA CCT CTC	Sequencing

TSC1-AS1293	AAT CCT CGG TCG TTT GAC TGT CTG TGA AGG	Sequencing
TSC1-S2296	GAC ACC ATG GTG ACC CAA CTG CAT AGC CAG	Sequencing
TSC1-AS2400	TCC ACC CGA AGC TCC GCA ATC ATG TTT CTG	Sequencing
TSC2-S1175	AGG AGC TAT GTG ACC AGA ACG AGT TCC ATG	Sequencing
TSC2-AS1332	CTG AAG AAC CTC TCC ATC AAC AAC TGC AAG	Sequencing
TSC2-S2485	AAG CTC ACA CAC ATT TCT GCC ACA GCC AGC	Sequencing
TSC2-AS2600	TGG TGT ATG GCA AGG AGA TGG CAA ACA CGC	Sequencing
TSC2-S4001	CCT ACA GCC GGT CAT CCT CAG CAT CTA GCC	Sequencing
TSC2-AS4120	CAA AGG CTG TGA GGG TTG GAA GGA GAG GTC	Sequencing
p110DNCAAX-AS	AGG AGG GTT TCT GGA ATT CCA CTT GAC AGA	Dominant negative mutant of PI3K p110 alpha
p110DNCAAX-S	GAA TTC CAG AAA CCC TCC TGA TGA GAG TGG	Dominant negative mutant of PI3K p110 alpha
p110a-S	CAC CAT GCC TCC ACG ACC ATC TTC GGG TGA	Mouse PI3K p110 alpha ORF cloning to pENTR-D-TOPO
Rheb-SSVM-AS	TCA CAT CAC CGA GCT CGA AGA CTT TCC T	CSVM to SSVM
bGHpA-S	ATG CGG TGG GCT CTA TGG CTT CTG AGG CGG	Sequencing
ERas-3'-79bp-S	GGG ATT CTA ACT TAA CCA TGT TGA TTC AGC	Reporter assay
ERas-3'-79bp-AS	ACT CGA GCT GTG AAG GAG AAA TCA GGT GAG	Reporter assay
AKT-T308A-S	CCA CTA TGA AGG CAT TCT GCG GAA CG	Dominant negative mutant of Akt1
AKT-T308A-AS	CGT TCC GCA GAA TGC CTT CAT AGT GG	Dominant negative mutant of Akt1
AKT-S473A-S	CTT CCC CCA GTT CGC CTA CTC AGC CAG TGG	Dominant negative mutant of Akt1
AKT-S473A-AS	CCA CTG GCT GAG TAG GCG AAC TGG GGG AAG	Dominant negative mutant of Akt1
MeERas-Cis-FS1	GTT TTG GGA AGG TAG AAG TAG GGG GAT TGT	Bisulphite sequencing
MeERas-Cis-FAS1	GAA TAA CTA CCT ACC AAC ATC TTT ACA CTA	Bisulphite sequencing
Rheb-HRas-AS1	CAT GCA GCC GGG GCC ACT CTC ATC CTT TTC TGC TTC CAA A	Rheb-Hras chimeric gene
Rheb-HRas-AS2	TCA GGA TAG AAC ACA CTT ACA GCT CAT GCA GCC GGG GCC A	Rheb-Hras chimeric gene
hERas-C2S-S	GAA GGC CAC CTC CCA CTC AGG CTG CTC TGT	Mutation in palmitoylation sites of human ERas
hERas-C2S-AS	ACA GAG CAG CCT GAG TGG GAG GTG GCC TTC	Mutation in palmitoylation sites of human ERas
ERas-TOPO-gw-S	CAC CAT GGC TTT GCC TAC AAA	**ERas and derivative mutants cloning to pENTR-D-TOPO**
Kras-S	CACCATGACTGAATATAAACTTGTGGTAGT	human Kras cloning to pENTR-D-TOPO
KRas4B-AS	TTACATAATTACACACTTTGTCTTTGACTT	human Kras4B cloning to pENTR-D-TOPO
KRasV12-S	CACCATGACTGAATATAAACTTGTGGTAGTTGGAGCTGTTGGCGTAGGCA	Mutation G12 of Kras to Valine
Nras-S	CACCATGACTGAGTACAAACTGGTGGTGGT	human Nras cloning to pENTR-D-TOPO
Nras-AS	TTACATCACCACACATGGCAATCCCATACA	human Nras cloning to pENTR-D-TOPO
NRasV12-S	CACCATGACTGAGTACAAACTGGTGGTGGTGGTTGGAGCAGTTGGTGTTGGGA	Mutation G12 of Nras to Valine

Appendix 3 (Antibody List)

Primary antibodies

Name	Supplier	Spiecies	Blocking	Dilution rate	Wash
AKT	Cell signaling	Rabbit	5% skim milk in TBST for 1h at RT	1 : 1000 in 5% BSA/TBST, O/N at 4°C	TBST 5 mins x 3 at RT
phospho-Ser473-AKT	Cell signaling	Rabbit	5% skim milk in TBST for 1h at RT	1 : 1000 in 5% BSA/TBST, O/N at 4°C	TBST 5 mins x 3 at RT
phospho-Thr308-AKT	Cell signaling	Rabbit	5% skim milk in TBST for 1h at RT	1 : 1000 in 5% BSA/TBST, O/N at 4°C	TBST 5 mins x 3 at RT
p70S6K	Cell signaling	Rabbit	5% skim milk in TBST for 1h at RT	1 : 1000 in 5% BSA/TBST, O/N at 4°C	TBST 5 mins x 3 at RT
phospho-Thr389-p70S6K	Cell signaling	Rabbit	5% skim milk in TBST for 1h at RT	1 : 1000 in 5% BSA/TBST, O/N at 4°C	TBST 5 mins x 3 at RT
Flag (M2)	Sigma	Mouse	5% skim milk in TBST for 1h at RT	1 : 1000 in 0.5% skim milk/TBST for 1h at RT or O/N at 4°C	TBST 10 mins x 3 at RT
HA (3F10)	Roche	Rat	5% skim milk in TBST for 1h at RT	1 : 600 in 0.5% skim milk/TBST for 1h at RT or O/N at 4°C	TBST 10 mins x 3 at RT
GFP	MBL	Rabbit (antiserum)	5% skim milk in TBST for 1h at RT	1 : 2000 in 0.5% skim milk/TBST for 1h at RT or O/N at 4°C	TBST 10 mins x 3 at RT
p110 alpha	Cell signaling	Rabbit	5% skim milk in TBST for 1h at RT	1 : 1000 in 5% BSA/TBST, O/N at 4°C	TBST 5 mins x 3 at RT
Oct3/4	Santa Cruz	Mouse	1% skim milk in TBST for 1h at RT	1 : 600 in 0.5% skim milk/TBST for 1h at RT or O/N at 4°C	TBST 10 mins x 3 at RT
Stat3	Santa Cruz	Rabbit	5% skim milk in TBST for 1h at RT	1 : 1000 in 5% BSA/TBST, O/N at 4°C	TBST 10 mins x 3 at RT
phospho-Tyr705-Stat3	Cell signaling	Rabbit	5% skim milk in TBST for 1h at RT	1 : 1000 in 5% BSA/TBST, O/N at 4°C	TBST 5 mins x 3 at RT
Cdk4	Santa Cruz	Goat	5% skim milk in TBST for 1h at RT	1 : 200 in 5% BSA/TBST for 1h at RT	TBST 10 mins x 3 at RT
Nanog	Yamanaka-Lab	Rabbit (antiserum)	5% skim milk in TBST for1h at RT	1 : 1000 in 0.5% skim milk/TBST for 1h at RT or O/N at 4°C	TBST 10 mins x 3 at RT
ERas	Yamanaka-Lab	Rabbit (antiserum)	5% skim milk in TBST for 1h at RT	1 : 500 in 0.5% skim milk/TBST for 1h at RT or O/N at 4°C	TBST 10 mins x 3 at RT
4EBP1	Santa Cruz	Goat	2% skim milk in TBST for 1h at RT	1 : 1000 in 2% skim milk/TBST for 1h at RT or O/N at 4°C	TBST 10 mins x 3 at RT
phospho-Ser9-GSK3β	Cell signaling	Rabbit	5% skim milk in TBST for 1h at RT	1 : 1000 in 5% BSA/TBST, O/N at 4°C	TBST 5 mins x 3 at RT
phospho-Thr308-AKT	Cell signaling	Rabbit	5% skim milk in TBST for 1h at RT	1 : 1000 in 5% BSA/TBST, O/N at 4°C	TBST 5 mins x 3 at RT
phospho-Ser380-PTEN	Cell signaling	Rabbit	5% skim milk in TBST for 1h at RT	1 : 1000 in 5% BSA/TBST, O/N at 4°C	TBST 5 mins x 3 at RT
phospho-Ser241-PDK1	Cell signaling	Rabbit	5% skim milk in TBST for 1h at RT	1 : 1000 in 5% BSA/TBST, O/N at 4°C	TBST 5 mins x 3 at RT
phospho-Ser256-FKHR	Cell signaling	Rabbit	5% skim milk in TBST for 1h at RT	1 : 1000 in 5% BSA/TBST, O/N at 4°C	TBST 5 mins x 3 at RT
Myc (9E10)-AC	Santa Cruz	Mouse	None	1 : 50 in lysis buffer	None
Myc	Santa Cruz	Rabbit	5% skim milk in TBST for 1h at RT	1 : 600 in 0.5% skim milk/TBST for 1h at RT or O/N at 4°C	TBST 10 mins x 3 at RT

Secondary antibodies

Name	Supplier	Dilution rate
Anti-Mouse IgG-HRP	Cell signaling	1:3000 in 5% skim milk
Anti-Rabbit IgG-HRP	Cell signaling	1:2000 in 5% skim milk
Anti-Goat IgG HRP	Santa Cruz	1:3000 in 5% skim milk
Anti-Rat IgG-HRP	Chemicon	1:5000 in 1% skim milk
Anti-Rabbit IgG-Cy3	Chemicon	1:100 in 5% skim milk
Anti-Mouse IgG-Cy3	Chemicon	1:100 in 1% BSA